A REPLACEABLE CONNECTION FOR CONCENTRICALLY BRACED FRAMES

DESIGN AND TESTING OF A REPLACEABLE CONNECTION FOR STEEL CONCENTRICALLY BRACED FRAMES

By

DANIEL M. STEVENS, B.ENG.MGT.

A Thesis Submitted to the School of Graduate Studies in Partial Fulfillment of the Requirements for the Degree Master of Applied Science

McMaster University

MASTER OF APPLIED SCIENCE (2016) (Civil Engineering)

McMaster University Hamilton, Ontario

TITLE: Design and Testing of a Replaceable Connection for Concentrically Braced Frames

AUTHOR: Daniel M. Stevens, B.Eng.Mgt.
(McMaster University)

SUPERVISOR: Dr. Lydell A. Wiebe

NUMBER OF PAGES: x, 114

LAY ABSTRACT

Earthquakes can cause major, devastating damage to city structures. The cost of repairs and the time needed to make those repairs can be crippling, to the point where it is easier to tear down the structures than properly repair them. Designers and engineers need improved ways to design these structures to be more easily repaired, without driving up the initial cost of the structure.

This research developed, tested and modelled a new, replaceable connection for earthquake resistant braces. The new connection is easier to install, easier to replace and provides added safety when compared to traditional designs.

ABSTRACT

There is increasing demand, from both engineers and their clients, for structures that can be rapidly returned to occupancy following an earthquake, while also maintaining or reducing initial costs. One possible way towards this goal is to ensure that seismic damage occurs only within elements that can be removed and replaced following a damaging earthquake. For concentrically braced frames that use hollow structural sections, the current design practice requires field welding of the brace to the gusset in a way that causes the brace to buckle out-of-plane. In the event of a damaging earthquake, the out-of-plane brace buckling may damage both the gusset plate and also any adjacent exterior cladding. The plate cannot be easily replaced, resulting in expensive and time-consuming repairs, and the damaged cladding could endanger the lives of people evacuating the building and of other pedestrians.

Through multiple design iterations, a new steel concentrically braced frame connection type was developed that can be bolted into place and that confines damage to replaceable components. The proposed connection is expected to result in reduced erection costs and be easier to repair following a major earthquake. Moreover, the new connection causes buckling to occur in-plane, preventing dangerous damage to the cladding.

Large scale experimental testing on two variations of the new connection was performed. The cyclic, uniaxial testing of a brace with the new connection demonstrated the connection's ability to behave in a desirable manner, with tensile yielding, brace buckling and connection rotation occurring during the expected drift levels associated with earthquake loading. A nonlinear finite element model of a brace with the new connection was developed and discussed. The finite element model was able to replicate the results of the experiment and will allow for further research and development of the new connection. The new connection shows promise as a replaceable connection for the seismic design of concentrically braced frames.

ACKNOWLEDGEMENTS

I would first like to thank my supervisor Dr. Lydell Wiebe, whose constant encouragement and support were the driving forces in completing this research. I was always strengthened by his positive attitude and his confidence in me when I wasn't feeling very confident or positive myself.

I would like to thank the amazing lab technicians we have at the Applied Dynamics Laboratory, Kent Wheeler and Paul Heerema, who helped make my laboratory experience an enjoyable success. They always knew how to make what I needed work. Their advice and assistance during the design, construction and operation of the experimental program was greatly appreciated.

My fellow graduate students in the program were a source of great ideas and help when needed. I would like to in particular thank Vahid Mohsenzadeh for helping during the experiment when he could and the work he will be doing to expand this research.

Funding for this research was provided by the National Sciences and Engineering Research Council (NSERC), Ontario Centres of Excellence (OCE), the Canadian Institute of Steel Construction (CISC) and the Ontario Erectors Association (OEA). Funding, fabrication services and consultation was provided by Walters Inc. This research would not have been possible without these generous sponsors.

Finally, I need to thank my friends, family and especially my wife Karlee for their love, support and prayers as I completed this research.

TABLE OF CONTENTS

LIST OF FIGURES

LIST OF TABLES

Chapter 1: Introduction

1.1 Motivation

Current seismic design codes, including the National Building Code of Canada (NBCC), focus on life safety of the occupants in very rare earthquake events. While this has been a very beneficial advancement in structural engineering, recent earthquakes, such as the 2010 and 2011 earthquakes in Christchurch, New Zealand have highlighted the need for improved solutions. Costs associated with the demolition, rebuilding, repair and economic downtime have been estimated at 20% of New Zealand's GDP (Canterbury Earthquake Recovery Authority 2012). However, the terrible economic implications of an earthquake are not limited to high seismic regions. A recent study commissioned by the Insurance Bureau of Canada has indicated that the direct losses associated with structural damage and business interruption of a 7.1 Magnitude earthquake near Quebec City would be over $30 billion, in part due to the unpreparedness of the region for a major earthquake. (AIR Worldwide 2013). It is critical that new building designs consider ways to prevent or reduce the extent of damage caused by an earthquake and to lower the time for repair after an earthquake.

While innovative solutions such as rocking frames and base isolation exist that fundamentally alter the seismic response of a structure and prevent structural damage from occurring, these systems are not commonly implemented, in part due to the higher upfront costs and lack of design familiarity by practicing engineers. Even traditional seismic force resisting systems, such as steel moment resisting frames or steel braced frames, are, due to increased initial cost, often ignored by designers in favour of conventional construction techniques which do not benefit from the improved performance of modern seismic design. It is necessary to find

solutions that are cost efficient and are easily understood by current design engineers to allow widespread application of more resilient building practices in current construction. A method towards this is to develop alternatives to traditional seismic force resisting system designs which are more constructible and more easily replaceable to allow lower time and cost for initial installation and allow for quick and cost efficient repairs to rapidly return a building to safe occupancy after an earthquake. One type of seismic force resisting system that could use this improvement is steel concentrically braced frames.

1.2 Design of Steel Concentrically Braced Frames

Steel concentrically braced frames (CBFs) are a commonly used lateral force resisting system (LFRS) for resisting the loads and demands imposed on a structure by wind and seismic ground motion. CBFs are used throughout North America, including in regions with high seismic risk. CBFs are desirable for their high stiffness, which allows them to resist seismic forces with less structural and non-structural deformations, and their low cost when compared to other seismic force resisting systems, such as steel moment resisting frames.

In Canada, CBFs can be designed as limited-ductility concentrically braced frames or moderately-ductile concentrically braced frames. In the United States, CBFs are labelled as either ordinary concentrically braced frames or special concentrically braced frames. CBFs are designed using the traditional approach to seismic design, which is to allow certain portions to yield and dissipate energy to prevent damage to the rest of the building in the event of a major earthquake.

In the case of seismically designed concentrically braced frames, the major source of ductility comes from the tensile yielding and compression buckling of the brace during large storey drifts, with some yielding also occurring in the connection and surrounding framing elements during more severe earthquakes (Roeder 2011). An example of the anticipated behaviour of a seismically designed concentrically braced frame at different seismic risk levels can be seen in Figure 1.1

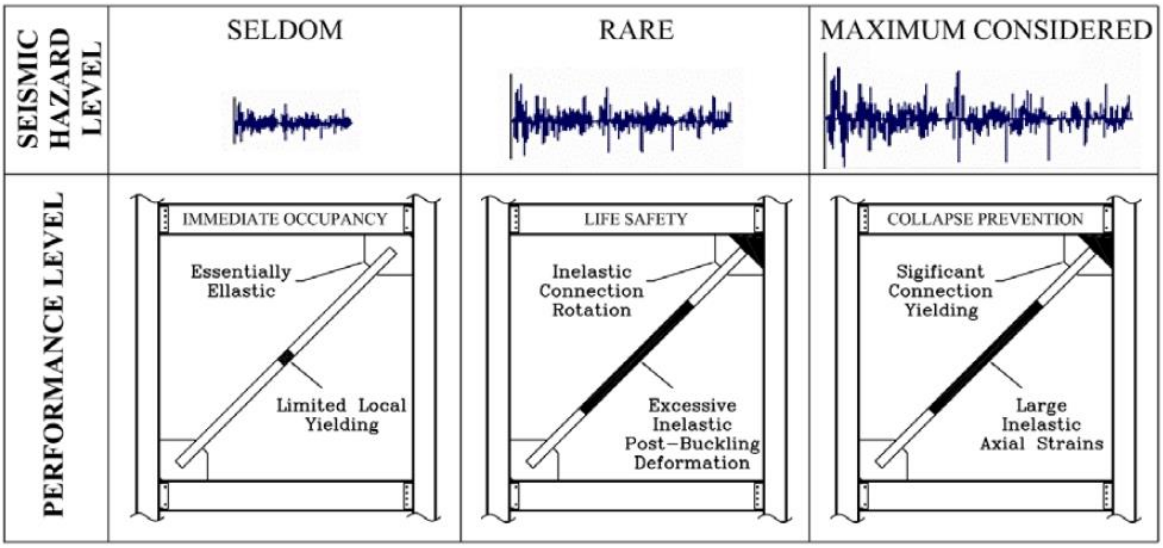

Figure 1.1: Braced frame performance at various hazard levels (Johnson 2005)

To ensure that the brace exhibits the required ductile behaviour during a seismic event, careful design of the braces and all connections and framing elements in the load path is required. The design process for CBFs as laid out in the Canadian code is to first assess the lateral loads expected to occur in the structure during an earthquake using either a static or dynamic procedure (NRCC 2010). These loads are reduced by a ductility value assigned based on the LFRS chosen. For limited-ductility CBFs, this reduction factor is 2.6 and for moderately-ductile CBFs the reduction factor is 3.9. Braces are then sized and selected based on these design forces. Braces are required to be used in opposing pairs due to the lower

strength of the brace in compression, especially after multiple buckling cycles. Braces can be configured in multiple different ways as seen in Figure 1.2. After brace selection, all other connections and elements in the load path of the braces must be designed to resist the probable forces of the braces when they have achieved their full tensile and buckling strength. This method of designing surrounding elements to be stronger than the yielding component, called capacity design, ensures that significant energy dissipation occurs in the brace before any brittle failure modes in the surrounding elements. Finally, brace buckling must be accommodated in one of two ways. The first is to design the brace end connections to be sufficiently stiff to allow three plastic hinges to occur within the brace. Since this connection strength can be difficult to achieve, the more commonly used method is to allow plastic hinging to occur in the brace end gusset plate connections and a single plastic hinge in the brace midspan. This has historically been done using a linear clearance rule equal to two times the thickness of the gusset plate as seen in Figure 1.3 (Astaneh-Asl et al, 1985).

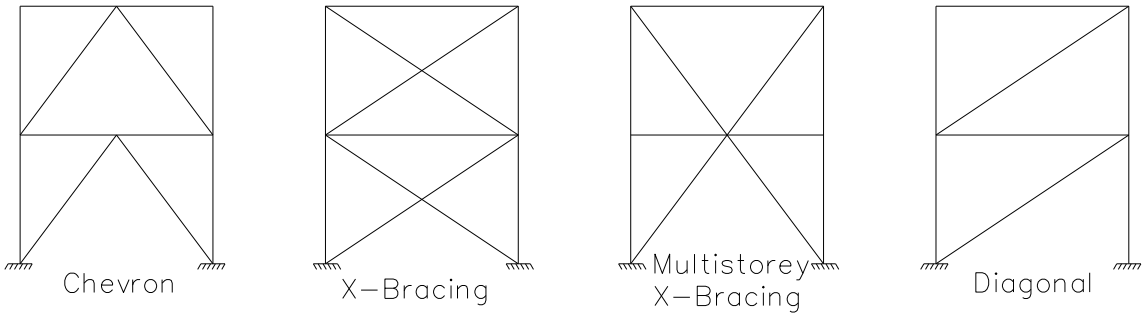

Figure 1.2: Possible Braced Frame Configurations

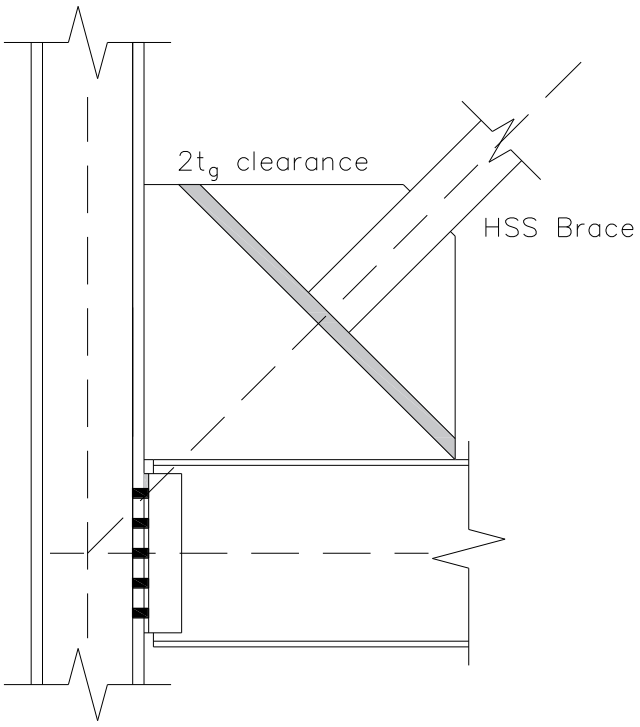

Figure 1.3: Typical Gusset Plate Design

When selecting brace size, opposing braces are assumed to equally carry the design lateral, force which causes the compressive strength of the brace to be the limiting factor in design. For this reason, hollow structural sections (HSS) are an economical and popular choice for braces due to their high compressive strength relative to other shapes. HSS braces have also been shown to provide higher postbuckling compressive resistance than other shapes which promotes a more regular structural response. A typical connection detail when using HSS braces can be seen in Figure 1.3. This detail consists of a gusset plate welded to the beam and column and a brace that is slotted and welded to the gusset plate. In this connection, when the brace buckles in compression, a plastic hinge forms in the gusset plate at the end of the brace.

There are a few issues with the typical connection design. The first is that it involves field welding of one or more components of the connection. Field welding is more time consuming than shop welding or field bolting, increases costs and can complicate quality control. Additionally, if the brace and gusset plate are damaged during a major seismic event, replacing the brace and gusset plate would require cutting out the gusset plate, field welding a new gusset plate and field welding a new brace to the gusset plate. These expensive and time consuming processes would delay the building's return to safe occupancy. Another issue with this connection is that the plastic hinges that form in the gusset plate cause the brace to buckle out-of-plane. This out-of-plane movement can cause damage to exterior cladding and could result in sections falling, endangering the lives of people evacuating the building and of other pedestrians. (Sen et al. 2013). If the cladding has sufficient strength such that it restricts the buckling of the brace, the intended behaviour of the system would be altered and could invalidate a number of design assumptions and cause the system to fail in a less ductile manner, such as gusset plate buckling due to the unexpectedly high compression force.

The typical connection also presents a complication due to the influence of the gusset plate on the beam-column connection and the associated consequences. Beam-column connections of braced frames are often assumed to be pin-ended connection, but the large storey drifts caused by seismic loading can make this assumption invalid. The storey drift can cause distortional forces to occur in the gusset plate caused by the rotation of the beam-column connection, leading to early buckling of the gusset plate (Lopez et al. 2004). The increased rigidity of the beam-column connection caused by the gusset plate increases the strength and stiffness of the structure and can allow for better transfer of forces between

floors and reduce the chance of accumulating inelastic demand in one storey (i.e. a "soft storey"). However, the higher stiffness of the beam-column connection imposes larger forces and inelastic demand on the beam and column while reducing the energy dissipation provided by the brace. This increased demand in the beam and column can lead to excessive damage there, increasing the number of members that would need to be repaired or replaced after an earthquake.

1.3 Summary of Past Research

1.3.1 CBF Experimental Testing

Over the past few decades, numerous experiments and studies have been done on braces, brace and connection assemblies, braced bays, and multistory braced frames under quasi-static cyclic and earthquake loading. In 1980, testing was done by Black et al. (1980) on a large variety of brace shapes under quasi-static cyclic loading. The testing showed that the effective brace slenderness ratio was the most important parameter for determining the hysteretic behaviour of a brace. Brace sections were shown to have reduced compressive strength with increasing number of cycles. The testing indicated hollow structural sections had a greater post buckling strength compared to other shapes. Testing done by Tang & Goel (1987) further confirmed the improved post-buckling strength of HSS braces while exhibiting a more limited fracture life, influenced by the width-to-thickness ratios of the brace. Figure 1.4 shows the hysteretic behaviour of a single HSS brace with pinned end conditions tested by Black et al. (1980).

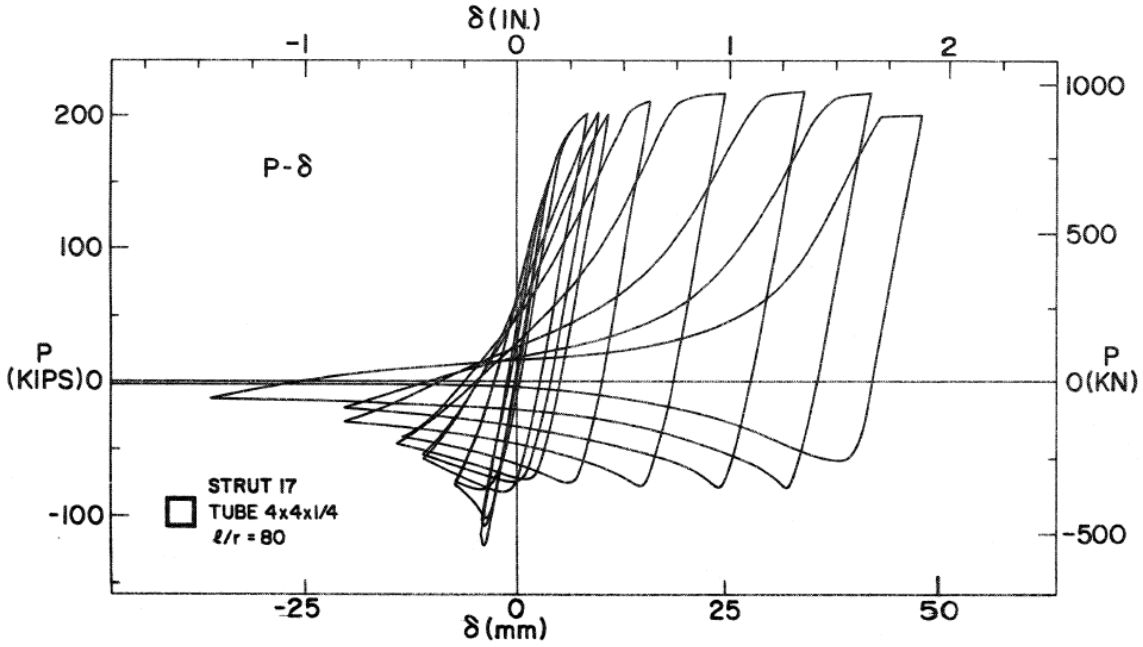

Figure 1.4: Hysteresis of a pinned end HSS brace (Black et al. 1980)

Further testing in the 1980s focused on the cyclic loading of braces connected to gusset plates. Testing done by Astaneh-Asl et al. (1985) showed that it was important to provide clearance in the gusset plate to allow for the out-of-plane buckling of the brace in compression and was the basis for the commonly used two times the gusset plate thickness linear clearance rule applied to gusset plate design. This testing also showed the need for the gusset plates to be able to resist the full tensile and compressive strength of the attached braces.

In an effort to improve the design of gusset plates, single bay diagonal brace frame testing was done by multiple researchers at the University of Washington (Johnson 2005, Kotulka 2007, Powell 2010). Thirty-four tests were done on a frame setup meant to represent a second storey braced bay. The research was focused on improving the design characteristics of gusset plate connections, with variations on gusset plate shape and connection attributes

such as weld type and length and bolted vs welded connections. The research provided new design tools for engineers when designing CBFs. The first is an elliptical clearance rule meant to replace the linear clearance rule proposed by Astaneh-Asl et al. (1985). Another tool that was developed was the balanced design procedure for concentrically braced frames. This procedure seeks to adjust the normal code equations to better select and size the connection region with the intent to increase the ductility of the CBF (Roeder et al. 2011). The research showed that the seismic performance of the braced frame was influenced by the inclusion of beams and columns to the testing. In these tests, the beam column connection could resist moment caused by the storey drift and allowed increased post-buckling strength of the system at the expense of yielding within the beams and columns. Figure 1.5 show the hysteretic behaviour of one of the braces tested which is typical of most tests performed in the University of Washington experimental program.

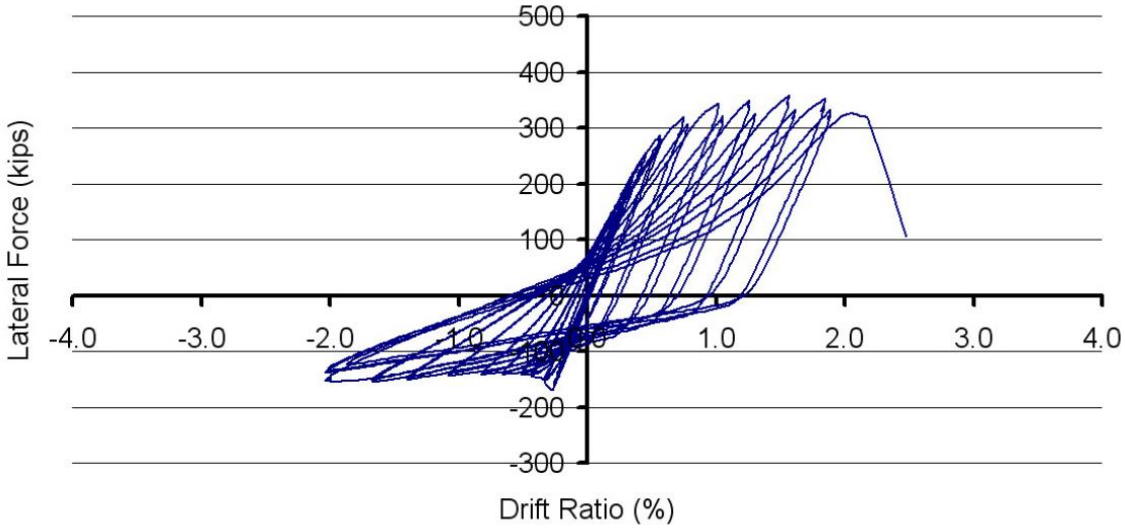

Figure 1.5: Single bay Hysteresis (Kotulka 2007)

Multi-storey planar testing done by Lumpkin (2009) based on the same representative structure as the previous University of Washington testing further showed the importance of

beams and columns to the performance of CBFs. Stiffer connections increased the contribution of the frame to the performance while also increasing the damage to the beam and columns. The addition of an opposing brace at each storey creates a more uniform overall storey force-drift hysteresis as seen in the second storey hysteresis shown in Figure 1.6.

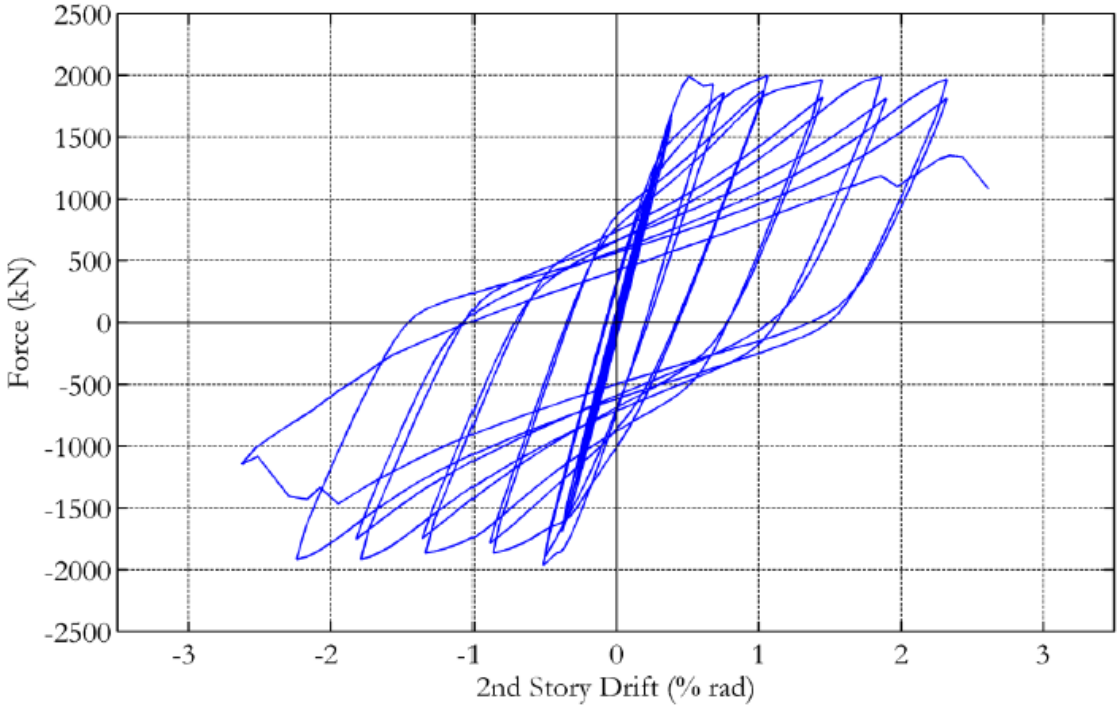

Figure 1.6: Paired brace Hysteresis (Lumpkin 2009)

1.3.2 Bolted Gusset Connections

Due to the desire for more economical and constructible connections, some research has been done to establish a suitable bolted connection for use in CBFs with HSS braces. Tests on bolted splice connections between the brace and gusset plate were completed by Kotulka (2007) and Powell (2010). Kotulka's (2007) test consisted of a plate welded to a slotted brace which was then bolted on one side to a gusset plate. This connection detail did not work as

anticipated, with gusset plate weld tearing occurring at the gusset to column interface before any brace buckling or tensile yielding could occur as seen in Figure 1.7(a). This early weld failure prevented any inelastic deformation from occurring in the brace, and instead concentrated the deformation in the splice plate. Eventually, the splice plate fractured. An alternative configuration, tested by Powell (2010), consisted of a two WT sections connected on either side of the gusset plate to the brace to equally spread the load on either side of the gusset plate. This connection formed multiple plastic hinges in the connection region, again preventing the brace from buckling, as seen in Figure 1.7(b). This behaviour is similar to the multiple hinge formation found in Buckling Restrained Braced frame testing with weak gusset plates (Chou and Chen 2009).

(a) (b)

Figure 1.7: Bolted gusset failures: (a) Single splice (Kotulka 2007) (b) Two WT sections (Powell 2010)

The performance of single sided and double sided bolted splice connections in concentrically X-braced frames using HSS sections was investigated by Davaran et al. (2009, 2015). The testing and analysis showed that compressive resistance of simple splice connections was lower than the expected brace compressive strength for all analyzed specimens. As noted by

Davaran (2015), this early connection failure would not be permitted for seismically designed CBFs as the braces would not experience flexural buckling before connection failure.

A study that demonstrated the successful performance of a bolted connection was performed for multiple brace sizes and lengths by de Oliveira et al. (2008). The bolted connection consisted of a cast steel connector welded to the end of a circular HSS and bolted to a gusset plate as shown in Figure 1.8. With this connection, the cast steel connector is much stiffer than either the brace or gusset, preventing multiple plastic hinges from forming as seen in other bolted gusset plate connections and allowing brace flexural buckling to occur. While this connection is easier to install than a field welded connection, the gusset plate would still need to be removed and replaced in the event of a major earthquake.

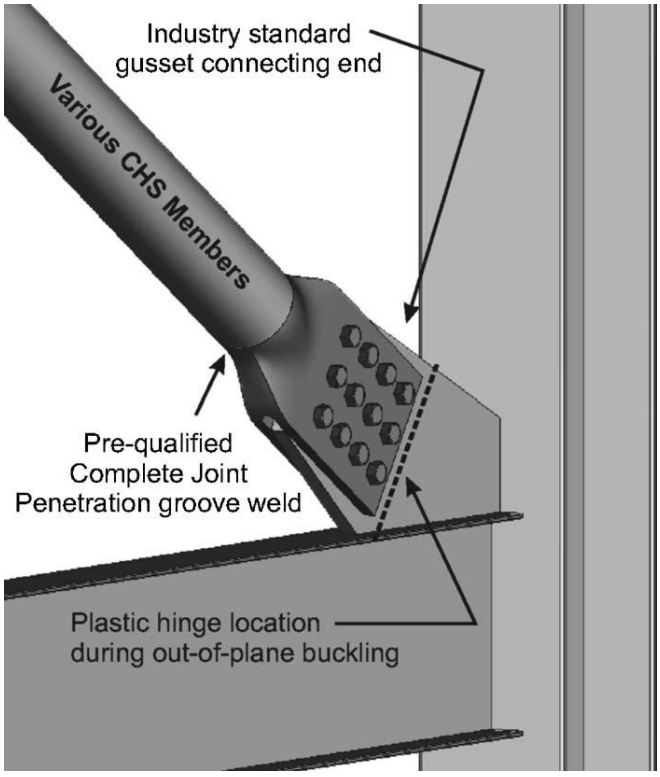

Figure 1.8: Cast steel bolted connection (de Oliveira et al. 2008)

1.3.3 In-Plane Buckling Connection

A number of experiments have been performed on a braced frame connection that allows buckling to occur in-plane. The connection, referred to as a "knife plate" connection and shown in Figure 1.9, was first tested by Lumpkin (2009) as an extension of the test program performed at the University of Washington. A 3t clearance limit was recommended for this connection to prevent the tearing in the knife plate present in Figure 1.10. Further full scale testing was performed using this knife plate connection and the results showed that the connection was able to provide the desired in-plane behaviour while sustaining similar drifts to traditional gusset connections (Tsai et al. 2013, Sen et al. 2016).

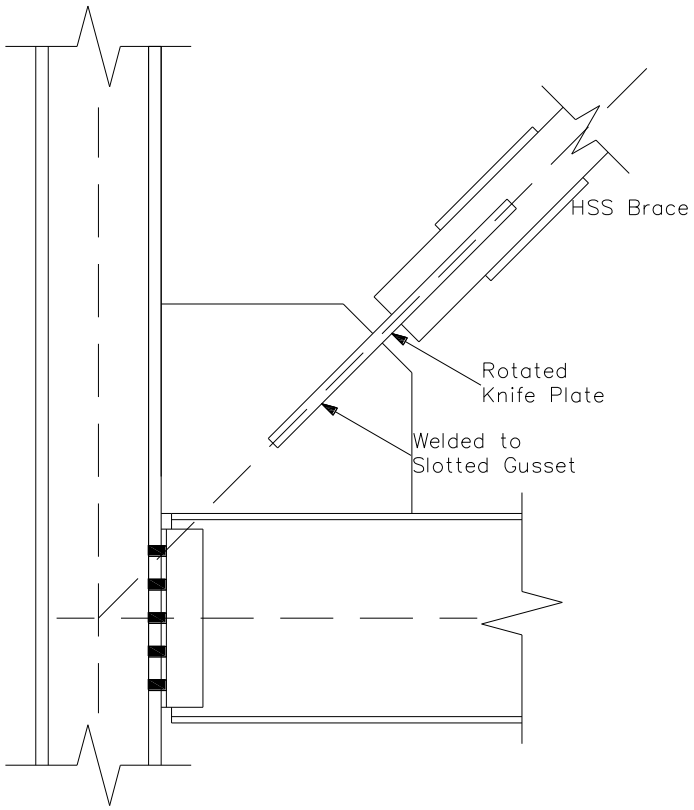

Figure 1.9: Rotated "knife plate" connection

Figure 1.10: Knife plate damage with insufficient hinge clearance (Lumpkin 2009)

The success of this new in-plane knife plate connection detail has caused it to be recommended as an alternative gusset plate connection in educational materials targeted at design engineers (Sabelli et al. 2013, AISC 2015). However, this connection has some issues. The first is that in some of the tested cases, buckling still occurred out-of-plane due to a plastic hinge occurring in the gusset plate instead of the hinge plate (Sen et al. 2016). This invalidates the purpose of the knife plate by concentrating damage in the gusset plate, which may not have been correctly proportioned to accommodate plastic hinging. This connection also does not improve the constructability or replaceability of the braced frame since field welding is still required during installation and repair.

1.4 Research Objectives

Previous research has not developed a connection for concentrically braced frames that allows for easily installed and replaceable components while also allowing the brace to buckle

in plane. The goal of this research is to develop a new connection type for the seismic design of concentrically braced frames which meets the following three criteria:

1. The new connection design should be easy to install and easy to replace in the event of damage. To facilitate this, the connection should not require any field welding. If the brace is damaged in an earthquake, the damage should be confined to a region that can be unbolted and replaced as a unit.
2. It should allow the brace to buckle in-plane to minimize damage to the surrounding walls and cladding.
3. It should provide comparable seismic performance to the current design practice. This includes similar yield and failure progression and similar energy dissipation behaviour.

The following research was performed to assess the new connection's performance, both experimentally and numerically, to ensure that it can meet the desired criteria.

1.5 Thesis Organization

Chapter 1 introduces the motivation of the research and provides an overview of the seismic design of concentrically braced frames. Previous research is discussed to give an understanding of the progression of findings in the field. Research of bolted and in-plane connection details is investigated, with the need for improvement highlighted. Finally, the research objectives of the project are stated.

Chapter 2 discusses the concept development of a new connection for use in the seismic design of steel concentrically braced frames. Early theories and ideas are presented and the

associated problems identified. The final proposed connection design is introduced and discussed. Preliminary finite element modelling is performed to assess the monotonic compressive capacity of the new connection.

Chapter 3 discusses the first large scale experimental testing of the new braced frame connection design that was proposed in Chapter 2. This chapter assesses the performance of the eight specimens that were tested under quasi-static axial loading. Hysteretic behaviour and damage progression are presented, with comparisons made between specimens.

Chapter 4 discusses a finite element model created to replicate the results of the experiment performed in Chapter 3. The finite element modelling approach is described and the analysis results are compared to the experimental results. Recommendations of further development and application of the finite element model are given.

Chapter 5 summarizes the findings and conclusions of the research that has been performed. It provides recommendations for the continued research and development of the new connection.

Appendix A consists of two design examples of the new connection design used in a 4 storey structures located in Vancouver, BC following simple code based procedures. It is meant to aid in understanding the steps necessary to design a structure using the new connection.

Appendix B consists of additional experimental data not included in the discussion chapters such as the instrumentation used and other measurement data. It also includes the full drawings of the experimental program.

Chapter 2: Concept Development of New Connection Design

2.1 Design Iterations

In order to meet the proposed objectives for the new seismically designed concentrically braced frame connection listed in Chapter 1, several different connection designs and details were created and evaluated. Initial designs focused on modifying a knife plate design that has been investigated in previous studies (Tsai et al. 2013). When using a knife plate, most of the yielding and rotation that would otherwise occur in the gusset plate occurs in the knife plate instead. Typically, the knife plate is slotted and welded directly to the gusset plate. Figure 2.1(a) shows an example of a typical knife plate connection.

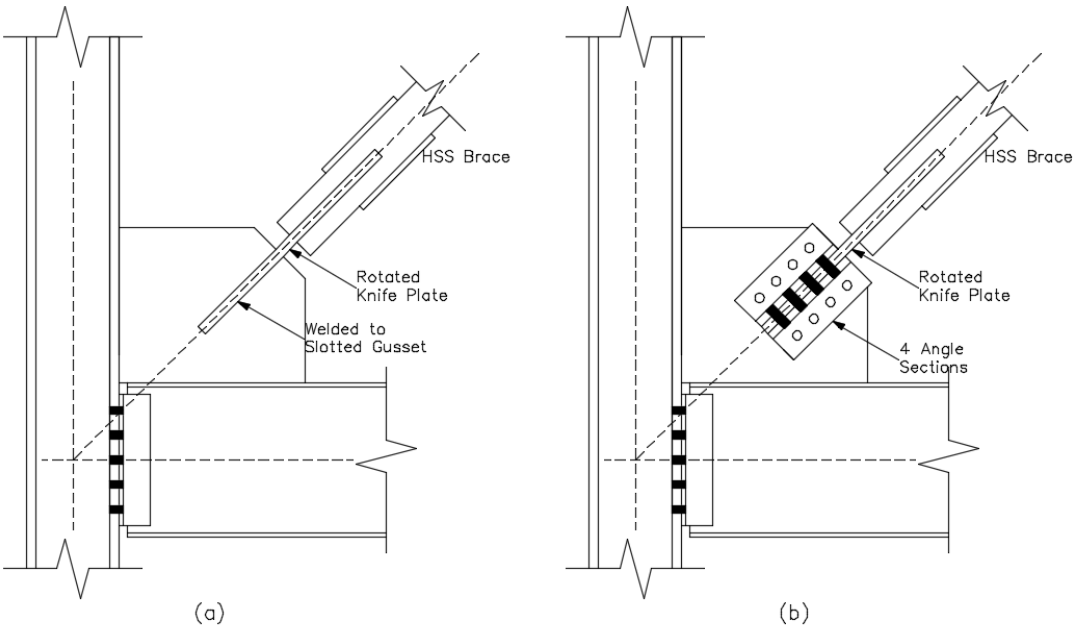

Figure 2.1: (a) Knife plate welded to gusset plate; (b) Knife plate bolted to gusset plate

For a knife plate design to meet all the objectives of the proposed new design, the weld connecting the knife plate to the gusset plate must be replaced with a bolted connection.

Figure 2.1(b) shows a design that was considered. This connection consists of the typical knife plate design but with 4 angles bolted around the gusset and knife plate to replace the knife plate to gusset plate weld.

This connection would meet the stated design objectives but has a number of associated concerns. The primary issue is the poor force transfer that would occur between the knife plate and the gusset plate. The angles have very little room to develop the high tensile forces that would need to be transferred between the gusset and the knife plate. This could result in significant rotation and warping of the angles, which is problematic under the cyclic loading an earthquake would impose on the connection.

The next iteration of design investigated using an end plate connection attached to a hinge plate to bolt the connection directly to the beam or column. Two examples of this are found in Figure 2.2. The connections for these braces would be assembled and welded together before being sent to site and would be bolted to the beam or column as a unit. This connection would meet the proposed goals and would be relatively easy to install and replace on site. The primary issues with this iteration of the design were geometric. First, if connected directly to the column as in Figure 2.2(a), there is very little possibility that the workpoint of the brace would pass through the desired location at the intersection between the beam and column centrelines. This eccentricity would induce a large moment in the column, which could require expensive stiffeners or a significantly larger column (Gross and Cheok 1988). There is also a concern that the high eccentricity could cause irreparable damage to the column under the large cyclic loading cause by a major earthquake. Second, the bolts nearest to the hinge plate could be very difficult to install.

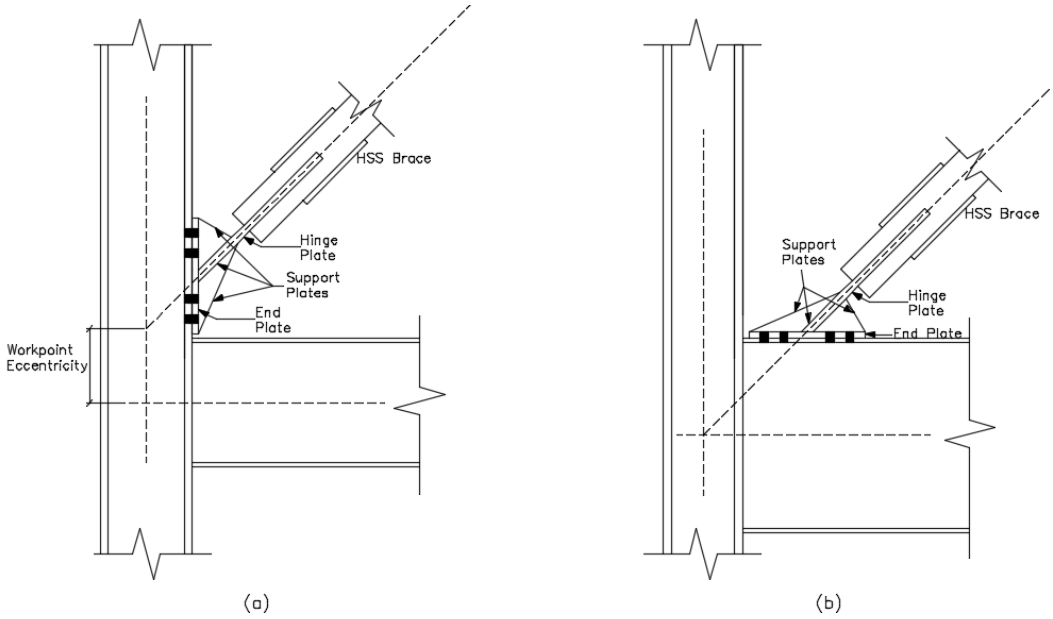

Figure 2.2: Hinge & plate connections: (a) Bolted to the column flange; (b) Bolted to the beam flange

If connected directly to the beam as shown in Figure 2.2(b), workpoint eccentricity can usually be avoided. However, in order to prevent this eccentricity, the connection end would usually need to be very close to the beam edge. This proximity to the beam edge could create problems for the design of the beam-column connection. The beam-column connection would need to be more robust to accommodate the increased shear from connecting the brace directly to the beam, and this would create interference problems between it and the bolts and stiffeners required for the brace connection. There would also be a concern that the large tension force on the bolts in the beam flange would require excessive stiffeners or welded plates to increase the flange thickness.

2.2 Proposed Connection Design

Working in consultation with industry experts, a solution was proposed that would meet all of the design objectives while limiting the negative effects of the previous proposals. The final proposal combines a knife plate design with a support that is attached directly to the beam, as shown in Figure 2.3. For this design, a hinge plate is welded to a slotted HSS and is then bolted to support plates that have been welded to the beam flange in the fabrication shop.

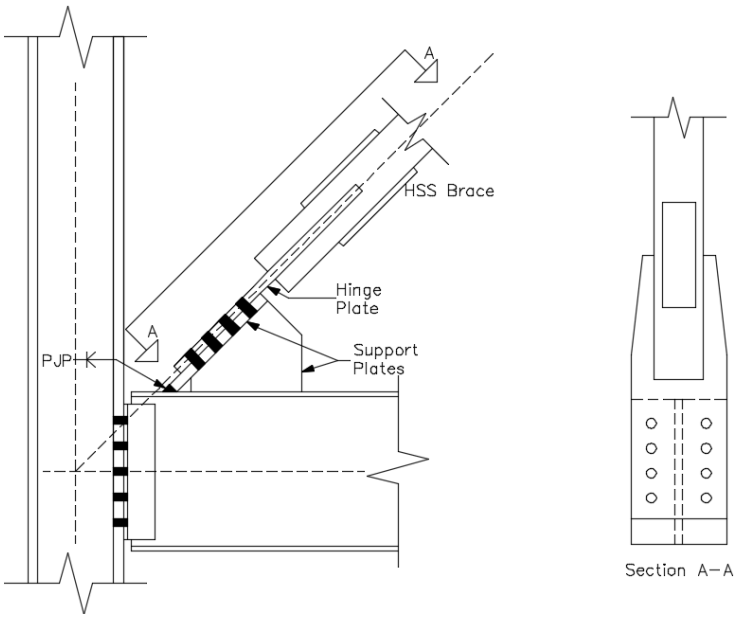

Figure 2.3: Proposed connection design

In addition to meeting all of the design objectives, this design provides other benefits. The proposed design would be very easy to install due to the simple single splice bolted connection. Hinging is unlikely to occur outside the brace and hinge plate due to the stiffness of the support, meaning that in all but the most catastrophic earthquakes, the only damaged components would be those that are easily replaceable. Since the hinge plate would be

welded to the brace in the shop, there would be the option of slotting both the hinge plate and the brace, as suggested by Martinez-Saucedo et al. (2008) and shown in Figure 2.4. This would eliminate the need for the costly cover plates that are typically required on slotted HSS braces to prevent net section fracture. A potential issue with the proposed connection is the eccentricity due to the single sided splice connection. Eccentricities are typically avoided because they can increase the deformation demand on the connection, leading to earlier fracture (Gross and Cheok 1988).

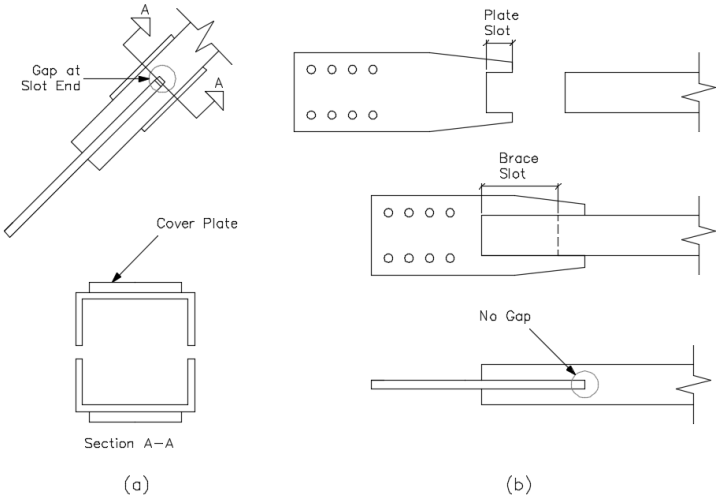

Figure 2.4: Slotting of brace and hinge plate: (a) Only the brace is slotted; (b) Brace and plate are slotted

There are two main design criteria that need to be considered for this connection that are not present in a typical gusset plate connection. The most significant design criterion is the selection of the hinge plate thickness to allow buckling to occur in the brace before failure in the connection. A thicker plate allows for higher initial buckling capacity by provided greater end rotation restraint, but it also tends to concentrate more damage in the brace during cyclic loading, reducing the total drift capacity of the system (Roeder et al. 2011). Determining the correct balance of strength and ductility will be essential for optimizing the performance of

the proposed connection. The calculation of the connection capacity is also challenging because of the unique configuration of the eccentric hinge plate. Most equations for determining the ultimate capacity of a single-sided splice are unable to adequately account for one plate being significantly stiffer than the other (Fang et al. 2015, Davaran et al. 2015, Packer et al. 2010). Another special design criterion is the sizing of the support plates to provide the required strength and stiffness in an efficient manner.

An alternative form of the proposed connection design has splice plates that eliminate the connection eccentricity, as shown in Figure 2.5. This may improve the connection performance under repeated cyclic loading. Although the eccentricity is prevented, this connection also has an increased risk of achieving a sway buckling mode where both the hinge plates and the splice plates bend, resulting in a brace that does not buckle, as seen in Figure 2.6. If that occurred, the deformation would be confined to the connection, which is very undesirable.

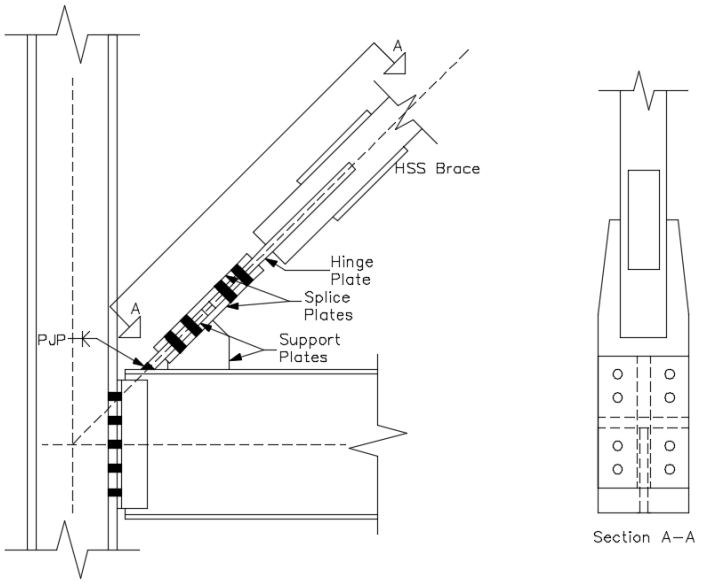

Figure 2.5: Concentric variation of proposed connection

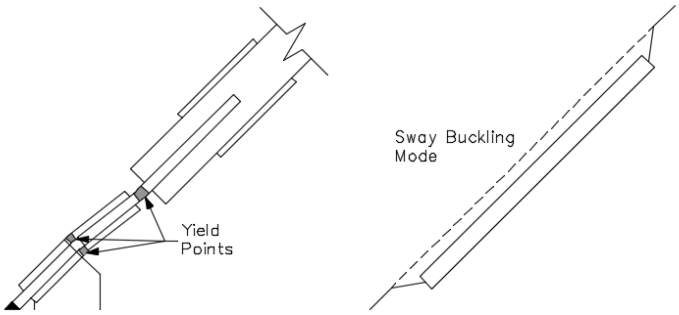

Figure 2.6: Sway buckling mode of concentric connection

2.3 Preliminary Finite Element Model of Proposed Design

2.3.1 Model description

In order to assess the viability of the proposed design, a finite element (FE) model was created using the general nonlinear analysis package ABAQUS (Dassault Systemes 2012). The model was created to simulate the behaviour of a future physical experiment that is described in Chapter 3 and included the full brace, support plates, hinge plates and bolts, as seen in Figure 2.7. The braces modelled ranged from HSS 89x89x6.4 to HSS 102x102x6.4 with lengths around 3m. The beams were not modelled and were assumed to provide rigid support to the support plates. The compressive load was applied as a uniform displacement at one support plate. Movement of the support plate ends along the axes perpendicular to the path of loading were prevented and the rotation degrees of freedom were fixed. An initial geometric imperfection was introduced into the model in proportion to the first buckling mode of the brace. This imperfection was scaled to a midspan deflection of 0.1% of the brace length. Two analysis steps were used in the model. The first step was a buckling analysis that was used for creating the imperfection. The second step was a nonlinear Riks

arc-length analysis that was used to determine the critical buckling load and to observe the yielding behaviour at various compression strains.

The brace was modelled using 4-noded quadrilateral shell elements, while the support plates, hinge plates and bolts were modelled using 8-noded brick elements. Contact surfaces were modelled using hard contact behaviour with no penetration in the normal direction. Friction was modelled using the penalty method with a coefficient of friction of 0.2. Tie connections were used to simulate the fillet welds between the brace and the knife plate. The material model was simulated using an isotropic hardening model with Von Mises yield criterion. The region of a typical braced bay that was modelled is highlighted in Figure 2.7.

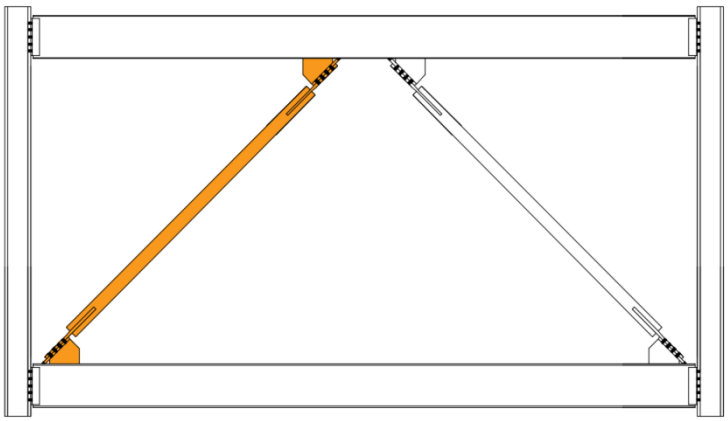

Figure 2.7: Modelled region of a typical braced bay

The modelling approach and selection of elements was based on two previous FE studies that validated models from companion physical experiments. Modelling of the brace was based on a study of concentric tubular braces subjected to seismic loading (Haddad 2015). The modelling of the hinge and support plates was based on a study of the compressive strength of single sided splice connections (Fang et al. 2015).

2.3.2 Modelling Results

The results of the model were used to confirm that the system would exhibit the desired failure behaviour and to estimate the critical buckling load. The stress distribution at critical buckling load is shown in Figure 2.8. The connection retains its strength and does not yield before the brace buckles. Figure 2.9 shows the stress distribution at an axial displacement of 1% of the brace length, approximately 5 times the yield strain. Significant yielding is observed in the hinge zone and the middle of the brace. This yielding does not spread to the support plates, meaning that any damage due to yielding is expected to remain confined to the easily replaceable components.

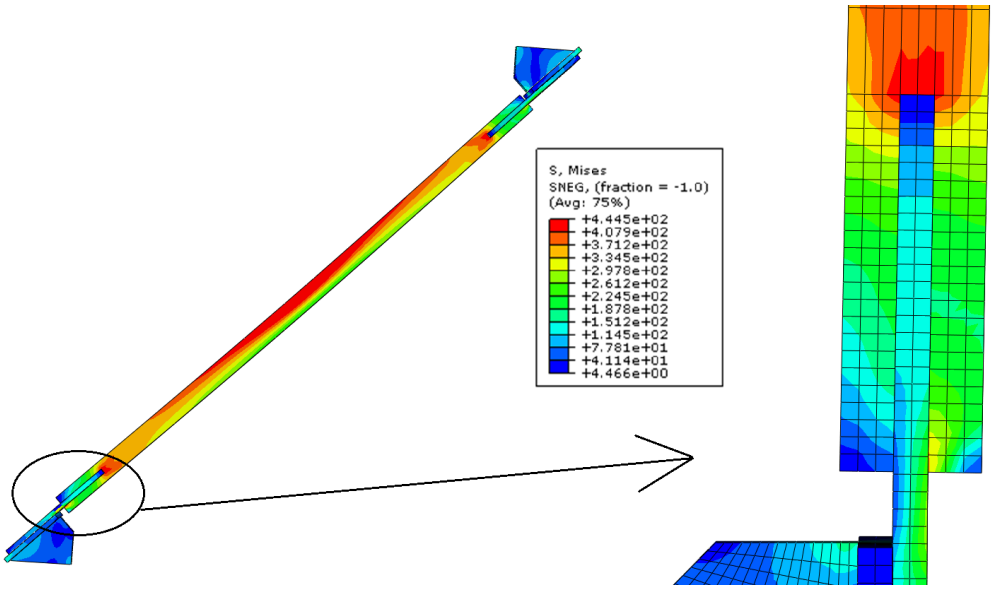

Figure 2.8: Von Mises stress of full system and hinge plate at buckling load

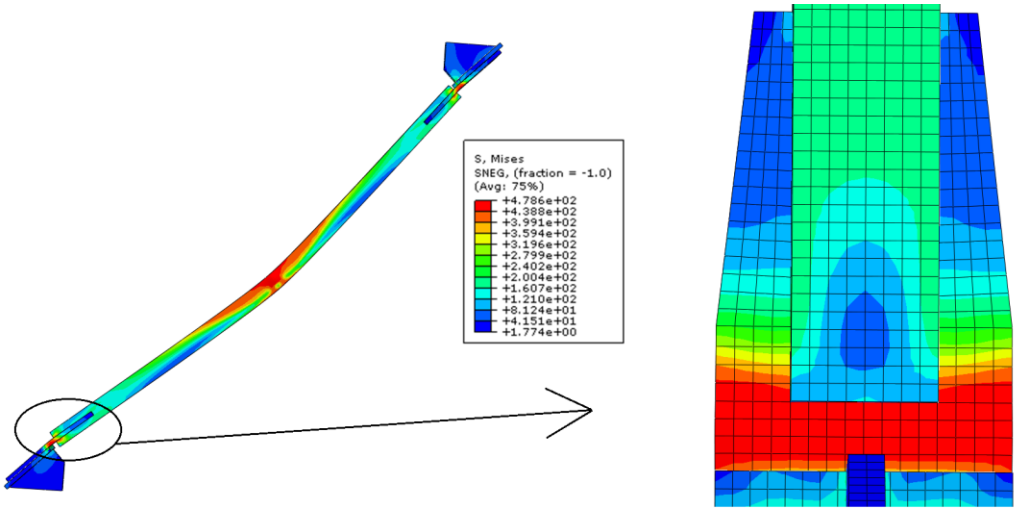

Figure 2.9: Von Mises stress of full system and hinge plate at 1% axial displacment

To estimate the peak compression load of the full system ($P_{u,full\ assemblage}$), the material yield and ultimate stresses were selected based on the material data sheets for the experiment detailed in Chapter 3 ($F_{y,brace}$ = 444MPa, $F_{u,brace}$ = 500MPa, $F_{y,plate}$ = 375MPa, $F_{u,plate}$ = 464MPa). The loads were calculated for a 3082 mm 102x102x6.4 HSS section with varying hinge plate dimensions. The theoretical buckling load of the brace ($P_{cr,brace}$) was found using the same yield strength as the model and assuming a Class H section due to the model not incorporating residual stresses. An estimated value of K for the theoretical buckling load was based on the relative moment resistances of the brace and the hinge plate, as shown in Figure 2.10 (Takeuchi and Matsui 2015). This theoretical buckling load was compared to a FE model that only included the brace and hinge plate, and that was loaded concentrically. Good agreement was found between the theoretical and FE results, as shown in Table 2.1. The ultimate compressive resistance of the eccentric splice connection was calculated using Equation 2.1, which is adapted from the procedure outlined in AISC Design Guide 24 for the compressive strength of single sided shear splice connections for HSS members (Packer

et al. 2010). In this equation, P_u is the axial strength of the connection, P_r is the compressive resistance of the thinner splice plate with an effective length of 1.2 times the length of the connection, M_u is the ultimate moment, which is taken as half of P_u times the connection eccentricity, and M_r is the plastic flexural capacity of the thinner plate.

$$\frac{P_u}{P_r} + \left(\frac{8}{9}\right)\left(\frac{M_u}{M_r}\right) = 1 \tag{2.1}$$

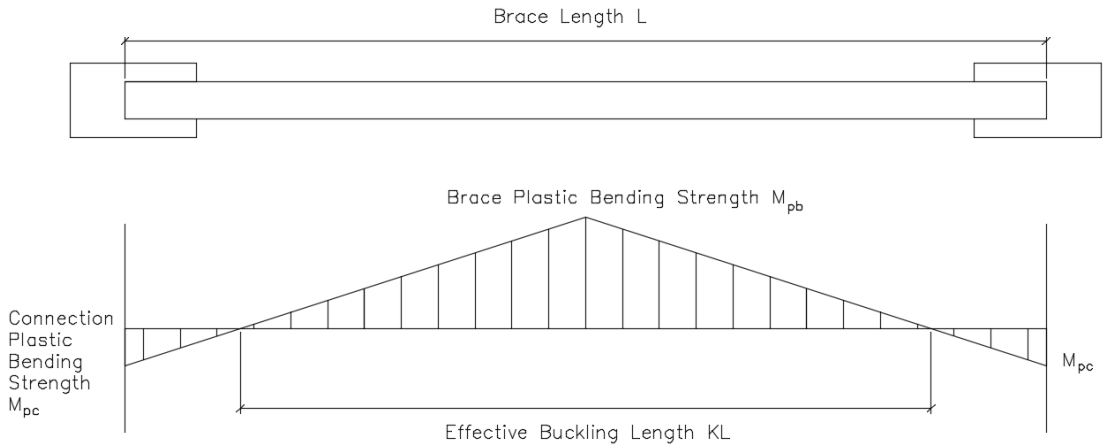

Figure 2.10: Determination of effective buckling length factor K

The results of the FE model ($P_{u,full\ assemblage}$) are compared to the theoretical calculations in Table 2.1. The hinge plate thickness of 25 mm was chosen because, according Equation 2.1, it was capable of reaching the critical buckling load of the brace with a K value of 1, the value typically assumed for a CBF. The FE model demonstrated that it could reach this load and brace buckling was the governing failure mode. The FE model and Equation 1 also agreed well for the thinnest plate considered, with connection failure occurring near the predicted value. The FE model and Equation 2.1 do not agree well for the intermediate plate thicknesses, with the variation of $P_{u,full\ assemblage}$ being more proportional to the brace buckling

strength than the connection strength. This inconsistency between the predicted strength and the actual strength remains true for other methods of calculating the connection strength (Fang et al. 2015, Davaran et al. 2015).

Table 2.1: FE and theoretical compressive strength for HSS 102x102x6.4 with varying hinge plate thicknesses

Hinge Plate Thickness	K	$P_{cr,brace}$ (Theory)	$P_{cr,brace}$ (FE)	$P_{u,connection}$ (Eq. 1)	$P_{u,full\_assemblage}$ (FE)	Failure Mode
25	0.75	850	864	673	640	Brace Buckling
22	0.80	805	810	567	608	Brace Buckling
19	0.84	767	776	464	585	Brace Buckling
16	0.88	730	740	364	345	Connection Failure
~	1.00	620	627	~	~	~

These results are typical of what was found for the eight specimens that were eventually tested, and they suggested that the connection would achieve the desired failure hierarchy, but that improved guidance for determining the connection strength may be necessary.

2.4 Conclusions

This chapter documents the development of a novel replaceable connection for the seismic design of concentrically braced frames. The objectives of the proposed new design were listed and some early design iterations were discussed and evaluated. The proposed new design was presented and the results of a preliminary finite element model were analyzed. The proposed new connection is expected to be easy to install, easy to replace if damaged, and to cause the brace to buckle in plane, thereby avoiding damage to exterior cladding. The FE model verified that the connection confines yielding to the easily replaceable components.

Chapter 3: Experimental Testing of the New Connection

3.1 Experimental Program

To verify that the new connection design could satisfy the desired criteria, an experimental program was performed to assess the connection's performance and failure behaviour under quasi-static cyclic uniaxial loading. The dimensions of the test represented a 3/4 scale of a reference structure designed to resist the seismic demands in Vancouver, British Columbia. Figure 3.1 shows the reference structure and Figure 3.2 shows the scaled second storey braced bay. For this experiment, the tested region consisted of the brace and the new connection, with angled supports to represent the boundary condition of the beam. Figure 3.3 shows a typical experiment setup for the HSS brace specimens that were tested. The angled supports at either end of the brace were reused for all tests of the same connection type.

Load was applied to the specimen using an actuator bolted to one of the angled supports and secured to the strong floor. The loading was applied cyclically and quasi-statically following the ATC-24 testing protocol (ATC 1992). The displacement for each cycle was applied in increments of yield drift (Δ_y), defined as the expected drift at which first buckling occurs. If the brace did not fracture by the end of the protocol shown in Figure 3.4, paired cycles at +1 Δ_y relative to the previous displacement were performed until failure.

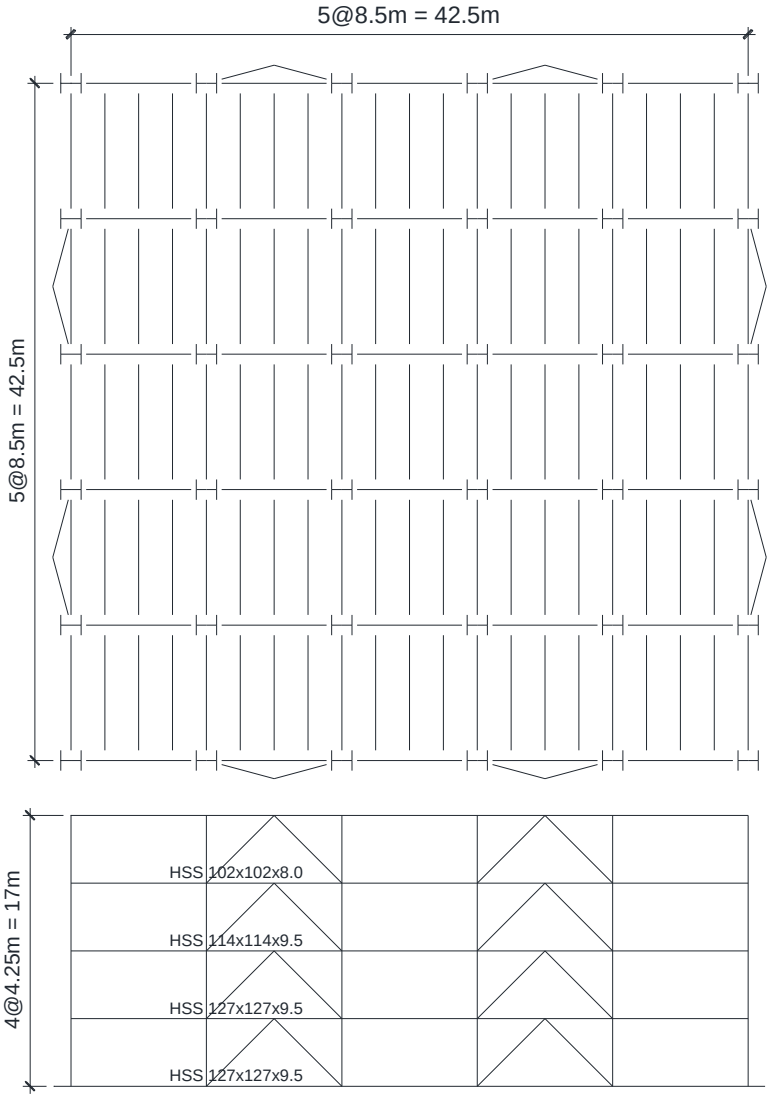

Figure 3.1: Reference Structure in Vancouver, BC

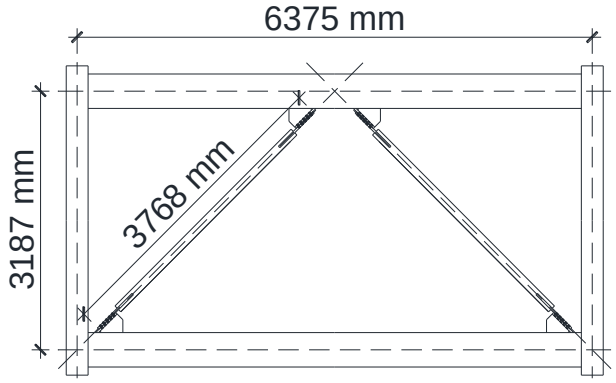

Figure 3.2: Scaled frame dimensions for selecting brace size

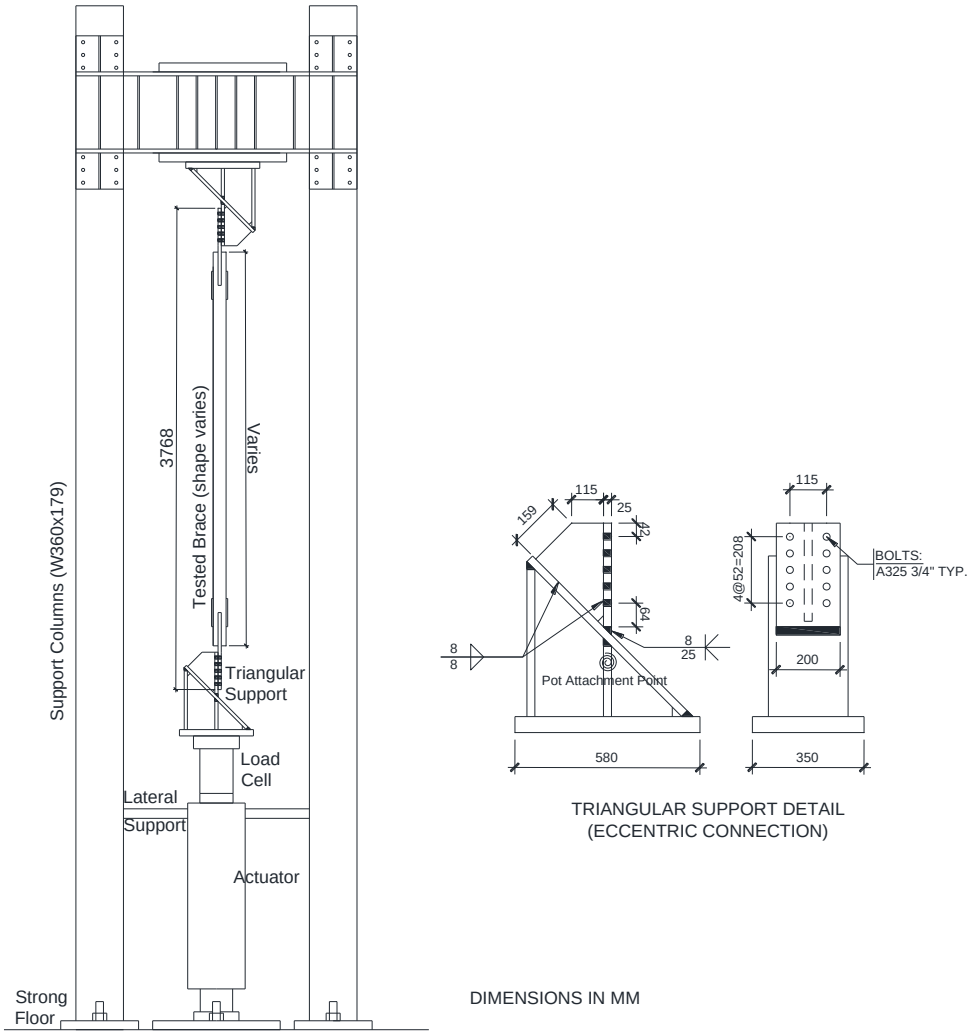

Figure 3.3: Typical Experimental Setup

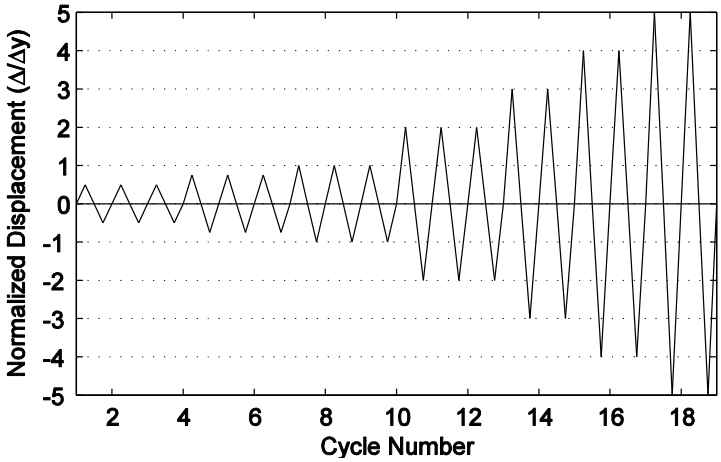

Figure 3.4: Loading Protocol

3.2 Test Specimens

Eight cold-formed HSS braces were tested for this experimental program. The distance between connection ends was kept constant between all specimens (3768 mm) and the brace lengths were adjusted according to the length of each connection. Five braces were tested with the Eccentric (Type E) connection and three braces were tested with the Concentric (Type C) connection. All specimens were designed to satisfy the requirements for moderately ductile concentrically braced frames in the CSA S16-14 seismic provisions (CSA 2014). The bolted connections of all specimens used ¾" A325 bolts that were pretensioned to 70% of their expected tensile loading using a torque wrench, but were not designed for a specified slip load. This was done because designing the connections as slip-critical would have required significantly more bolts, resulting in a much longer connection and shorter brace, thereby reducing the energy dissipation capacity of the brace.

Table 3.1 summarizes key parameters of the test specimens, including the brace shape, the connection type, the brace yield (F_y) and ultimate stress (F_u), actual brace lengths, and key connection dimensions. The hinge length, defined as the distance between the brace end and the end of the support plate in connection type E and the end of the splice plate in connection type C, was typically designed to be two times the hinge plate thickness to align with previous recommendations for gusset plates (Astaneh-Asl et al. 1985). The hinge plate thickness was designed to provide sufficient tensile resistance along the first line of bolts for the full capacity of the brace. In addition, the hinge plates of connection type E were designed to account for the eccentricity present in the connection as recommended by AISC Design Guide 24 for the compressive strength of single sided shear splice connections for

HSS members (Packer et al. 2010). The hinge plate thickness was selected to satisfy the constraint:

$$\frac{P}{P_u} + \left(\frac{8}{9}\right)\left(\frac{M}{M_u}\right) < 1 \tag{3.1}$$

where P is the axial force in the connection, P_u is the available strength in axial compression of the thinner splice plate with an effective length of 1.2 times the length of the connection, M is the moment in the connection, which is taken as P times half the connection eccentricity, and M_u is the plastic flexural capacity of the thinner plate. This resulted in hinge plates that were 14%-24% thicker than if eccentricity had not been considered.

Table 3.1: Test Specimens

Specimen	HSS Square Brace Shape	Connection Type	F_y (MPa)	F_u (MPa)	Brace Length (mm)	Hinge Plate Thickness (mm)	Hinge Length (mm)	Splice Plate Thickness (mm)
E-1	102x102x6.4	Eccentric	444	501	3082	25	50	-
E-2	89x89x8.0	Eccentric	513	578	3096	22	44	-
E-3	89x89x6.4	Eccentric	458	531	3200	19	38	-
E-4	102x102x6.4	Eccentric	444	501	3034	25	75	-
E-5	102x102x6.4	Eccentric	444	501	3108	19	38	-
C-1	102x102x6.4	Concentric	444	501	2863	19	44	16
C-2	89x89x8.0	Concentric	513	578	2886	19	38	16
C-3	89x89x6.4	Concentric	458	531	3105	16	32	10

Specimens E-1, E-2 and E-3 were three different brace sizes with the eccentric connection. Specimens C-1, C-2 and C-3 were the same three brace sizes but with the concentric connection instead. Specimen E-4 was the same as E-1 except that a larger hinge length of three times the hinge plate thickness was used. Specimen E-5 was not designed to account for the eccentricity in the connection and therefore had a hinge plate that was 24% thinner than the hinge plate of E-1.

3.3 Experimental Results

The following sections discuss the experimental results in terms of the yield and failure progression, the measured drift and force capacities, and the bolt slip behaviour. The loads were measured using a load cell connected to the head of the actuator. The displacements were measured using a string potentiometer attached to just below the support plates on either end of the test assemblage, as seen in Figure 3.3, which corresponds to the just under the beam flange of the reference frame. The displacements were converted to an equivalent storey drift based on the scaled design building used to select the braces, with a 1% drift corresponding to a 23 mm axial displacement as measured by the potentiometer.

3.3.1 Yield and Failure Behaviour

All eight tested specimens experienced yielding and failure only in the intended locations. The initial yield mechanism was brace buckling, followed by brace tensile yielding and hinge plate yielding to allow more significant brace buckling under compression. Severe buckling of the brace when loaded in compression caused local buckling to occur near midlength of the brace, which led to tears forming in the corners of the HSS under tension loading. These tears then extended to cause complete fracture of the brace in tension, as seen in Figure 3.5. This is consistent with the failure behaviour observed with more conventional gusset plate connections (e.g. Roeder et al. 2011).

(a) (b) (c)

Figure 3.5: Specimen E-1: (a) Local buckling; (b) Tearing; (c) Fracture

For braces with the eccentric connection, the location of hinge plate yielding varied depending on the end of the brace and the direction of buckling. Figure 3.6 shows an example of this asymmetrical hinge plate yielding. The hinge plate at the top rotated towards the support plate, confining yielding to the region between the brace end and the support plate. Yielding in the bottom plate was spread over a larger area, with the most significant yielding occurring along the first row of bolts. Despite hinging occurring along the bolt line, no tears or unintended damage developed in the hinge plate of any of the eccentric brace specimens, including the thin hinge plate of specimen E-5.

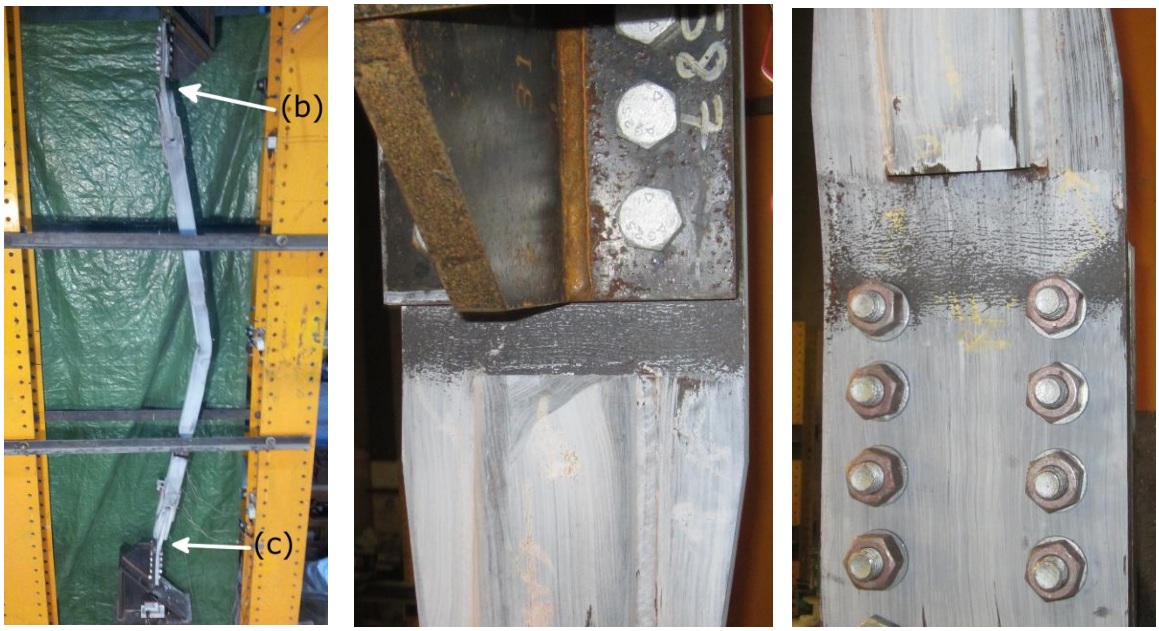

(a) (b) (c)

Figure 3.6: Eccentric hinge yield lines: (a) buckling direction; (b) top hinge; (c) bottom hinge

For braces tested with the concentric connection, end rotation was typically confined to the hinge plate. However, one end of specimen C-3 had rotation and yielding appear first in the splice plates, starting at 1% drift. Minor yielding became visible in the hinge plate at 1.6% drift, and at larger drifts the rotation occurred primarily in the hinge plate. Figure 3.7 compares the yielding of the splice plates in specimen C-3 with the desire hinge plate behaviour of the concentric connection. Although the appearance of two plastic hinges within the connection did not lead to undesirable results in this case, it was not considered acceptable because it could have led to deformation concentrating in the connection rather than the brace.

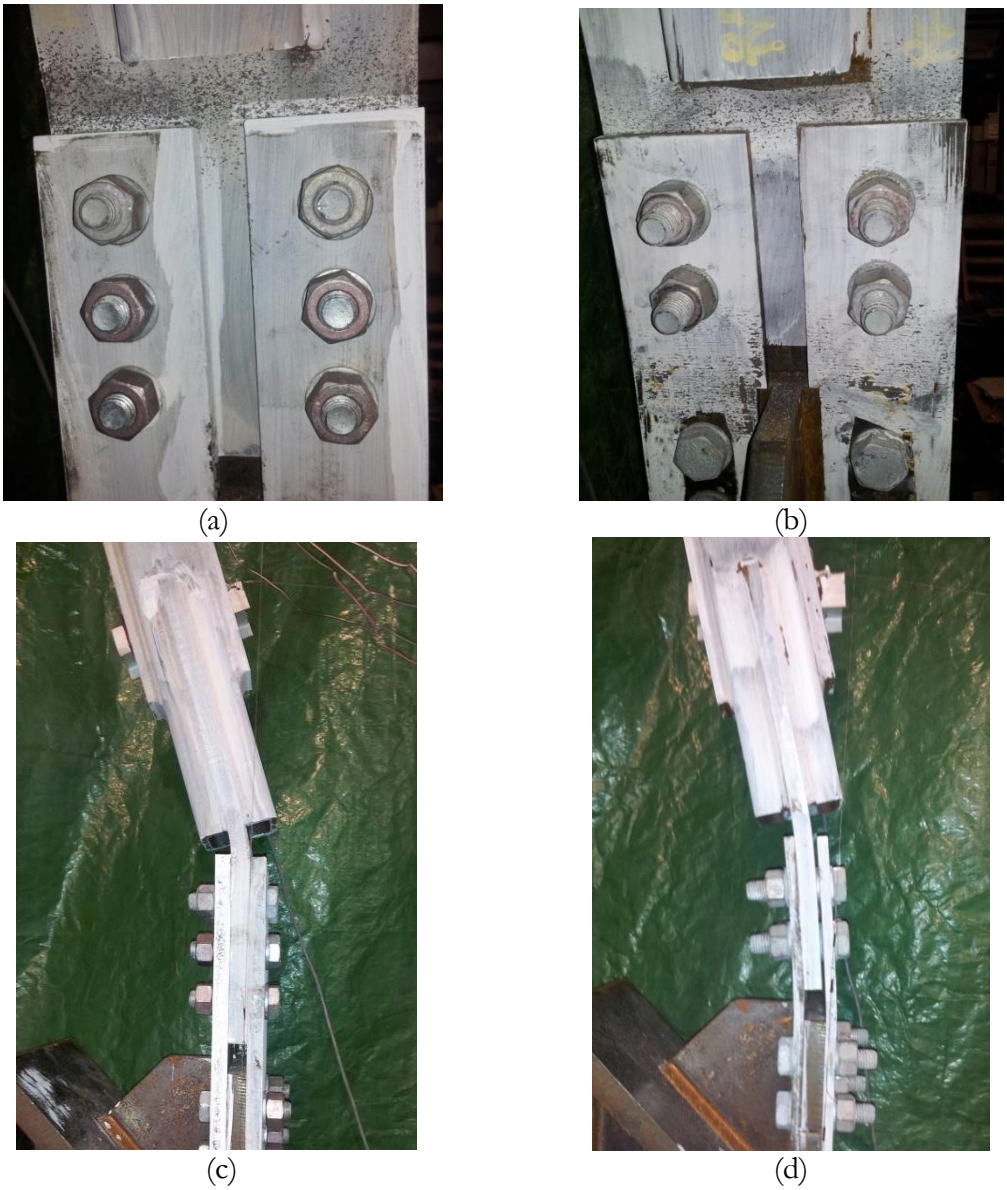

Figure 3.7: Concentric hinge behaviour: (a) Single hinge line (C-1); (b) Multiple hinge lines (C-3); (c) Profile with single hinge (C-1); (d) Profile with multiple hinges (C-3)

3.3.2 Drift and Force Capacity

Figure 3.8 shows the load-displacement curves of the eight specimens tested in the experimental program. All of the tested specimens reached at least the 18th load cycle shown in Figure 3.4. The maximum drift ranges, shown in Table 3.2, varied from 3.3% to 6.4%, which was within the expected range of traditional gusset plate connections (Roeder et al. 2011). The drift range of each test specimen was primarily influenced by the brace shape used. Specimens using the HSS102x102x6.4 section (E-1, E-4, E-5, C-1) all had drift ranges of 3.3% to 3.4%, the smallest of all brace shapes tested. The HSS 89x89x6.4 specimens E-3 and C-3 had drift ranges of 5.4% and 5.1%, respectively. The variation in drift range between different brace shapes was mostly related to how quickly local buckling occurred in the midlength plastic hinge of the brace, which is heavily influenced by the local slenderness of the brace, as seen in previous experiments (e.g. Han et al. 2007). Very similar drift ranges were found between specimens with the same brace type but different connections (E-1, E-4, E-5 and C-1, E-2 and C-2, E-3 and C-3). Although the HSS 89x89x8 specimens E-2 and C-2 had the largest drift ranges of 5.9% and 6.4% respectively, this may have been influenced by the tension load on these specimens being limited by the actuator capacity.

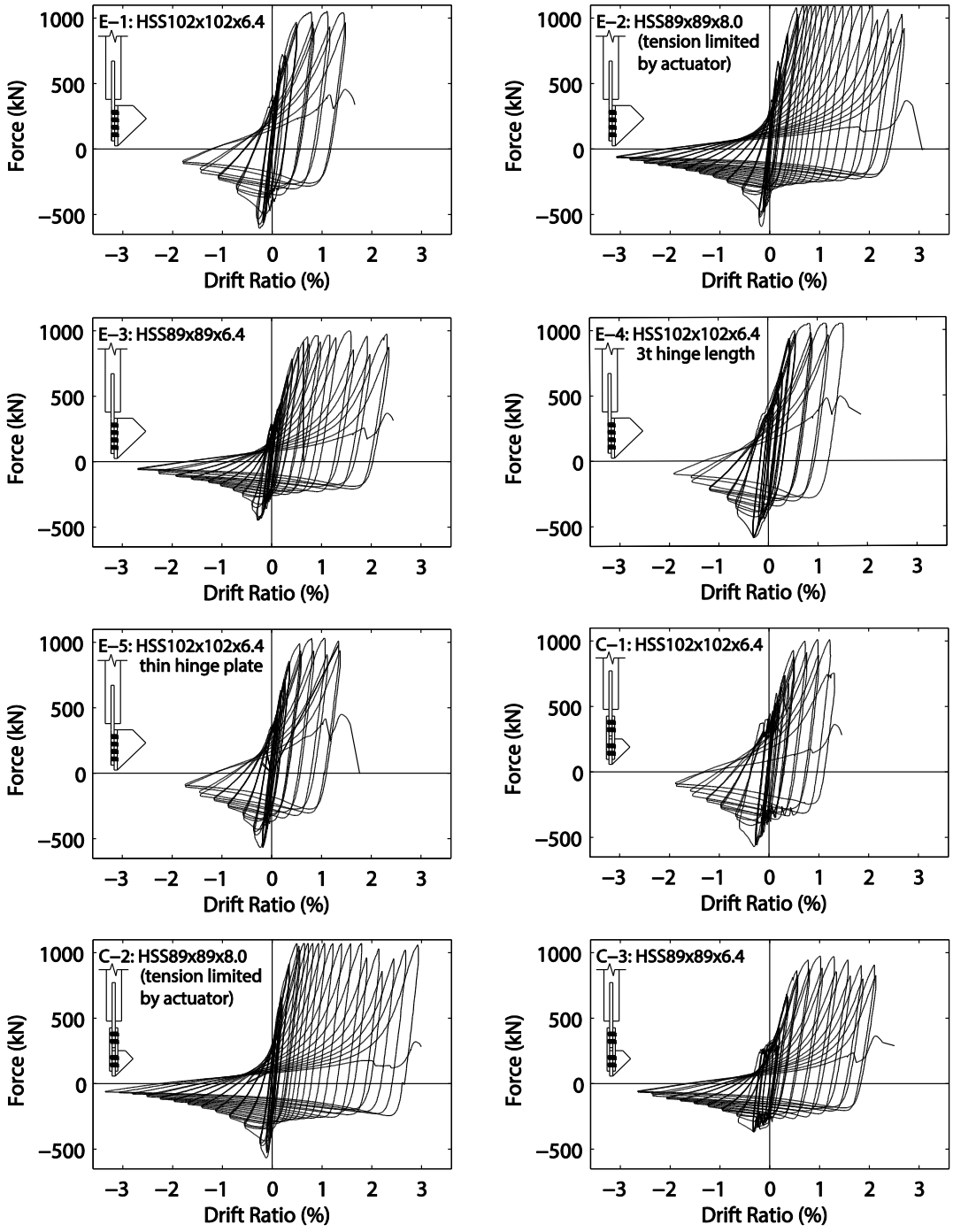

Figure 3.8: Experimental load-displacement curves for all specimens

The braces and connections of all specimens sustained the anticipated tension and compression forces before ultimate failure of the brace. The maximum predicted and measured tension and compression values for each test are shown in Table 3.2. The predicted tensile resistance, T_r, was calculated as A_gF_y where A_g is the gross area of the brace. The maximum tension forces in the experiment, T_{max}, were typically within 10% of the expected yield values, except for specimens E-2 and C-2, which used the same brace section and in which tension forces were limited by the actuator capacity.

Table 3.2: Summarized Test Results

	Drift (%)			Peak Tension Forces		Peak Compression Forces				Slip Loads (kN)	
Specimen	Min	Max	Range	T_r	T_{max}	C_r (K=1)	C_{max}	K_t	K_e	Predicted	Actual[a]
E-1	-1.8	+1.6	3.4	1030	1047	-494	-605	0.77	0.84	374	370
E-2	-3.1	+2.8	5.9	1236	1091[b]	-420	-592	0.81	0.78	374	375
E-3	-2.7	+2.4	5.1	911	1000	-337	-451	0.81	0.80	299	285
E-4	-1.9	+1.5	3.4	1030	1052	-501	-590	0.77	0.86	374	445
E-5	-1.8	+1.5	3.3	1030	1031	-490	-569	0.85	0.88	374	360
C-1	-1.9	+1.4	3.3	1030	1011	-540	-572	0.85	0.94	449	340
C-2	-3.4	+3.0	6.4	1236	1067[b]	-467	-568	0.85	0.87	449	555
C-3	-2.7	+2.2	4.9	911	975	-349	-371	0.86	0.95	299	260

[a]Average of slip loads after initial slip
[b]Limited by actuator

The predicted compression resistance, C_r, was calculated using the flexural buckling equation from S16-14 with n being 1.34 for a cold formed HSS and KL being the length between hinge zones (K=1), as recommended in the CISC Commentary of S16-14 and previous research (CSA 2014, Tremblay et al. 2003). A theoretical effective length factor, K_t, was also calculated using the relative plastic moment capacities of the brace and hinge plates as seen in Equation 3.2 (Takeuchi & Matsui 2015) where M_{ph} is the plastic moment capacity of the hinge plate and M_{pb} is the plastic moment capacity of the brace:

$$K_t = \frac{1}{1+\left(\frac{M_{ph}}{M_{pb}}\right)} \quad (3.2)$$

The maximum recorded compression forces, C_{max}, were 6%-40% larger than the estimated compressive resistance found when using KL equal to the length between hinge zones. However, experimentally derived effective length factors, K_e, were within 12% of the effective length calculated using equation 3.2 (K_t). All specimens with the concentric connection (C-1, C-2 and C-3) had a lower compression force than the same brace size with the eccentric connection (E-1, E-2 and E-3), despite having a shorter brace length. The reduced compressive strength resulted from the increased connection flexibility caused by the splice plates, even in specimens C-1 and C-2, which had plastic rotation only in the hinge plate (Figure 3.7(a)). Specimen C-3 had a maximum compressive force 18% smaller than E-3 due to the early yield of the splice plates at one end, which greatly increased the flexibility in the connection. If early yield had occurred in the splice plates at both ends, brace buckling might not have occurred, with inelastic deformation concentrating in the connection instead. Specimen E-5, which used a thin hinge plate, had a peak compressive load only slightly smaller than Specimen E-1 and did not have its compressive strength limited by the connection strength. The support plates provided sufficient fixity to the connection to prevent the connection failure modes found in standard lap splice connections in compression (Davaran et al. 2015). This indicates that designing the hinge plate of the eccentric connection to resist the additional moment due to the eccentricity was unnecessarily conservative.

3.3.3 Bolt Slip

Due to the bolted connections of the tested specimens being designed only for strength, bolt slip appeared during the experiment. Initial bolt slip typically occurred before initial brace buckling and at a load greater than the predicted slip load of the connection (see Table 3.2), which was calculated using the formula for bolt slip in S16-14 assuming a clean mill scale surface (CSA 2014). Slip continued in pre-yield cycles but generally in smaller increments and at lower loads than the initial slip, the average load of which is shown in Table 3.2. However, bolt slip diminished and eventually stopped occurring after the brace compressive strength degraded to less than the slip load after the first several post-buckling cycles, as seen in Figure 3.9(a). After this, the compressive load no longer exceeded the residual slip load and the connection remained fully slipped in the tensile direction. This meant that slip did not continue to affect the hysteretic response beyond 0.2% to 0.4% drift, as seen in the full specimen hystereses in Figure 3.8. Despite multiple instances of slip occurring in each direction, the hinge and support plates were sufficiently thick to prevent noticeable deformation of the bolt hole. Bolt slip was larger in specimens with the concentric connection because there was an additional bolted shear transfer at each brace end. Figure 3.9(b) is an example of this larger slip compared to the equivalent eccentrically connected brace in Figure 3.9(a). Nevertheless, even with this connection, the slip did not affect the hysteretic response beyond the low drift levels.

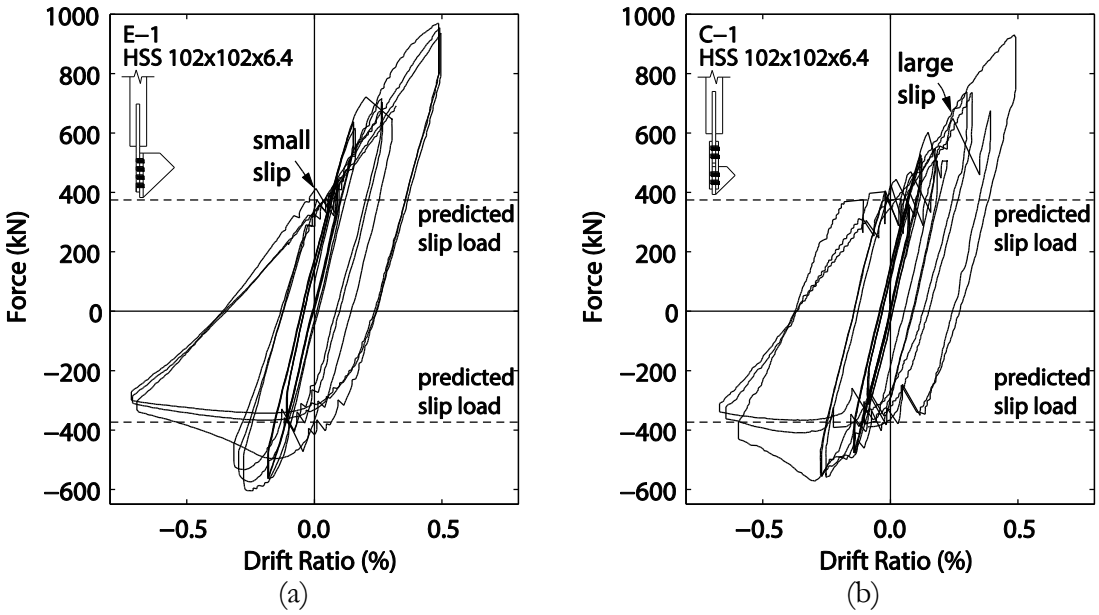

Figure 3.9: Bolt slip comparison: (a) Eccentric connection; (b) Concentric connection

3.4 Conclusions

An experimental study of eight different braces was conducted using the new replaceable connection. The study focused on the yielding and failure behaviour of the brace and hinge plate of the new connection without considering frame effects. The study found that:

1. All braces tested with the new connection failed in the intended manner, with significant yielding occurring at the center and ends of the replaceable brace module before ultimate failure in the brace. The brace performance was primarily influenced by the brace shape rather than connection parameters. Drift ranges were within expected values based on previous studies of more conventional gusset plate connections.
2. Eccentricity in the brace connection did not result in any undesirable yielding or failure. Additionally, designing the hinge plate for extra forces due to eccentricity was

unnecessarily conservative, provided that the support plates had sufficient rotational restraint to prevent multiple plastic hinges from forming in the connection.

3. Bolt slip had little effect on the brace hysteresis after the compressive strength of the brace decayed to less than the slip load. Bolt slip at low displacements was larger in the concentric connection than in the eccentric connection.
4. Within this experimental program, the performance of the eccentric connection was equal to or better than that of the concentric connection, with no observed negatives associated with the eccentricity in the connection, less risk of early connection failure and less bolt slip than the concentric connection. For these reasons and the improved constructability of a single splice connection, the eccentric connection is the recommended choice for further development and experimentation as an alternative connection for concentrically braced frames.

This study focused on specimens designed for a specific scaled brace bay, and the experiments were limited to testing of the brace and connection behaviour without considering the interaction with the rest of the braced frame. Future experimental testing should consider the proposed connection within a frame in order to investigate how this affects the connection performance, and to determine what design considerations are required for the beam and beam-column connections that are used with the new replaceable connection.

Chapter 4: Finite Element Modelling of Experiment Results

4.1 Model Description

The experimental behaviour of specimen E-1, detailed in Chapter 3, was simulated using the finite element modelling software package ABAQUS (Dasault Systemes 2012). The new model built on some of the ideas in the model presented in Chapter 2, but was improved to account for the full cyclic behaviour of the experimental test. Figure 4.1 shows the region that was modelled, which included the full brace, hinge plate, bolts, and the support plates. Boundary conditions and displacement controlled loading were applied uniformly at the bottom surfaces of the support plates at either end. The brace was modelled using 4-noded quadrilateral shell elements with five integrations points along the thickness. A dense mesh with an aspect ratio of 1 was used in the midspan and connection regions of the brace to better capture the nonlinear behaviour in these regions. The hinge and support plates were modelled using 8-noded brick elements with 4 elements along the thickness. The bolts were modelled using a combination of 8-noded brick and 6-noded wedge elements to ensure a symmetrical mesh throughout the bolt. The material model for the brace and plates was a combined nonlinear isotropic and kinematic hardening model that used the yield stress of the tested material along with isotropic and kinematic constants from previous experiments of cold formed brace steel (Nip et al. 2010) and hot rolled plate steel (Korzekwa and Tremblay 2009) with similar yield and ultimate failure properties to the tested specimen. A summary of the material parameters is shown in Table 4.1.

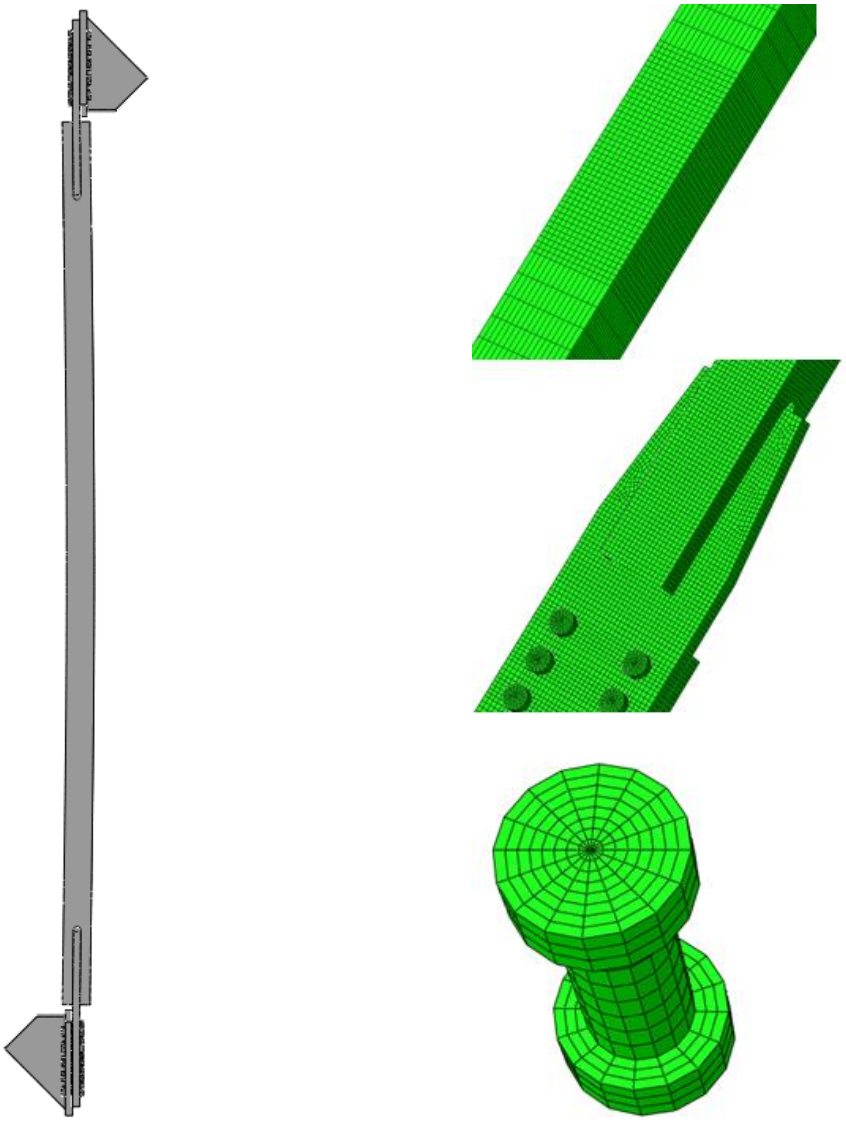

(a) (b)

Figure 4.1: Finite element model of specimen E-1: (a) Full view; (b) Meshed Regions

Table 4.1: Finite element model material properties

	Brace Steel	Plate Steel
Yield Stress at zero plastic Strain σ (MPa)	353	350
Isotropic hardening constant, Q (MPa)	35.9	110
Isotropic hardening rate, b	1.47	4
Kinematic hardening constant, C (MPa)	82500	8000
Kinematic hardening rate, γ	700	75

These material parameters are combined by the following two equations to determine the isotropic stress (σ_i) and kinematic stress (σ_p) of the material at different plastic strains (ε_p).

$$\sigma_i = Q\left(1 - e^{-b\epsilon_p}\right) \tag{4.1}$$

$$\sigma_k = \frac{C}{\gamma}(1 - e^{-\gamma\epsilon_p}) \tag{4.2}$$

A monotonic stress strain curve of the brace material model stress-strain curve is shown in Figure 4.2. The 0.2% offset line to determine yield stress is also shown and intersects with the brace material model at a value (449MPa) approximately equal to the brace yield strength for specimen E-1 (444 MPa) shown in Table 3.1.

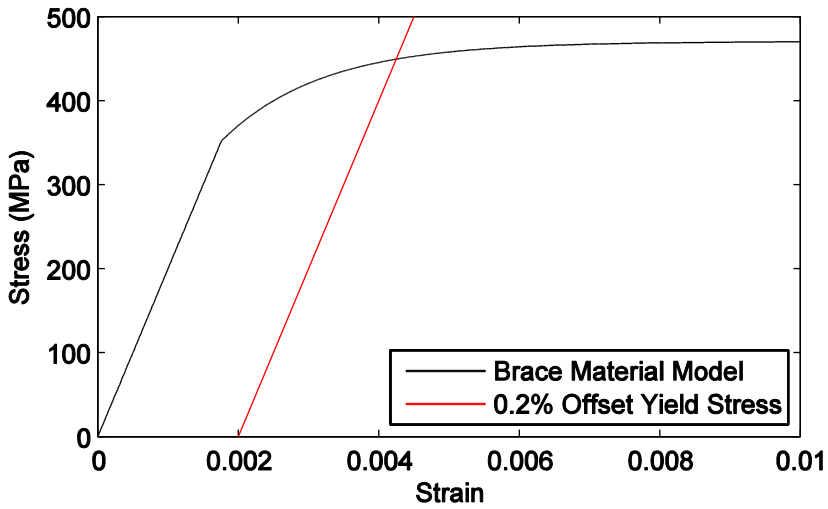

Figure 4.2: Brace material model

Hard contact rules were applied in the normal direction of all points of contact between the hinge plates, support plates and bolts. The tangential contact between the bolt shank and bolt hole was kept frictionless while all other tangential contacts between the bolt heads, hinge plate and support plate used a friction coefficient of 0.44 applied using the penalty

method. The bolts and their associated holes were modelled as the same diameter, meaning no large displacement slip occurs during loading. Each bolt was pretensioned to 70% of their expected tensile resistance at the start of the analysis.

A 0.1% imperfection in the shape of the first buckling mode was introduced into the model to allow for the initiation of buckling. The cyclic displacement was applied uniaxially and statically through the support plates at one end of the model while all other support plate end translational degrees of freedom remained fixed. The displacement history was selected to best match the actual displacement experienced by the brace assembly during testing and accounting for the lack of large displacement slip in the model.

4.2 Model Results

The load vs brace axial displacement curve of the finite element model superimposed on the experimental results is shown in Figure 4.3. The brace axial displacement was chosen as the comparison value because bolt slip did not occur in the finite element model and so measuring by the brace deformation kept consistency between the experimental and numerical results. The model shows good agreement with the experimental results. Peak compression and tension loads are close to the experimental values and overall behaviour is aligned well with the experiment.

The model exhibits high plastic strains in the same regions seen in the experiment. Different hinge lines formed at either end of the brace (Figure 4.4) as was observed during the experiment (Figure 4.5). The model confirms that there is a more concentrated plastic strain demand in the connection hinge that bends towards the support plates than in the

connection hinge that bends away. The shell elements in the brace sufficiently capture the inelastic local buckling and cupping of the brace midspan as shown in Figure 4.6. The centre of the midspan plastic hinge was 20 mm away from the exact centre of the brace due to the different hinge behaviour at either end of the brace. This was similar to the difference between the midspan and plastic hinge during the experiment.

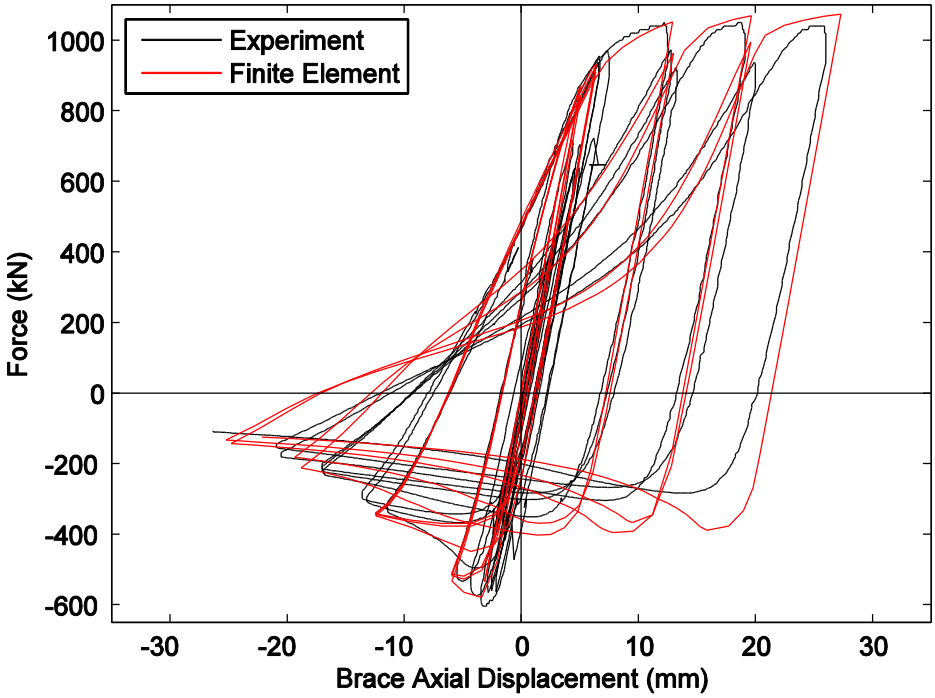

Figure 4.3: Experimental and finite element load-displacement curves for Specimen E-1

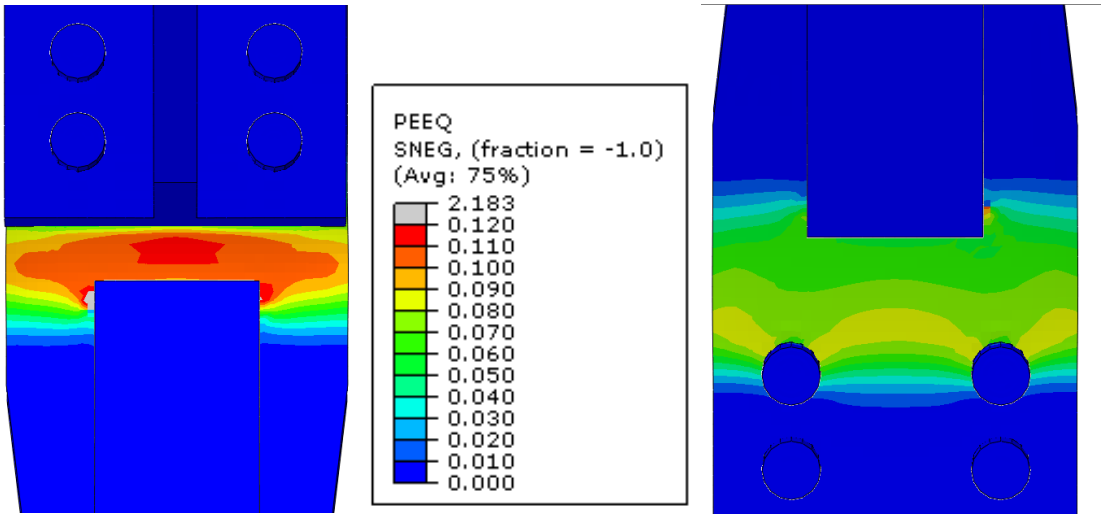

(a) (b)

Figure 4.4: Equivalent plastic strain at -1.8% drift: (a) Top Hinge; (b): Bottom Hinge

(a) (b)

Figure 4.5: Plastic yielding from experiment: (a) Top Hinge; (b): Bottom Hinge

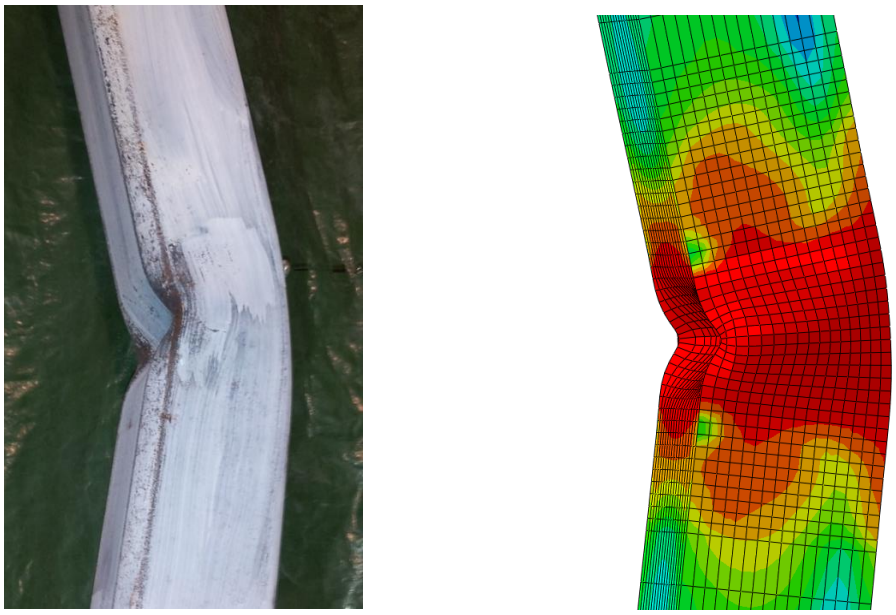

(a) (b)

Figure 4.6: Midspan cupping at -1.8% drift: (a) Experiment (b): Stress distribution of FEM

4.3 Conclusions

A finite element model was created in ABAQUS to simulate the behavior of Specimen E-1 from the experimental testing of the new connection. The model was an improved version of the model presented in Chapter 2 that was altered to model the full cyclic loading and the strength deterioration of the specimen after multiple post-yielding cycles. The model was able to replicate the yielding and hysteretic behaviour seen during the experiment. Future development of the model should focus on modelling all of the specimens tested during the experiment and using those results to test brace angles, sizes, and connection parameters that were not fully investigated during the experiment. The model could also be adapted to test the connection performance within a full braced frame.

Chapter 5: Conclusions and Future Research

5.1 Summary

This thesis proposed a new connection for the seismic design of steel concentrically braced frames with HSS braces. The new connection was designed to be cheaper and easier to install than a traditional gusset plate connection by replacing field welding with more economical field bolting. The bolted connection was designed to confine damage within easily replaceable components in the event of a major earthquake, lowering the cost of repairs and reducing the length of time before the structure can be reoccupied. Finally, the new connection was designed to allow buckling to occur in-plane, preventing damage to exterior cladding that could pose a danger to pedestrians and people evacuating the building.

The design of the connection required multiple iterations that drew influence from previous research into bolted splice connections and in-plane buckling designs. A connection type with two variations, one with an eccentric single splice connection, and the other with a concentric double lap splice connection, was selected for detailed development. A preliminary finite element model of the new connection was developed to assess some connection design parameters that would need to be considered with the new connection.

Large scale experimental testing the new connection was performed at the Applied Dynamics Laboratory at McMaster University. The test consisted of quasi-static cyclic testing on braces fitted with the new connection. Both connection variants and three different brace sizes were included in the eight specimens tested. Braces were repeatedly cycled until fracture and comparisons were made between specimens. The performance parameters of interest were

the maximum drift range of the samples, the load capacity and the observed progression of yielding and failure that occurred in the brace and the connection.

Using results from the experiment, the finite element model was further refined and developed. The finite element model explicitly modelled the bolted connection and incorporated nonlinear isotropic and kinematic hardening models to capture the behaviour of the brace during cyclic loading. The finite element model was able to replicate the results of the experiment reasonably well and could be used to perform a larger, parametric study of the new connection behaviour.

5.2 Conclusions

The connection design that was developed and tested was capable of meeting the three objectives proposed at the start of the research program: It can be bolted into place and easily replaced in the event of damage to the brace, it allows buckling to occur in-plane, and it performed under cyclic loading in the manner required for use within seismically designed concentrically braced frames and consistent with previous testing of other connection details.

Both iterations of the finite element model and the results of the finite element model indicate that the new connection type is not as susceptible to multiple plastic hinges forming within the connection as seen in previous research on bolted splice connections between HSS braces and gusset plates. The stiff support plates confine plastic hinging to the easily replaceable hinge plates and ensure that ductile buckling of the brace occurs before any connection failure. The testing and the preliminary model both demonstrated that designing

for beam-column effects due to eccentricity in the bolted connection is unnecessarily conservative.

From the results of the experimental testing and the observations made during concept development, the eccentric variation of the new connection design is the preferred choice. The eccentric connection is more compact and easier to install than an equivalent concentrically designed connection. During testing, the concentric connection was shown to be more susceptible to forming multiple plastic hinges within the connection and experienced much larger bolt slips. In addition, the experimental study demonstrated no negatives associated with the eccentricity present in the eccentric connection.

5.3 Future Research

The experimental and numerical research of the new connection has thus far been limited to quasi-static cyclic loading of a brace and connection assembly, and a limited range of brace lengths and shapes that have been designed to fit within a chevron braced frame. The finite element model developed during this research should be used within a full parametric study to determine the impacts the new connection has under a range of brace length shapes, and orientations. Developing models and experiments that represent the brace behaviour within a full braced frame assembly will help investigate issues of high beam forces and beam-column connection flexibility when compared to other connections. This will help to determine if designers can use simple shear connections between beam and column or if moment resisting connections are necessary. Finally, dynamic testing will help to evaluate if bolt slip, which had minimal impact on the quasi static hysteretic behaviour of the brace, would present issues under certain earthquake ground motions.

References

AIR Worldwide (2013). "Study of Impact and the Insurance and Economic Cost of a Major Earthquake in British Columbia and Ontario/Quebec."

American Institute of Steel Construction (AISC) (2010). "Seismic Provisions for Structural Steel Buildings. ANSI/AISC 341-10." Chicago, United States.

American Institute of Steel Construction (AISC) (2015). "Vertical Bracing Corner Connections." American Institute of Steel Construction, webinar, Chicago, United States.

Applied Technology Council (ATC) (1992). "Guidelines for cyclic seismic testing of components of steel structures." ATC 24.

Astaneh-Asl A., Goel S., Hanson R. (1985). "Cyclic out-of-plane buckling of double-angle bracing," *Journal of Structural Engineering*, 111(5), 1135-1153.

Black R., Wenger W., Popov E. (1980). "Inelastic buckling of steel struts under cyclic load reversals." Earthquake Engineering Research Center, University of California, Berkeley, CA, Tech. Rep. UCB/EERC Report No. 80-40, 1980.

Canadian Standards Association (CSA) (2014). "Limit States Design of Steel Structures." *CSA Standard S16-14*, Rexdale, Canada.

Canterbury Earthquake Recovery Authority (2012). "Christchurch Central Recovery Plan."

Chou, C.C. Chen, P.J. (2009). "Compressive behavior of central gusset plate connections for a buckling-restrained braced frame." *Journal of Constructional Steel Research*, 65, 1138-1148.

Dassault Systemes Simulia Corp. (2012). "ABAQUS Analysis User's Manual." Simulia DCS, Providence, RI, US.

Davaran, A., Hoveidae, N. (2009). "Effect of mid-connection detail on the behavior of cross-bracing systems." *Journal of Constructional Steel Research*, 65, 985-990.

Davaran A., Gelinas, A., Tremblay, R. (2015). "Inelastic Buckling Analysis of Steel X-Bracing with Bolted Single Shear Lap Connections." *Journal of Structural Engineering*, 141(8), 04014204.

de Oliveira C., Packer J., Christopolous C. (2008). "Cast Steel Connectors for Circular Hollow Section Braces under Inelastic Cyclic Loading." *Journal of Structural Engineering*, 34(3), 374-383.

Fang C., Yam M.C.H., Cheng J.J., R.Zhang Y. (2015). "Compressive Strength and Behaviour of Gusset Plate Connections with Single-Sided Splice Members." *Journal of Constructional Steel Research*, 106, 166-183.

Gross J.L. and Cheok G. (1988). "Experimental Study of Gusseted Connections for Laterally Braced Steel Buildings" U.S. Department of Commerce, Gauthersburg, MD, US.

Haddad M. (2015). "Concentric Tubular Steel Braces Subjected to Seismic Loading: Finite Element Modeling." *Journal of Constructional Steel Research*, 104, 115-166.

Han S.W., Kim W.T., Foutch D.A. (2007). "Seismic behavior of HSS bracing members according to width-thickness ratio under symmetric cyclic loading." *Journal of Structural Engineering,* 133,(2).

Johnson S.M. (2005). "Improved Seismic Performance of Special Concentrically Brace Frames," MASc. thesis, University of Washington, Seattle, WA

Korzekwa R., Tremblay R. (2009). "Numerical simulation of the cyclic inelastic behaviour of buckling restrained braces." *International Specialty Conference on Behaviour of Steel Structures in Seismic Area (STESSA).*

Kotulka B.A. (2007). "Analysis for a Design Guide on Gusset Plates used in Special Concentrically Braced Frames." MASc thesis, University of Washington, Seattle, WA.

Lee K., Bruneau M. (2005). "Energy dissipation demand of compression members in concentrically braced frames." *Steel and Composite Structures*, 4(5), 235-358.

Lehman D., Roeder C., Herman D., Johnson S., Kotulka B. (2008). "Improved seismic performance of gusset plate connections." *Journal of Structural Engineering*, 134, 890-901.

Lope, W.A., Gwie D.S., Lauck T.W., Sanders C.M. (2004). "Structural Design and Experimental Verification of a Buckling-Restrained Braced Frame System." *Engineering Journal,* AISC, 41(4), 177–186.

Lumpkin, E.J. (2009). "Enhanced seismic performance of multi-story special concentrically braced frames using a balanced design procedure." MASc. thesis, University of Washington, Seattle, WA

Martinez-Saucedo G., Packer J.A. and Christopoulos C. (2008). "Gusset Plate Connections to Circular Hollow Section Braces under Inelastic Cyclic Loading." *Journal of Structural Engineering*, 134, 1252-1258.

National Research Council of Canada (NRCC) (2010). "National Building Code of Canada."

Nip K.., Gardner L., Davies C., Elghazouli A. (2010). "Extremely low cycle fatigue tests on structural carbon steel and stainless steel." *Journal of Constructional Steel Research,* 66, 96–110.

Packer J., Sherman D., Lecce M. (2010). "Steel Design Guide 24: Hollow Structural Section Connections." American Institute of Steel Construction, Chicago, IL, US.

Powell J. A. (2010). "Evaluation of Special Concentrically Braced Frames for Improved Seismic Performance and Constructability." MASc. thesis, University of Washington, Seattle, WA.

Roeder C.W., Lumpkin E.J., Lehman D.E. (2011). "A balanced design procedure for special concentrically braced frame connections." *Journal of Constructional Steel Research*, 67, 1760-1772.

Sabelli, Rafael, Roeder, Charles W., Hajjar, Jerome F. (2013). "Seismic design of steel special concentrically braced frame systems: A guide for practicing engineers." NEHRP Seismic Design Technical Brief No. 8, produced by the NEHRP Consultants Joint Venture, MD, NIST GCR 13-917-24.

Sen A.D., Sloat D., Pan L., Roeder C.W., Lehman D.E., Berman, J.W. (2013). "Evaluation of the Seismic Performance of Two-Story Concentrically Braced Frames with Weak Beams." *5th International Conference on Advances in Experimental Structural Engineering*, NCREE, Taipei, Taiwan.

Sen A.D., Roeder C.W., Berman J.W., Lehman D.E., Li C.H., Wu A.C., Tsai K.C. (2016). "Experimental Investigation of Chevron Concentrically Braced Frames with Yielding Beams." *Journal of Structural Engineering*, 142(12), 04016123.

Takeuchi, T., Matsui, R. (2015). "Cumulative Deformation Capacity of Steel Braces under Various Cyclic Loading Histories." *Journal of Structural Engineering*, 141(7), 04014175.

Tang X., Goel S.C. (1987). "Seismic Analysis and Design Considerations of Braced Steel Structures." Report No. UMCEE 87-04, Dept. of Civil and Environmental Eng, University of Michigan, Ann Arbor, MI

Tremblay R., Archambault M., Filiatrault A. (2003). "Seismic response of concentrically braced steel frames made with rectangular hollow bracing members." *Journal of Structural Engineering,* 129(12), 1626-1636.

Tsai C.Y., Tsai K.C., Lin P.C., Ao W.H., Roeder C.W., Mahin S.A., Lin C.H., Yu Y.J., Wang K.J., Wu A.C., Chen J.C. and Lin T.H. (2013). "Seismic Design and Hybrid Tests of a Full-Scale Three-Story Concentrically Braced Frame Using In-Plane Buckling Braces." *Earthquake Spectra*, 29 (3), 1043-1067.

Appendix A: New Connection Design Examples

This appendix contains a design example to illustrate how the new connection might be implemented within the framework of current design codes. This example will primarily use Canadian codes (NBCC-10 and S16-14) and design methods with some reference to methods used in AISC design provisions. Equations are from S16-14 (CSA, 2014) unless otherwise noted.

The design examples presented are the second storey braces of the four storey office building shown in Figure A-1, located in Vancouver, BC. The first example is of an eccentric connection design with the beam connecting to the column web by a double angle shear connection. The second example is of a concentric connection design with a moment resisting extended plate beam-column connection.

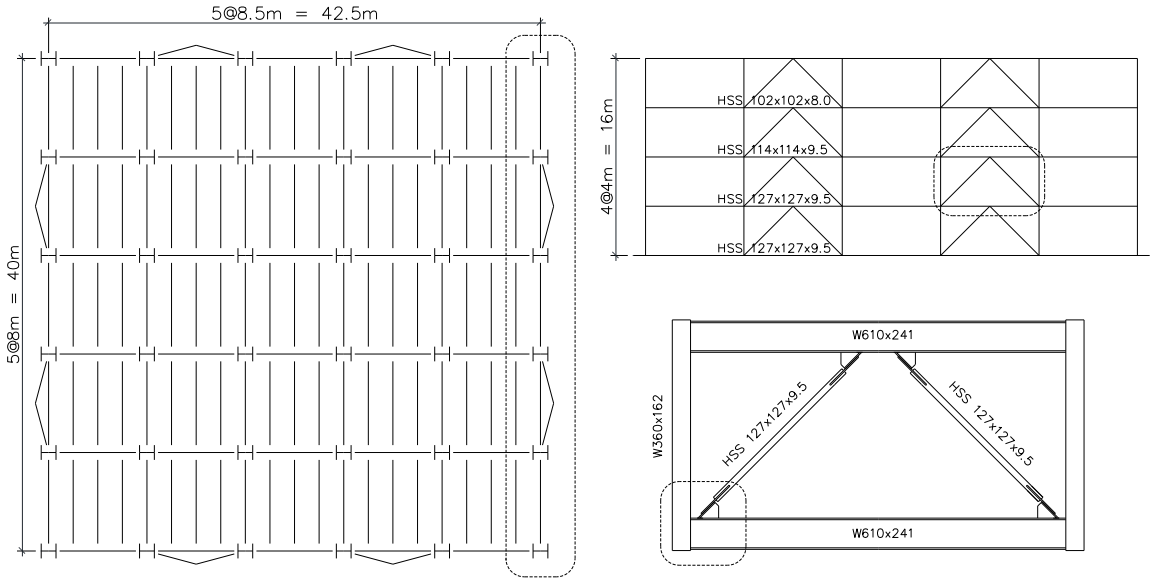

Figure A-1: Reference structure in Vancouver, BC

Example 1: Eccentric Brace to Beam Connection

The HSS 127x127x9.5 Class C brace is oriented 45° to the horizontal. The brace is connected using the new replaceable connection to a W610x241 beam which is connected to the W360x162 column by a double angle shear connection. All steel used is G40.21 350W

unless otherwise noted. All dimensions are in millimetres unless otherwise noted. The completed connection detail is shown in Figure A-2

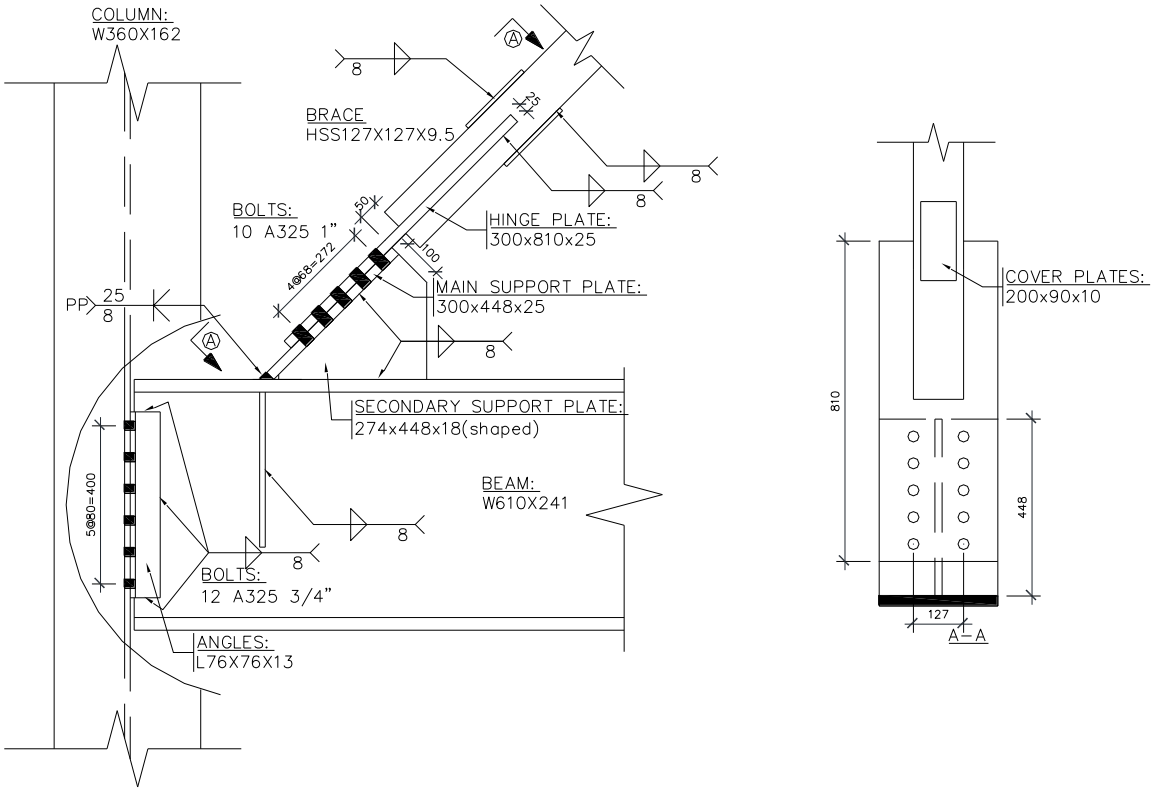

Figure A-2: Final eccentric connection design

From the 10th edition CISC *Handbook of Steel Construction* (CISC, 2010) Table 6-3, the material property is as follows:

G40.21 350W

$F_y = 350\ MPa \quad F_u = 450\ MPa$

From the CISC *Handbook of Steel Construction* (CISC, 2010) pages 6-102, 6-45 and 6-51, the geometric properties are as follows:

Brace HSS127x127x9.5

$A_g = 4240\ mm^2 \quad r = 47.5\ mm$

Beam W610x241

$d = 635\ mm \quad b = 329\ mm \quad t = 31\ mm \quad w = 17.9\ mm$

Column W360x162

$d = 364\ mm \quad b = 371\ mm \quad t = 21.8\ mm \quad w = 13.3\ mm$

Design Loads:

The required factored loads in the connection are taken from the probable brace resistances found in S16-14 Section 27.5.3.

Probable Tensile Resistance:

$$R_y F_y = 460\ MPa \tag{27.1.7}$$

$$T_u = A_g R_y F_y \tag{27.5.3.4}$$

$$T_u = (4240\ mm)(460\ MPa)$$

$$T_u = 1951\ kN$$

Probable Compressive Resistance:

The effective length used for calculating the compressive force of the brace should be based on the distance between the hinge zones. This effective length won't be determined until the connection geometry has been fully designed. A reasonable estimate for this example involves reducing the length between work points by 2 m to account for the beam depth and connection length. The n value is taken as 1.34 for a Class C brace.

$$KL = \sqrt{(4000\ mm)^2 + (4000\ mm)^2} - 2000\ mm$$

$$KL = 3657\ mm$$

$$F_e = \frac{\pi^2 E}{\left(\frac{KL}{r}\right)^2} \quad (13.3.1)$$

$$F_e = \frac{\pi^2 (200000\ MPa)}{\left(\frac{3657\ mm}{47.5\ mm}\right)^2}$$

$$F_e = 330\ MPa$$

$$\lambda = \sqrt{\frac{R_y F_y}{F_e}} \quad (13.3.1)$$

$$\lambda = \sqrt{\frac{460\ MPa}{330\ MPa}}$$

$$\lambda = 1.18$$

$$C_r = A_g R_y F_y (1 + \lambda^{2n})^{(-1/n)} \quad (13.3.1)$$

$$C_r = (4240\ mm)(460\ MPa)\left(1 + (1.18)^{2(1.34)}\right)^{(-1/1.34)}$$

$$C_r = 968\ kN$$

$$C_u = 1.2 C_r$$

$$C_u = 1162\ kN$$

After designing the connection, the actual C_u value based on a true effective length of 3788mm, is 1117 kN. The brace and connection forces under the associated peak tension and compressive forces are shown in Figure A-3.

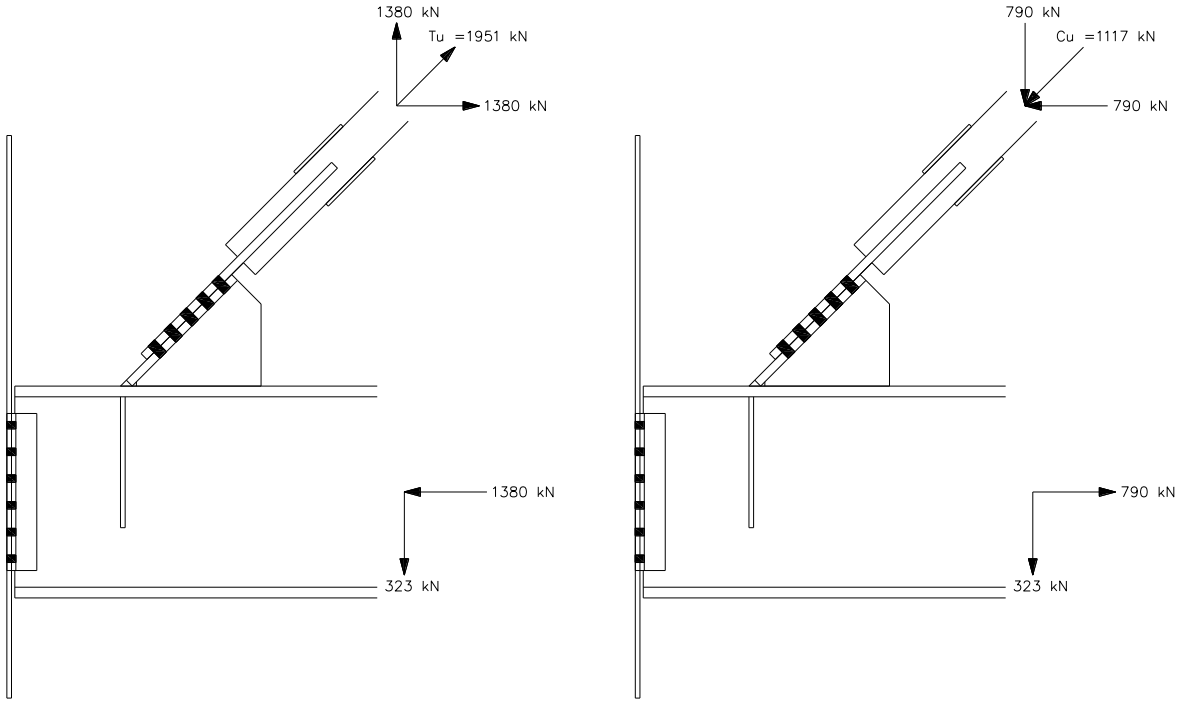

Figure A-3: Applied force in tension and compression

Hinge Plate Dimensions:

To determine the geometry of the connection, the hinge plate dimensions need to be calculated. The chosen width of the hinge plate should be less than the beam flange width to prevent interference with non-structural elements beyond the beam flange edge. A hinge plate width of 300mm is selected for this purpose.

Hinge to Support Plate Bolt Requirement:

Strength per A325 1" bolt in single shear bearing with threads excluded:

$$V_r = 0.6\phi_b A_b F_u \qquad (13.12.1.2)$$

$$V_r = 0.6(0.8)(507\ mm^2)(825\ MPa)$$

$$V_r = 201\ kN$$

The number of bolts required to resist the probable brace tensile resistance is

$$n_b \geq T_u / V_r$$

$$n_b \geq 1951\ kN/201\ kN$$

$$n_b \geq 9.7$$

Therefore, use 10 1" A325 bolts. Using 5 lines of two bolts with a minimum spacing of 68 mm, the connection dimensions are shown in Figure A-3. The bolts are aligned along the centreline of the brace walls to provide better force transfer while still maintaining spacing and edge length requirements.

Checking for reduced bolt shear strength due to length of splice plate:

$$L \leq 15d_b \qquad (13.12.1.2)$$

$$272 \leq 15(25.4)$$

$$272 \leq 381$$

Therefore, no reduction in bolt strength is required.

Hinge plate required thickness:

To prevent gross yield of the hinge plate:

$$A_g \geq \frac{T_u}{\phi F_y} \qquad (13.2(a)(i)))$$

$$t_h(300\ mm) \geq \frac{1951\ kN}{(0.9)(350\ MPa)}$$

$$t_h \geq 20.6\ mm$$

To prevent net section fracture along the first line of bolts:

$$A_{ne} \geq \frac{T_u}{\phi_u F_u} \qquad (13.2(a)(iii))$$

$$t_h\big((300\ mm) - 2(27\ mm)\big) \geq \frac{1951\ kN}{(0.75)(450\ MPa)}$$

$$t_h \geq 23.5\ mm$$

To prevent the three critical modes of block shear failure shown in Figure A-4:

$$\phi_u \left[U_t A_n F_u + 0.6 A_{gv} \frac{(F_y + F_u)}{2} \right] \geq T_u \qquad \text{(13.2(a)(ii)))}$$

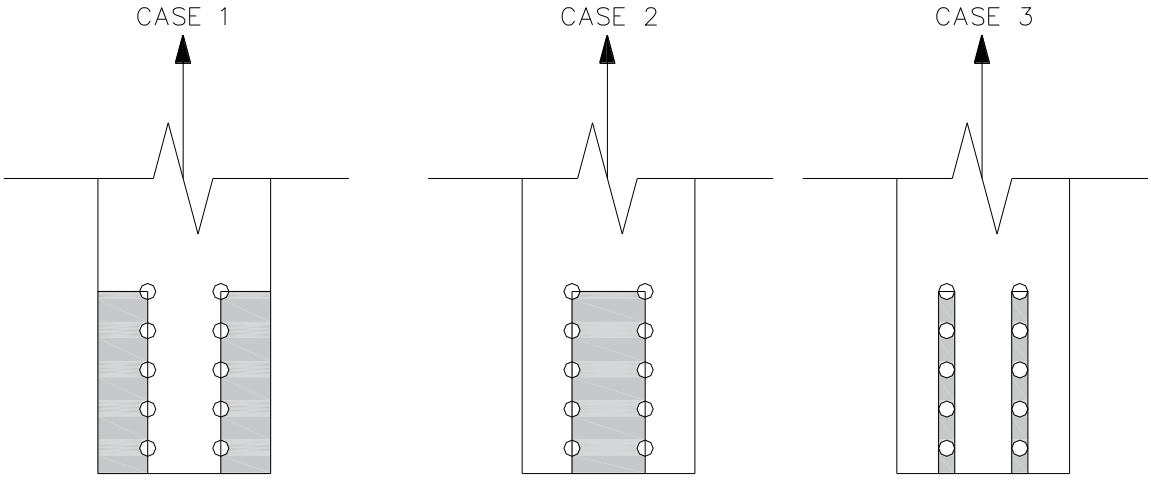

Figure A-4: Block shear failure modes

Case 1:

$$A_n = (2(87\ mm) - 27\ mm)t_h = 147 t_h\ mm$$

$$A_{gv} = 2(310\ mm)t_h = 620 t_h\ mm$$

$$t_h \geq \frac{T_u}{\phi_u \left[U_t (147\ mm) F_u + 0.6(620\ mm) \frac{(F_y + F_u)}{2} \right]}$$

$$t_h \geq \frac{1951\ kN}{(0.75) \left[(1)(147\ mm)(450) + 0.6(620\ mm) \frac{(350 + 450)}{2} \right]}$$

$$t_h \geq 12.1\ mm$$

Case 2:

$$A_n = \big(127\ mm - (27\ mm)\big)t_h = 100 t_h\ mm$$

$$A_{gv} = 2(310) t_h = 620\ mm$$

$$t_h \geq \frac{T_u}{\phi_u \left[U_t(100\ mm) F_u + 0.6(620\ mm) \frac{(F_y + F_u)}{2} \right]}$$

$$t_h \geq \frac{1951\ kN}{(0.75) \left[(1)(100\ mm)(450) + 0.6(620\ mm) \frac{(350 + 450)}{2} \right]}$$

$$t_h \geq 13.4\ mm$$

Case 3:

$$A_n = 0$$

$$A_{gv} = 4(310\ mm) t_h = 1240 t_h\ mm$$

$$t_h \geq \frac{T_u}{\phi_u \left[U_t(0\ mm) F_u + 0.6(1240\ mm) \frac{(F_y + F_u)}{2} \right]}$$

$$t_h \geq \frac{1951\ kN}{(0.75) \left[0.6(1240\ mm) \frac{(350 + 450)}{2} \right]}$$

$$t_h \geq 8.7\ mm$$

Therefore, the most critical condition of net section fracture along the first line of bolts is satisfied by using a 25 mm (1") plate.

Hinge plate buckling:

Hinge plate buckling should be checked in the region between the brace end and the first row of bolts. This distance can be conservatively taken as 94 mm. A typical value of K for hinge plate buckling is K=1.2.

$$\frac{KL}{r} = \frac{(1.2)(94)}{t_h/\sqrt{12}}$$

$$\frac{KL}{r} = \frac{(1.2)(94)}{(25)/\sqrt{12}}$$

$$\frac{KL}{r} = 15.6$$

Since KL/r < 25, yielding controls as per AISC Specification Section J4.4(a). Due to the eccentricity present in the connection, it may seem necessary to design for the combined compression and moment acting in this region using a beam-column equation such as those found in S16-14 Section 13.8. However, the testing presented in Chapter 3 of this thesis confirmed that this requirement is unnecessarily conservative for this application since the hinge plate will be expected to rotate about the hinge line during an earthquake. Additionally, the support plates provide enough rigidity to allow most of the moment to occur in the support plates rather than the hinge plate.

Hinge plate to brace weld:

Using an 8mm (single pass) E49XX fillet weld, the strength per mm of weld is:

$$V_r = 0.67\phi_w A_w X_u (1 + 0.5\sin^{1.5}\theta) M_w \qquad (13.13.2.1)$$

$$V_r = 0.67(0.67)\left(8\ mm/\sqrt{2}\right)(490\ MPa)(1 + 0.5\sin^{1.5}(0))(1)$$

$$V_r = 1.24\ kN/mm$$

The length of weld on each side of the connection:

$$L_w \geq \frac{T_u}{(4\ sides)(1.24\ kN/mm)}$$

$$L_w \geq 392\ mm$$

Therefore, select a weld length of 400 mm for the hinge plate to brace weld.

Brace Required Strength:

The only check left for the brace is to determine the size of cover plates necessary to prevent net section fracture of the brace at the end of the slot. Research has shown that this would not be necessary if the brace and gusset are each slotted and welded together in the shop (Martinez, 2008) but for this example cover plates will be used.

Brace net section:

Providing for a slightly wider slot than plate (2 mm larger), the net section area is:

$$A_n = A_g - 2(25\ mm + 2\ mm)(9.5\ mm)$$

$$A_n = 3727\ mm^2$$

The effective net section of a slotted HSS can be found by applying the equations in S16-14 section 12.3.3. AISC Specification Table D3.1 has a useful approximation for the eccentricity of the weld with respect to the centroid of a slotted HSS section where B and H are the depth and width of the rectangular HSS.

$$\bar{x} = \frac{B^2 + 2BH}{4(B + H)}$$

For a square HSS where B = H:

$$\bar{x} = \frac{3H}{8}$$

$$\bar{x} = \frac{3(127)}{8}$$

$$\bar{x} = 47.6\ mm$$

Brace effective net area:

$$A_{ne} = \left(1 - \frac{\bar{x}}{L_w}\right) A_n$$

$$A_{ne} = \left(1 - \frac{47.6\ mm}{400\ mm}\right)(3727\ mm^2)$$

$$A_{ne} = 3283\ \ mm^2$$

Brace net section tensile resistance:

$$T_r = \phi_u A_{ne} F_u$$

$$T_r = (0.75)(3283\ mm^2)(450\ MPa)$$

$$T_r = 1108\ kN$$

This resistance can be increased by S16-14 clause 27.5.4.2:

$$T_r = (1108\ kN)\ R_y/\phi$$

$$T_r = (1108\ kN)\ (1.2)/(0.9)$$

$$T_r = 1477\ kN$$

Brace slot cover plates

The remaining net section tension resistance that must be resisted by cover plates is:

$$T_r = 1951\ kN - 1477\ kN$$

$$T_r = 474\ kN$$

The cover plates will be 90 mm wide to allow clearance for welds on the HSS wall. Multiple iterations may be required to find a proper plate. Try a 10 mm thick plate:

$$T_r = (2\ cover\ plates)\phi_u \left(1 - \frac{\bar{x}}{L_w}\right) A_n F_u$$

$$T_r = (2\ cover\ plates)(0.75)\left(1 - \frac{66\ mm}{400}\right)(90)(10)(450)$$

$$T_r = 507\ kN \geq 474\ kN$$

Therefore, 90x10 mm cover plates are sufficient for net section net section resistance.

Cover plate to brace welds:

The welds need to be designed to resist the probable tensile resistance of each cover plate.

$$T_u = A_c R_y F_y$$

$$T_u = (90\ mm)(10\ mm)(1.1)(350\ MPa)$$

$$T_u = 347\ kN$$

Using 6 mm E49XX longitudinal fillet welds on each side of the plate, the required weld length is:

$$L_w \geq \frac{347\ kN}{(2\ sides)(0.933\ kN/mm)}$$

$$L_w \geq 186\ mm$$

Therefore, use 200x90x10 mm cover plates centred over the end of the slot with 6 mm longitudinal fillet welds along the plate length.

Support Plates:

Since the support plate will be under similar loading conditions to the hinge plate, the 300 mm wide and 25 mm thick plate will pass all the same tension and bolt checks as the hinge plate. The main support will be supported by the secondary support plate and will not be susceptible to plate buckling. The only new calculations involve connections to the beam and secondary support plate.

To determine the forces present at the connection, equilibrium must be established within the connection region. The method for this is adapted from the Uniform Force Method Special Case 3 which is for vertical brace connections with no gusset connection to the column. In this case, there is no eccentricity at the beam column connection so there is no additional moment present in the connection. The eccentricity between the centreline of the

hinge plate and main support plate centrelines causes a moment at the support plate to beam flange connection. The interface forces for the maximum tension and maximum compression are shown in Figure A-5.

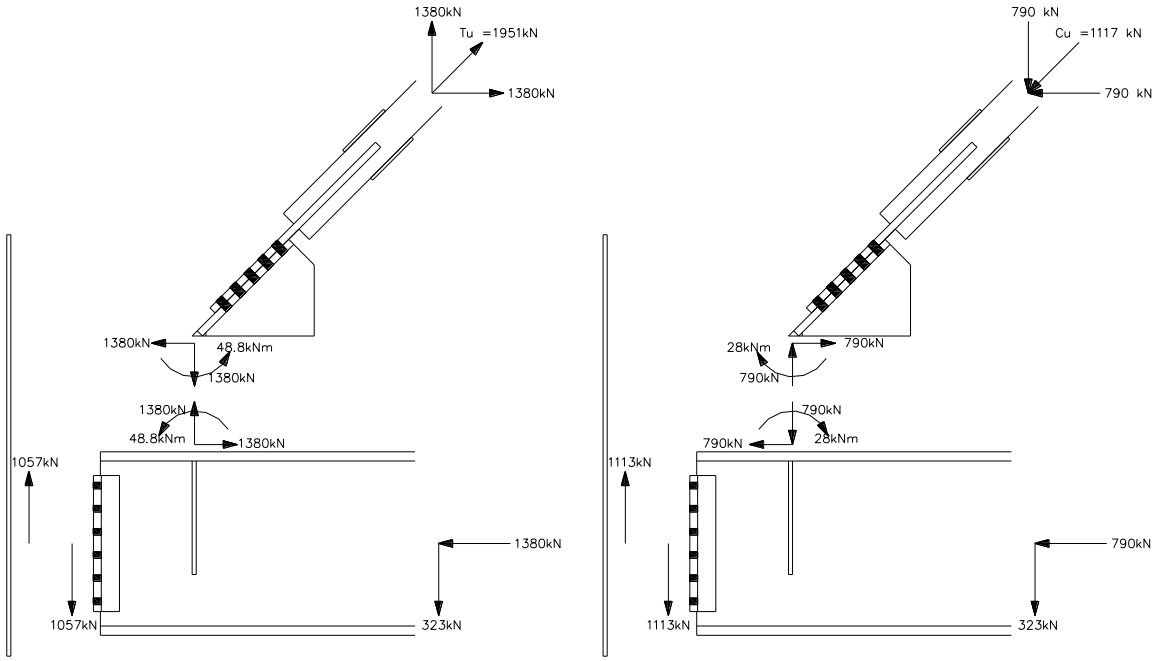

Figure A-5: Connection interface forces

It is assumed that the majority of the force normal to the beam will be transferred by the main support plate. The weld between the main support plate and the beam flange should be designed to transmit the full strength of the plate. The secondary support plate is designed to provide stability and rotational stiffness to the connection which confines rotation to the hinge plate. It also distributes the shear force at the support-beam connection along a longer length to allow better transfer to the beam web. However, it is not the primary means of load transfer. For this reason, the secondary support thickness is selected to be the same as the beam web and the welds connecting it to the main support plate and beam flange are the minimum required size for the associated material thickness.

Bearing strength of the beam:

The additional normal force in the main support plate that should be considered when designing the bearing stiffener is accounted for by distributing the moment about the normal projection of the main and secondary support plates.

$$I = 211.8 * 10^6\ mm^4$$

$$T = 1380\ kN + \frac{My}{I}A$$

$$T = 1380\ kN + \frac{(48.8\ kNm)(109\ mm)}{(211.8 * 10^6\ mm^4)}(300\ mm * 18\ mm)$$

$$T = 1522\ kN$$

$$C = 790\ kN + \frac{(28\ kNm)(109\ mm)}{(211.8 * 10^6\ mm^4)}(300\ mm * 18\ mm)$$

$$C = 871\ kN$$

Web Buckling:

$$B_r = 0.6\phi_{be}w^2\sqrt{F_y E} \qquad (14.3.2(b)(ii))$$

$$B_r = 0.6(0.75)(17.9\ mm)^2\sqrt{(350\ MPa)(200000\ MPa)}$$

$$B_r = 1206\ kN \geq C = 871\ kN$$

Therefore the web does not cripple under compressive bearing.

Web Yielding:

The web yielding strength of the beam using an end loaded case and a bearing area equal to the normal width of the main support plate (18mm) is:

$$B_r = \phi_{be} w(N + 4t)F_y \quad (13.3.2(b)(i))$$

$$B_r = (0.75)(17.9\ mm)\big((18\ mm) + 4(31\ mm)\big)(350\ MPa)$$

$$B_r = 667\ kN \leq T = 1522\ kN$$

Therefore, a bearing stiffener is needed in the web. The stiffener is required to resist 505kN in tension and a negligible force in compression. Therefore the minimum area of each bearing stiffener is:

$$T - B_r \leq \phi A_b F_y$$

$$A_b \geq \frac{(T - B_r)}{\phi F_y}$$

$$A_b \geq \frac{(1522\ kN - 667\ kN)}{(0.9)(350\ MPa)}$$

$$A_b \geq 2714\ mm^2$$

For a stiffener width of 121 mm on each side of the web, the minimum required bearing stiffener thickness is:

$$t_b \geq \frac{A_b}{(2)(121\ mm)}$$

$$t_b \geq 11.2\ mm$$

The bearing stiffener should be at least half the thickness of the connecting plate. Therefore, 14mm bearing plates are used.

Bearing Stiffener Weld:

Using two 6 mm welds on each stiffener (the minimum weld size for the 18 mm beam web), the minimum required length of the weld is:

$$L_w \geq \frac{855\ kN}{(4\ sides)(0.933\ kN/mm)}$$

$$L_w \geq 230\ mm$$

However, it is recommended that the stiffeners should extend at least 2/3 the depth of the beam to allow more uniform force transfer to the beam web and beam-column connection region. Therefore, the recommended bearing stiffener length is 392 mm.

Beam-Column Connection

A double angled beam connection will be used to connect the beam to the column. For this example, the beam connects directly to the column web. This eliminates any eccentricity or moment in the beam-column connection beyond what would be expected in a standard beam-column connection. Therefore, Tables 3-37 and 3-38 in the 10th edition of the CISC Handbook of Steel Construction (CISC, 2010) will be used to design the connection. The angles are bolted to the column web and welded to the beam web.

Peak Connection Force:

The maximum connection force occurs in the beam-column connection with a compression brace framing into the beam assuming the brace is under the maximum possible compression as seen in Figure A-5. The maximum connection shear force in this case is 1113 kN.

Connection Details:

To resist the 1113 kN shear force, G40.21 300W L76x76x13 angles are used. The 470 mm long angles are connected to the beam web with 8 mm welds and the column web with 6 ¾" bolts per angle and a gauge of 80 mm. The angle, beam and column thicknesses meet the requirements to allow the full connection capacity as listed in Tables 3-37 and 3-38.

Example 2: Concentric brace to beam connection

This example takes a connection on the second storey of the south side of the structure using the concentric version of the replaceable connection and a moment resisting end plate connection to connect the beam to the column flange. The final connection design is shown in Figure A-6.

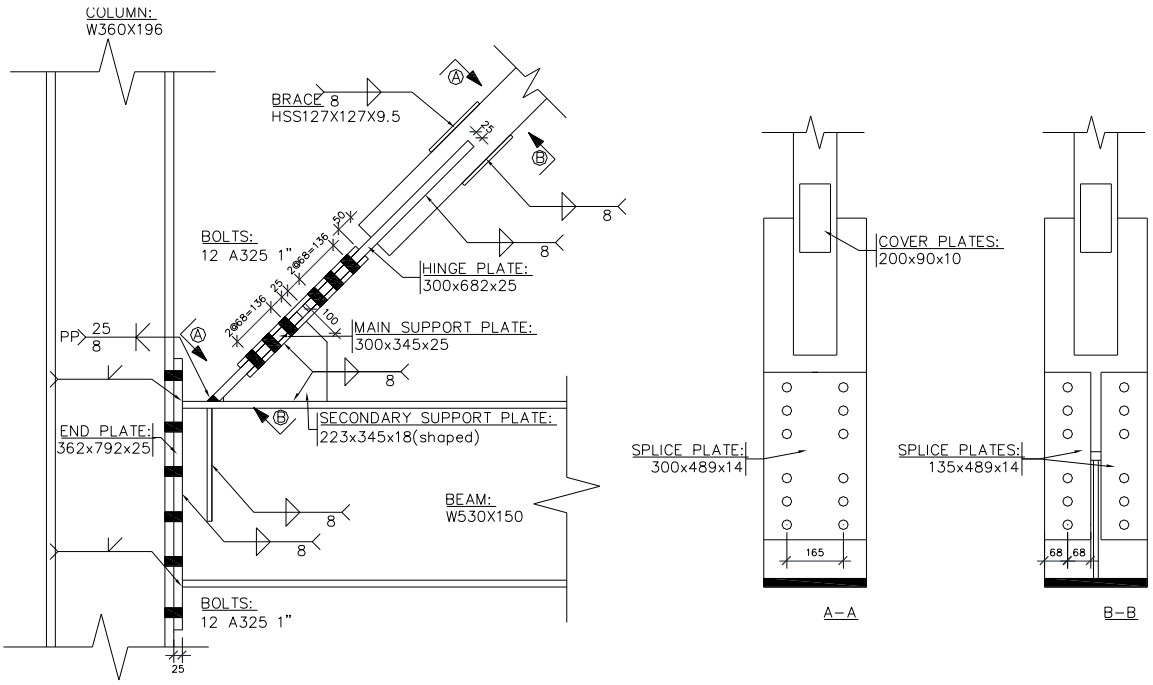

Figure A-6: Final concentric connection design

From the CISC *Handbook of Steel Construction* Table 6-3, the material properties are as follows:

G40.21 350W

$F_y = 350\ MPa \quad F_u = 450\ MPa$

From the CISC *Handbook of Steel Construction* pages 6-102, 6-45 and 6-51, the geometric properties are as follows:

Brace HSS127x127x9.5

$A_g = 4240\ mm^2 \quad r = 47.5\ mm$

Beam W530x150

$d = 543\ mm \quad b = 312\ mm \quad t = 20.3\ mm \quad w = 12.7mm$

Column W360x196

$d = 372\ mm \quad b = 374\ mm \quad t = 26.2\ mm \quad w = 16.4\ mm$

Design Loads:

The required factored loads in the connection are taken from the probable brace resistances found in S16-14 Section 27.5.3.

Probable Tensile Resistance:

$$R_y F_y = 460\ MPa \tag{27.1.7}$$

$$T_u = A_g R_y F_y \tag{27.5.3.4}$$

$$T_u = (4240\ mm)(460\ MPa)$$

$$T_u = 1951\ kN$$

Probable Compressive Resistance:

The effective length used for calculating the compressive force of the brace should be based on the distance between the hinge zones. This effective length won't be determined until the connection geometry has been fully designed. A reasonable estimate for this example involves reducing the length between work points by 2 m to account for the beam depth and connection length. The n value is taken as 1.34 for a Class C brace.

$$KL = \sqrt{(4000\ mm)^2 (4000\ mm)^2} - 2000\ mm$$

$$KL = 3657\ mm$$

$$F_e = \frac{\pi^2 E}{\left(\frac{KL}{r}\right)^2} \quad (13.3.1)$$

$$F_e = \frac{\pi^2 (200000\ MPa)}{\left(\frac{3657\ mm}{47.5\ mm}\right)^2}$$

$$F_e = 330\ MPa$$

$$\lambda = \sqrt{\frac{R_y F_y}{F_e}} \quad (13.3.1)$$

$$\lambda = \sqrt{\frac{460\ MPa}{330\ MPa}}$$

$$\lambda = 1.18$$

$$C_r = A_g R_y F_y (1 + \lambda^{2n})^{(-1/n)} \quad (13.3.1)$$

$$C_r = (4240\ mm)(460\ MPa)\left(1 + (1.18)^{2(1.34)}\right)^{(-1/1.34)}$$

$$C_r = 968\ kN$$

$$C_u = 1.2 C_r$$

$$C_u = 1162\ kN$$

After designing the connection, the actual C_u value based on a true effective length of 3611mm, is 1178 kN. The brace and connection forces under the associated peak tension and compressive forces is shown in Figure A-7

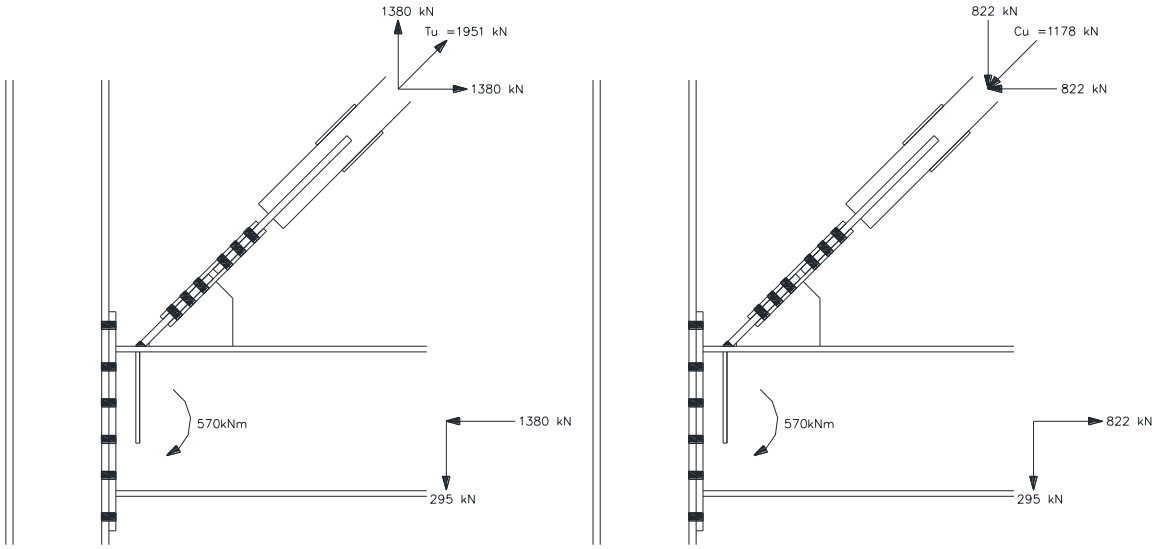

Figure A-7: Maximum Applied Forces

Hinge Plate Dimensions:

To determine the geometry of the connection, the hinge plate dimensions need to be calculated. The chosen width of the hinge plate should be less than the beam flange width to prevent interference with non-structural elements beyond the beam flange edge. A hinge plate width of 300mm is selected for this purpose.

Hinge to Splice Plates Bolt Requirement:

Strength per A325 1" bolt in double shear bearing with threads excluded:

$$V_r = 0.6\phi_b m A_b F_u \qquad (13.12.1.2)$$

$$V_r = 0.6(0.8)(2)(507\ mm^2)(825\ MPa)$$

$$V_r = 402\ kN$$

The number of bolts required to resist the probable brace tensile resistance is

$$n_b \geq T_u / V_r$$

$$n_b \geq 1951\ kN / 402\ kN$$

$$n_b \geq 4.8$$

Therefore, use six 1" A325 bolts. Use 3 lines of two bolts with a minimum spacing of 68 mm. To accommodate the splice plate geometry, the bolt line will align with the centreline of the small splice plates.

Checking for reduced bolt shear strength due to length of splice plate:

$$L \leq 15d_b \qquad (13.12.1.2)$$

$$204 \leq 15(25.4)$$

$$204 \leq 381$$

Therefore, no reduction in bolt strength is required.

Hinge plate required thickness:

To prevent gross yield of the hinge plate:

$$A_g \geq \frac{T_u}{\phi F_y} \qquad (13.2(a)(i)))$$

$$t_h(300\ mm) \geq \frac{1951\ kN}{(0.9)(350\ MPa)}$$

$$t_h \geq 20.6\ mm$$

To prevent net section fracture along the first line of bolts:

$$A_{ne} \geq \frac{T_u}{\phi_u F_u} \qquad (13.2(a)(iii))$$

$$t_h\big((300\ mm) - 2(27\ mm)\big) \geq \frac{1951\ kN}{(0.75)(450\ MPa)}$$

$$t_h \geq 23.5\ mm$$

To prevent the three critical modes of block shear failure:

$$\phi_u \left[U_t A_n F_u + 0.6 A_{gv} \frac{(F_y + F_u)}{2} \right] \geq T_u \qquad (13.2(a)(ii)))$$

Case 1:

$$A_n = (2(67\ mm) - 27\ mm)t_h = 107 t_h\ mm$$

$$A_{gv} = 2(180\ mm)t_h = 360 t_h\ mm$$

$$t_h \geq \frac{T_u}{\phi_u \left[U_t (107\ mm) F_u + 0.6(360\ mm) \frac{(F_y + F_u)}{2} \right]}$$

$$t_h \geq \frac{1951\ kN}{(0.75) \left[(1)(107\ mm)(450) + 0.6(360\ mm) \frac{(350 + 450)}{2} \right]}$$

$$t_h \geq 19.33\ mm$$

Case 2:

$$A_n = \big(165\ mm - (27\ mm)\big)t_h = 138 t_h\ mm$$

$$A_{gv} = 2(180) t_h = 360\ mm$$

$$t_h \geq \frac{T_u}{\phi_u \left[U_t (138\ mm) F_u + 0.6(360\ mm) \frac{(F_y + F_u)}{2} \right]}$$

$$t_h \geq \frac{1951\ kN}{(0.75) \left[(1)(138\ mm)(450) + 0.6(360\ mm) \frac{(350 + 450)}{2} \right]}$$

$$t_h \geq 17.5\ mm$$

Case 3:

$$A_n = 0$$

$$A_{gv} = 4(180\ mm)t_h = 1240t_h\ mm$$

$$t_h \geq \frac{T_u}{\phi_u \left[U_t(0)F_u + 0.6(720\ mm)\frac{(F_y + F_u)}{2}\right]}$$

$$t_h \geq \frac{1951\ kN}{(0.75)\left[0.6(720\ mm)\frac{(350 + 450)}{2}\right]}$$

$$t_h \geq 15.1\ mm$$

Therefore, the most critical condition of net section fracture along the first line of bolts is satisfied by using a 25 mm plate.

Hinge plate buckling:

Hinge plate buckling should be checked in the region between the brace end and the first row of bolts. This distance can be conservatively taken as 104 mm.

$$\frac{KL}{r} = \frac{(1.2)(104)}{t_h/\sqrt{12}}$$

$$\frac{KL}{r} = \frac{(1.2)(104)}{(30)/\sqrt{12}}$$

$$\frac{KL}{r} = 14.4$$

Since KL/r < 25, yielding controls as per AISC Specification Section J4.4(a).

Hinge plate to brace weld:

Using an 8mm (single pass) E49XX fillet weld, the strength per mm of weld is:

$$V_r = 0.67\phi_w A_w X_u (1 + 0.5\sin^{1.5}\theta) M_w \quad (13.13.2.1)$$

$$V_r = 0.67(0.67)\left(8\ mm/\sqrt{2}\right)(490\ MPa)(1 + 0.5\sin^{1.5}(0))(1)$$

$$V_r = 1.24\ kN/mm$$

The length of weld on each side of the connection:

$$L_w \geq \frac{T_u}{(4\ sides)(1.24\ kN/mm)}$$

$$L_w \geq 392\ mm$$

Therefore, select a weld length of 400 mm for the hinge plate to brace weld.

Splice Plates:

For this connection design, splice plates are used to connect the hinge plate to the support plates. These splice plates should provide the necessary connection forces and should provide enough moment resistance to confine the hinging to the hinge plate. There are 3 splice plates, one is the full width of the hinge plate and the other two are cut to accommodate the secondary support plate. The required plate thickness will be checked using the smaller splice plates and the same thickness will be applied to the larger splice plate.

Minimum Thickness:

The thickness of the splice plates to prevent net section failure must be greater than:

$$A_{ne} \geq \frac{T_u}{\phi_u F_u}$$

$$t_h\left((135\ mm) - (27\ mm)\right) \geq \frac{488\ kN}{(0.75)(450\ MPa)}$$

$$t_h \geq 13.4\ mm$$

Since the bolts are symmetrically placed, the only block shear failure that must be checked is bolt tearout. To prevent bolt tearout, the thickness of the plate greater than:

$$A_n = 0$$

$$A_{gv} = 4(180\ mm)t_h = 1240t_h\ mm$$

$$t_h \geq \frac{T_u}{\phi_u \left[U_t(0)F_u + 0.6(720\ mm)\frac{(F_y + F_u)}{2}\right]}$$

$$t_h \geq \frac{976\ kN}{(0.75)\left[0.6(720\ mm)\frac{(350 + 450)}{2}\right]}$$

$$t_h \geq 7.3\ mm$$

Therefore, 14mm splice plates are used.

Support Plates:

Since the support plate will be under similar loading conditions to the hinge plate, the 300 mm wide and 25 mm thick plate will pass all the same tension and bolt checks as the hinge plate. The main support will be supported by the secondary support plate and will not be susceptible to plate buckling. The only new calculations involve connections to the beam and secondary support plate.

To determine the forces present at the connection, equilibrium must be established within the connection region. The method for this is adapted from the Uniform Force Method Special Case 3 which is for vertical brace connections with no gusset connection to the column. (AISC, 20…) Minor alterations are made due to the unique shape of the connection.

It is assumed that the majority of the force normal to the beam will be transferred by the main support plate. The weld between the main support plate and the beam flange should be

designed to transmit the full strength of the plate. The secondary support plate is designed to provide stability and rotational stiffness to the connection which confines rotation to the hinge plate. It also distributes the shear force at the support-beam connection along a longer length to allow better transfer to the beam web. However, it is not the primary means of load transfer. For this reason, the secondary support thickness is selected to be the same as the beam web and the welds connecting it to the main support plate and beam flange are the minimum required size for the associated material thickness.

Since there is very little eccentricity in this connection, the moment at the support to beam connection is neglected and the force used to check the beam bearing strength will be conservatively taken as the normal component of the brace load. The force distribution is shown in Figure A-8.

The additional moment at the beam-column interface is calculated from the Uniform Force Method Special Case 3. It is calculated by multiplying the connection shear force caused by the brace by half the column depth

$$M = \frac{b_c}{2} V$$

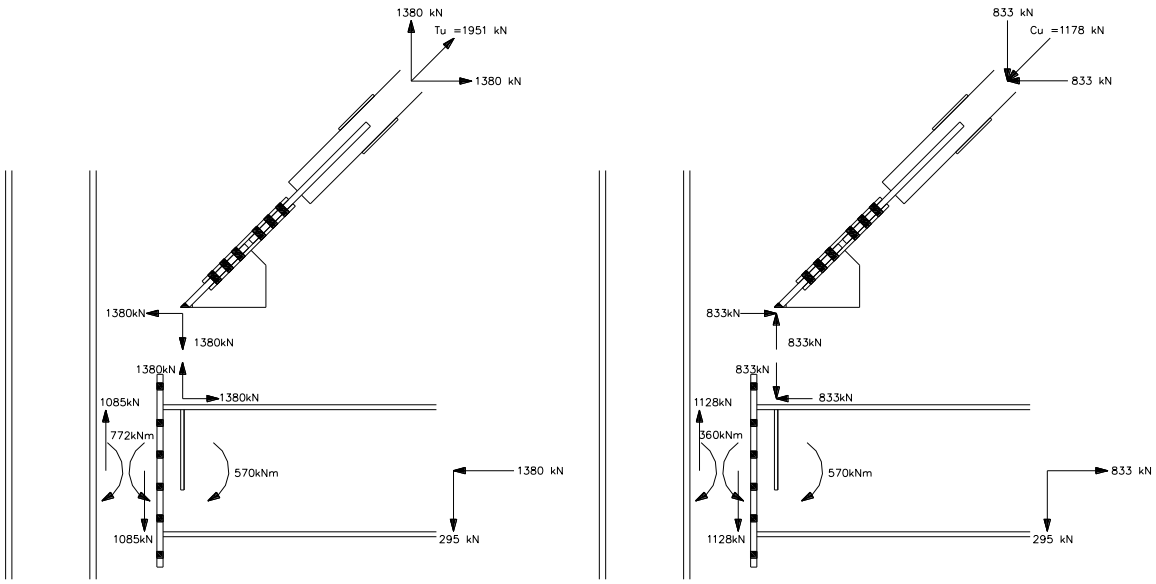

Figure A-8: Connection interface forces

Bearing strength of the beam:

Web Buckling:

$$B_r = 0.6\phi_{be} w^2 \sqrt{F_y E} \qquad (14.3.2(b)(ii))$$

$$B_r = 0.6(0.75)(12.7\ mm)^2 \sqrt{(350\ MPa)(200000\ MPa)}$$

$$B_r = 607\ kN \leq C = 790\ kN$$

Therefore the web will require a bearing stiffener to prevent web crippling.

Web Yielding:

The web yielding strength of the beam using an end loaded case and a bearing area equal to the normal width of the main support plate (21 mm) is:

$$B_r = \phi_{be} w(N + 4t)F_y \qquad (13.3.2(b)(i))$$

$$B_r = (0.75)(12.7\ mm)\big((19\ mm) + 4(20.3\ mm)\big)(350\ MPa)$$

$$B_r = 344\ kN \leq T = 1380\ kN$$

Therefore, a bearing stiffener is needed in the web. The stiffener is required to resist 505kN in tension and a negligible force in compression. Therefore the minimum area of each bearing stiffener is:

$$T - B_r \leq \phi A_b F_y$$

$$A_b \geq \frac{(T - C_r)}{\phi F_y}$$

$$A_b \geq \frac{(1380\ kN - 344\ kN)}{(0.9)(350\ MPa)}$$

$$A_b \geq 3289\ mm^2$$

For a stiffener width of 123 mm on each side of the web, the minimum required bearing stiffener thickness is:

$$t_b \geq \frac{A_b}{(2)(123\ mm)}$$

$$t_b \geq 13.4\ mm$$

Therefore 14 mm stiffeners will be used on each side of the beam.

Stiffener to Web:

Using two 8 mm welds on each stiffener, the minimum required length of the weld is:

$$L_w \geq \frac{916\ kN}{(4\ sides)(0.933\ kN/mm)}$$

$$L_w \geq 245\ mm$$

However, it is recommended that the stiffeners should extend at least 2/3 the depth of the beam to allow more uniform force transfer to the beam web and beam-column connection region. Therefore, the recommended bearing stiffener length is 260mm.

Beam-Column Connection

An extended bolted unstiffened end plate moment resisting connection is used to transfer the shear and moment caused by the braces to the column flange. The maximum shear and moment in the connection occur when the incoming brace is in compression. The connection must resist a 615 kNm moment and a 1101 kN shear. The CISC Moment Connections for Seismic Connections (CISC, 2005) is used to design the connection with some adjustments made because the beam is not expected to form a plastic hinge. Due to the high shear relative to the moment, additional bolts are added in the web region to resist the shear but are not assumed to contribute to the moment resistance.

The end plate connection as designed is shown in Figure A-9. The design checks are as follows:

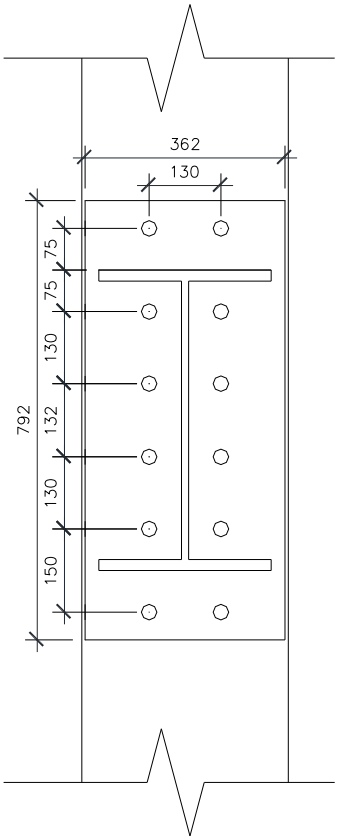

Figure A-9: Bolted End Plate Detail

Bolt Tension:

The top 4 bolts are assumed to resist the full tension force caused by the beam moment. The bolt area of each bolt must satisfy the following requirement:

$$0.75A_bF_u \geq \frac{M}{2(d_1 + d_2)}$$

$$0.75A_b(830\ MPa) \geq \frac{(615\ kNm)}{2(458\ mm + 608\ mm)}$$

$$A_b \geq 464\ mm^2$$

Therefore, the 1" bolts (A_b = 507 mm^2) satisfy this requirement.

Bolt Shear:

The connection shear is reduced by the remaining 8 bolts in the connection. The area of each bolt must satisfy the following requirement:

$$6A_b(0.5F_u) \geq V$$

$$6A_b\big(0.5(830\ MPa)\big) \geq 1101\ kN$$

$$A_b \geq 442\ mm^2$$

Therefore, the 1" bolts (A_b = 507 mm^2) satisfy this requirement.

End Plate Flexure:

To prevent end plate flexural yielding, the end plate thickness must satisfy the following requirement where $s = \sqrt{b_p g}$ and $F_{yp} = 250\ MPa$

$$t_p \geq \sqrt{\frac{M}{0.8F_{yp}\left\{(d_b - p_t)\left[\frac{b_p}{2}\left(\frac{1}{p_f}+\frac{1}{s}\right)+\left(p_f+s\right)\frac{2}{g}\right]+\frac{b_p}{2}\left(\frac{d_b}{p_f}+\frac{1}{2}\right)\right\}}}$$

$$t_p \geq \sqrt{\frac{615\ kNm}{0.8(250MPa)\left\{(543-75)\left[\frac{362}{2}\left(\frac{1}{75}+\frac{1}{217}\right)+(75+217)\frac{2}{130}\right]+\frac{362}{2}\left(\frac{543}{75}+\frac{1}{2}\right)\right\}}}$$

$$t_p \geq 24.7\ mm$$

Therefore, the 25mm thick end plate satisfies this requirement

End Plate Shear:

To prevent end plate shear yielding, the plate thickness must satisfy the following requirement:

$$t_p \geq \frac{M}{1.1F_{yp}b_p(d_b - t_b)}$$

$$t_p \geq 11.8\,mm$$

Therefore, the 25mm thick end plate satisfies this requirement

Beam Flange Tension:

If the column flange thickness meets the following requirement, no tension continuity plate is required.

$$t_c \geq \sqrt{\frac{\left(\frac{M}{d_b - t_b}\right)\left(\frac{g}{2} - k_1\right)}{2F_y c}}$$

$$t_p \geq \sqrt{\frac{\left(\frac{615\ kNm}{543\ mm - 20.3\ mm}\right)\left(\frac{130\ mm}{2} - 38\ mm\right)}{2(350\ MPa)(150\ mm)}}$$

$$t_c \geq 17.4\,mm$$

Therefore, the 26.2 mm column flange thickness satisfies this requirement and no continuity plates are required for tension.

Beam Flange Compression:

If the column flange thickness meets the following requirement, no compression continuity plate is required.

$$w_c \geq \frac{M}{(d_b - t_b)\left(6k_e + 2t_p + t_b\right)F_y}$$

$$w_c \geq \frac{615\ kNm}{(543\ mm - 20.3\ mm)\left(6(38\ mm) + 2(25\ mm) + (20.3\ mm)\right)(350\ MPa)}$$

$$w_c \geq 11.3\,mm$$

Therefore, the 16.4 mm column flange thickness satisfies this requirement and no continuity plates are required for compression.

Panel Zone Shear:

The panel zone shear is taken as the moment at the face plus the additional moment caused by the shear force at the column flange. The beam depth is taken as the distance between the centreline of the beam tension flange and the edge of the end plate on the compression side.

The applied panel zone shear force is equal to:

$$V_p = \frac{M + V\left(\frac{d_c}{2}\right)}{d_b}$$

$$V_p = \frac{615\ kNm + (1101\ kN)\left(\frac{372\ mm}{2}\right)}{668\ mm}$$

$$1227\ kN$$

The panel zone shear resistance is equal to:

$$V_r = 0.55\phi d_c w_c F_y \left[1 + \frac{3b_c {t_c}^2}{d_c d_b w_c}\right]$$

$$V_r = 0.55(0.9)(372\ mm)(16.4\ mm)(350\ MPa)\left[1 + \frac{3(374\ mm)(26.2\ mm)^2}{(372\ mm)(668\ mm)(16.4\ mm)}\right]$$

$$V_r = 1257\ kN$$

Therefore, the panel zone is strong enough to resist the shear forces without additional doubler plates.

References

American Institute of Steel Construction (AISC) (2010). "Seismic Provisions for Structural Steel Buildings. ANSI/AISC 341-10." Chicago, United States.

National Research Council of Canada (2010). "National Building Code of Canada."

Canadian Institute of Steel Construction (CISC) (2005). "Moment Connections for Seismic Applications." Markham, Ontario, Canada

Canadian Institute of Steel Construction (CISC) (2010). "Handbook of Steel Construction, 10th edition." Markham, Ontario, Canada

Canadian Standards Association (CSA) (2014). ""Design of Steel Structures. CSA Standard S16-14." Rexdale, Canada.

Muir, L., Thorton, W. 2014. "Steel Design Guide 29: Vertical Bracing Connections – Analysis and Design." American Institute of Steel Construction, Chicago, IL, US.

Appendix B: Experimental Setup and Additional Results

The purpose of this Appendix is to provide more experimental information than is present in Chapter 3.

Instrumentation

The generalized location of instrumentation is seen in Figure B-1. Table B-1 lists the exact measurements in mm of the instrumentation measurements.

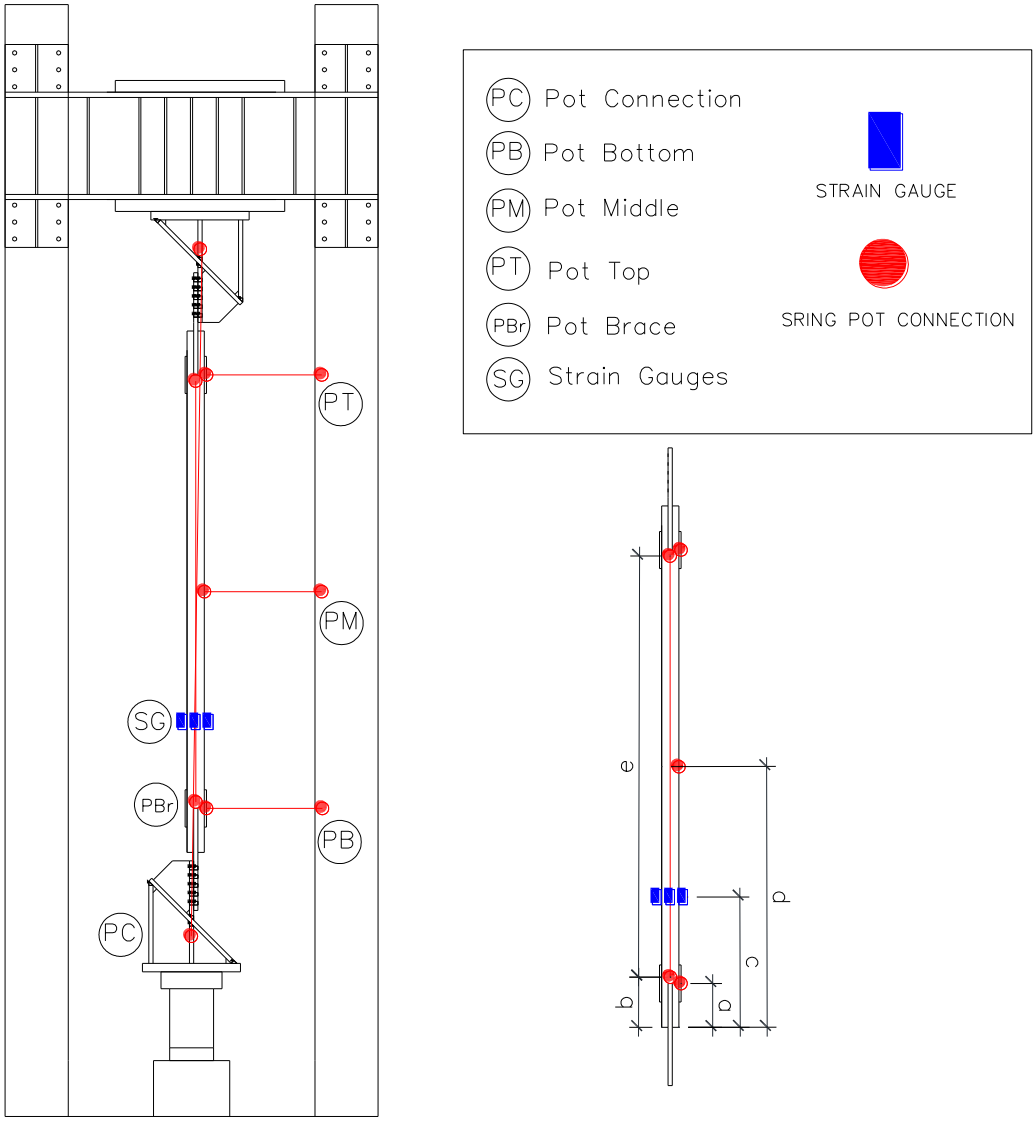

Figure B-1: Instrumentation setup

Table B-1: Instrumentation dimension values

Specimen	a	b	c	d	e
E-1	260	285	770	1541	2512
E-2	275	300	774	1548	2496
E-3	225	250	800	1600	2700
E-4	260	285	758	1517	2464
E-5	260	285	777	1554	2538
C-1	260	285	716	1432	2293
C-2	275	300	723	1443	2286
C-3	225	250	776	1553	2605

Test Data

The hysteresis curves of all 8 specimens in terms of raw displacement as measured by PC are shown in Figure B-2.

The corrected hysteresis curves of all 8 specimens in terms of raw displacement as measured by PBr are shown in Figure B-3. During testing, large bolt slips shifted the magnets of the pot attachment points on the brace for 4 of the specimens. For specimen E-1, the corrected values shown are thought to be accurate as there was a small, well-defined jump. For specimen C-3, a correction was made but the jump was larger and not as well defined. Specimen C-2 required correction but slip correction was attempted during the experiment by moving the magnets back to the intended position. It is not clear if this worked properly. Multiple slips and manual corrections were attempted for specimen C-1. Additionally, during portions of the C-1 test, the pot was inactive. Therefore, no numerical corrections were made to the results of C-1 and the brace displacement values likely do not reflect the true state of brace deformation during the experiment.

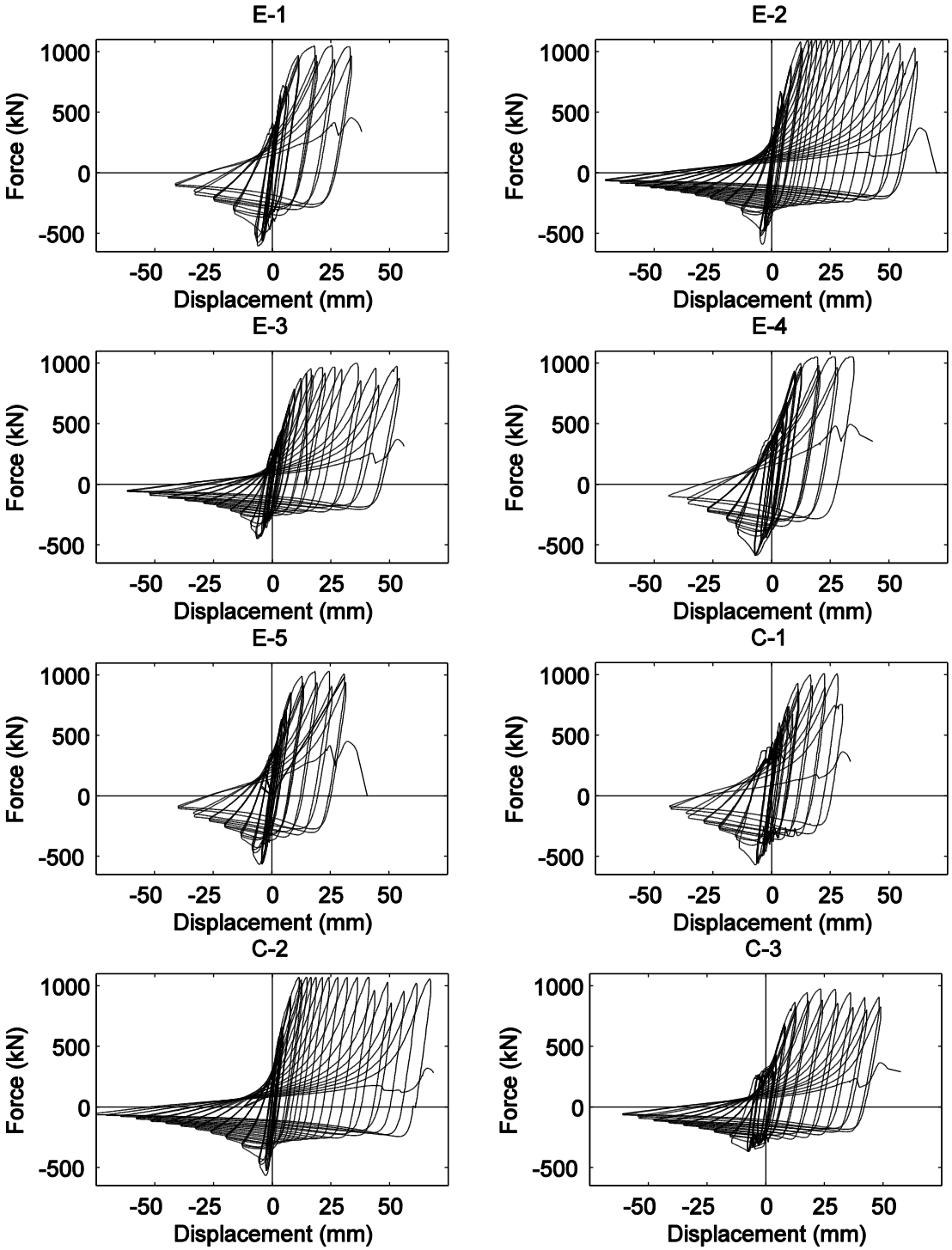

Figure B-2: Load vs. Pot Connection (PC) displacement

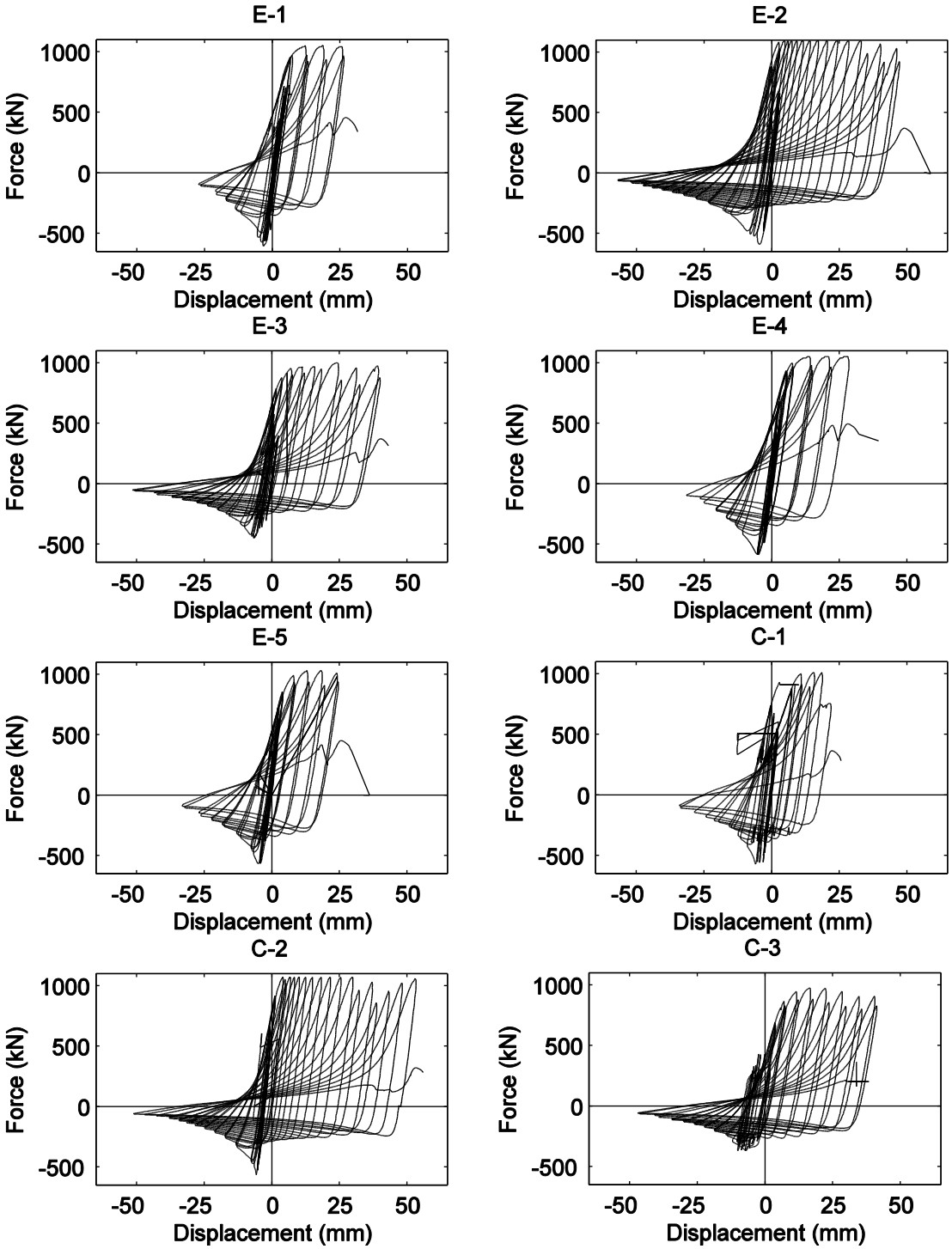

Figure B-3: Load vs. Pot Brace (PBr) Displacements

The midspan pot readings needed to be corrected to account for the shift of the pot on the brace while the pot on the support column remained stationary. The pot end and the typical brace connection point started 550mm from each other. The correction was based on the following formula:

$$PM_{corrected} = \sqrt{(550 + PM_{measured})^2 - \left(\frac{PC}{2}\right)^2} - 550$$

Which is based on trigonometric relationships between the attachment points. For braces that buckled towards the pot, this correction was higher than those that buckled away.

7 of the 8 brace midspan deflections are plotted vs the connection pot displacement. The middle pot did not operate correctly during test E-4 and its results are ignored. The results can be seen in Figure B-4

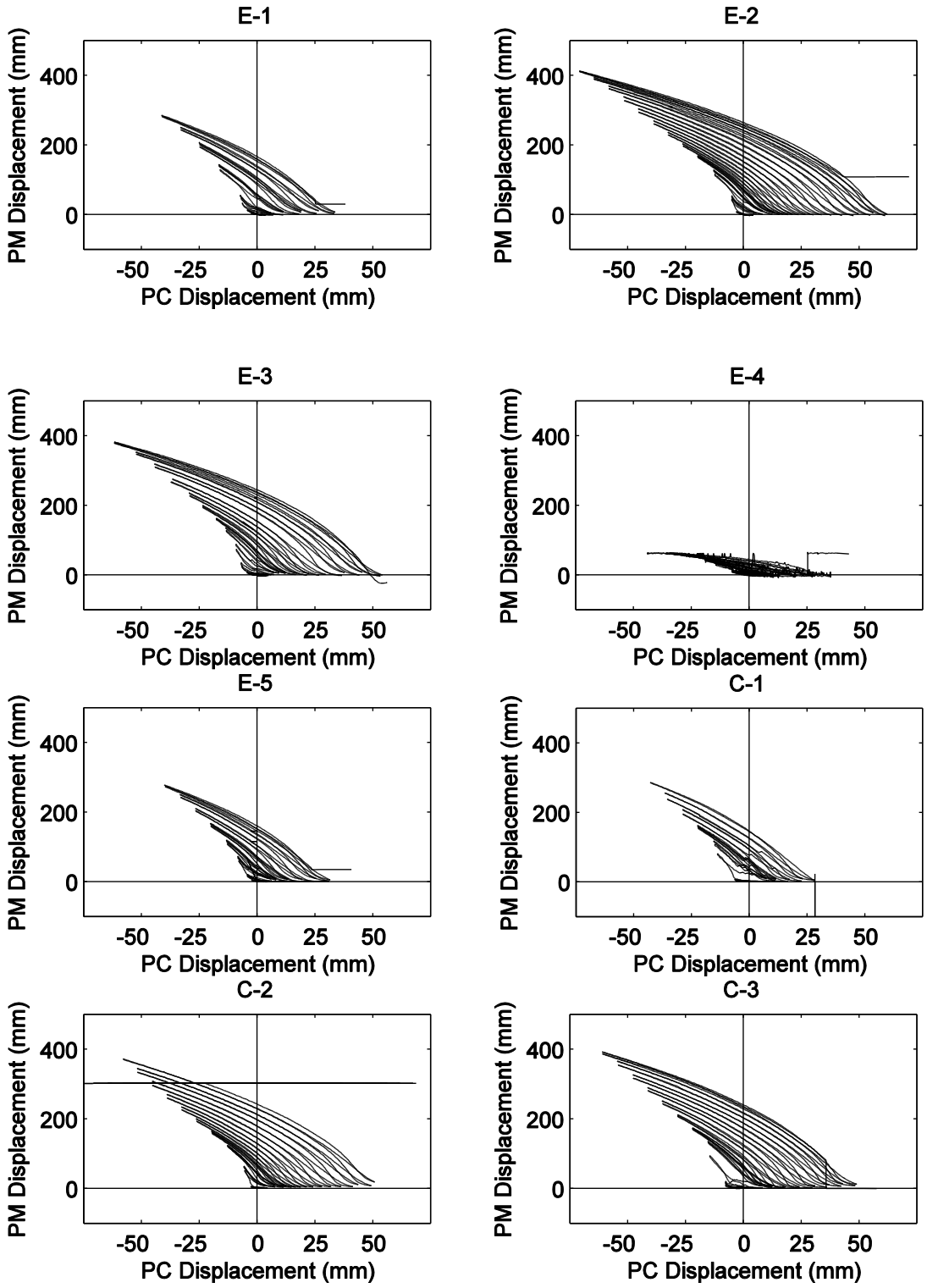

Figure B-4: Midspan (PM) displacement vs Connection (PC) displacement

Experiment Drawings

The following pages include the experimental steel information given to Walters Inc. for fabrication.

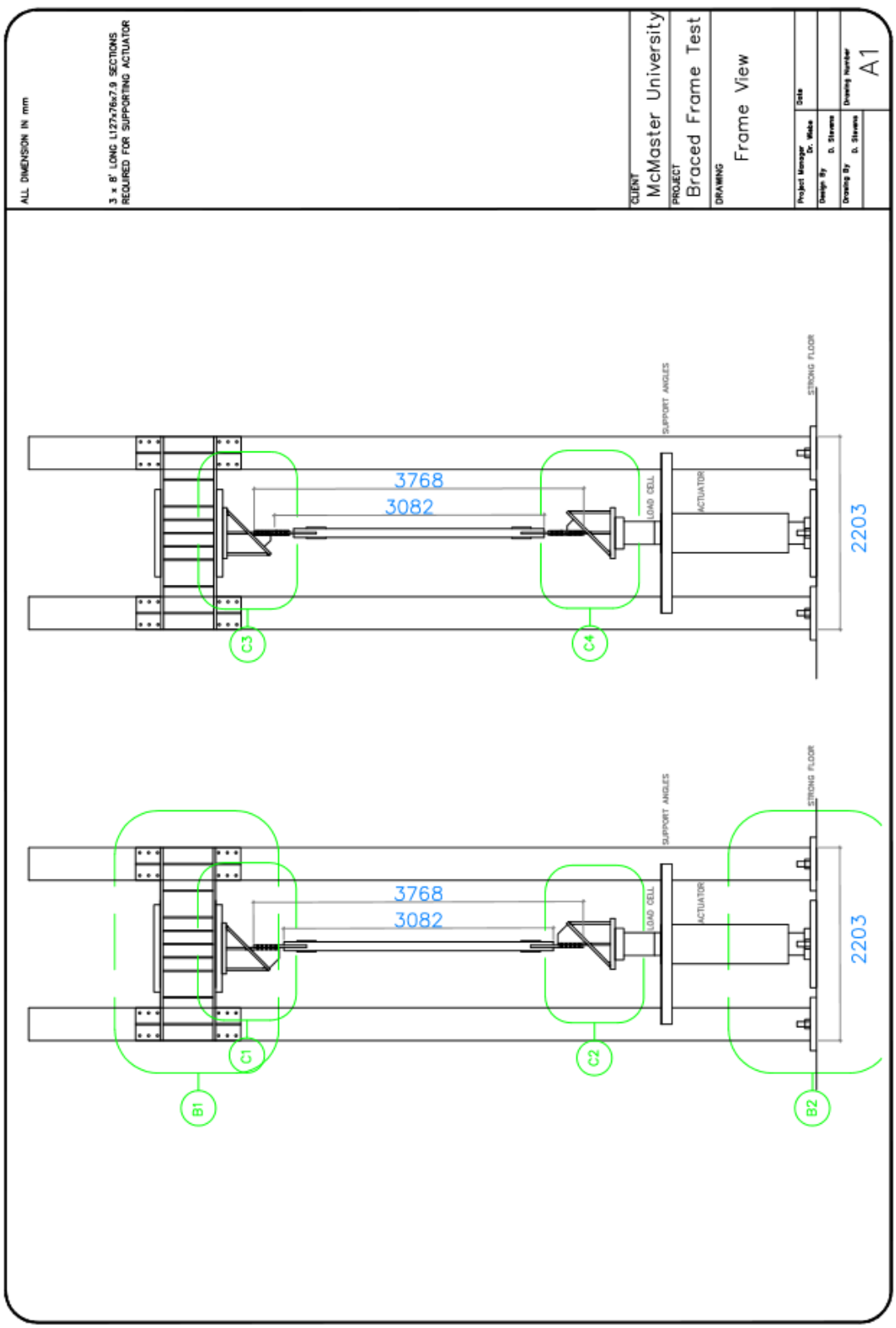
ALL DIMENSION IN mm
3 x 8' LONG L127x76x7.9 SECTIONS REQUIRED FOR SUPPORTING ACTUATOR
CLIENT
McMaster University
PROJECT
Braced Frame Test
DRAWING
Frame View
Project Manager
Dr. Wade
Design By
D. Stevens
Drawing By
D. Stevens
Date
Drawing Number
A1
SUPPORT ANGLES
STRONG FLOOR
LOAD CELL
ACTUATOR
3768
3082
2203
C3
C4
C1
C2
B1
B2

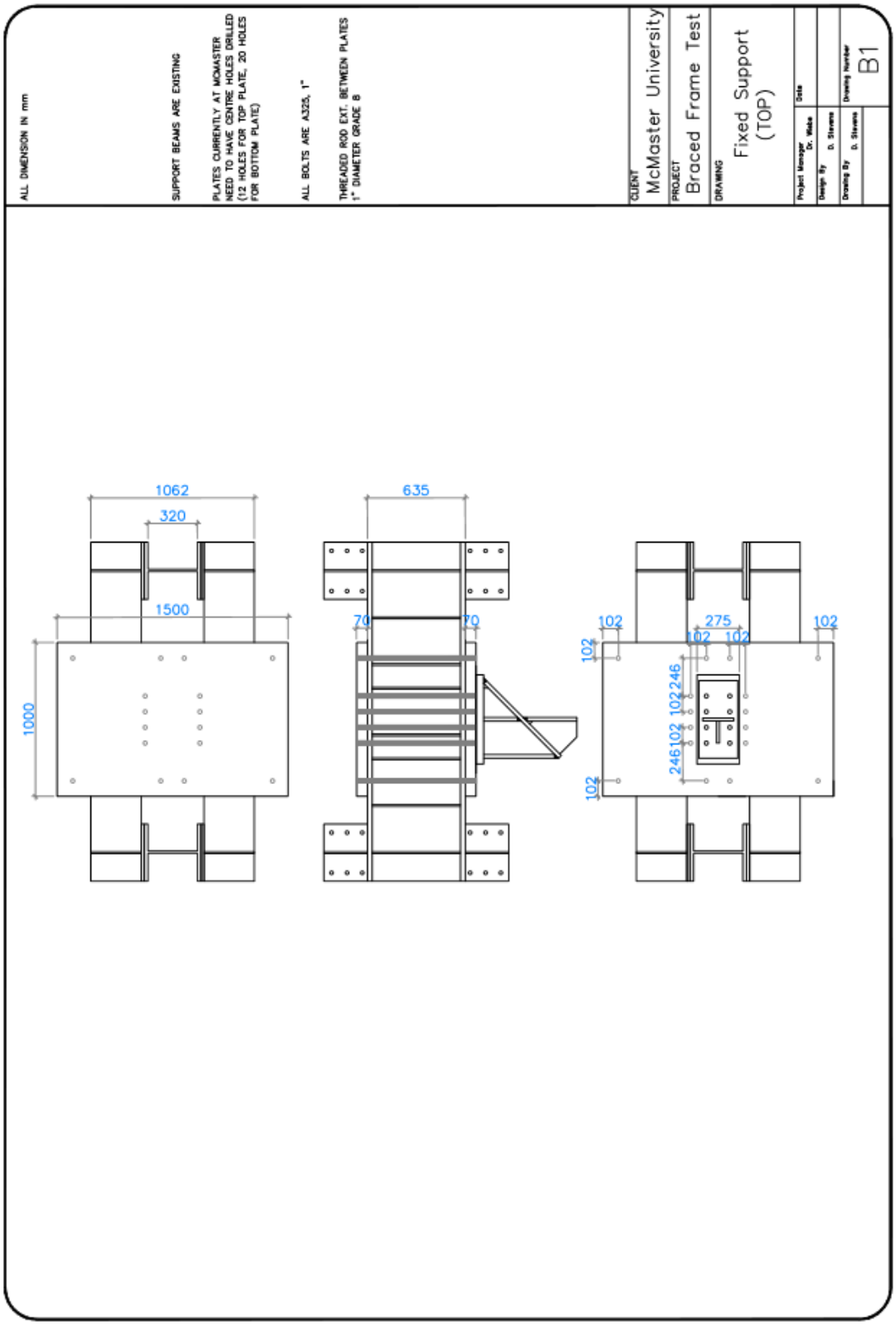
ALL DIMENSION IN mm
SUPPORT BEAMS ARE EXISTING
PLATES CURRENTLY AT MCMASTER NEED TO HAVE CENTRE HOLES DRILLED (12 HOLES FOR TOP PLATE, 20 HOLES FOR BOTTOM PLATE)
ALL BOLTS ARE A325, 1"
THREADED ROD EXT. BETWEEN PLATES 1" DIAMETER GRADE 8
CLIENT
McMaster University
PROJECT
Braced Frame Test
DRAWING
Fixed Support (TOP)
Project Manager Dr. Wade
Design By D. Stevens
Drawing By D. Stevens
Date
Drawing Number
B1
1062
320
1500
1000
635
70
70
102
275
102
102
102
102
102
102
246
102
246
102

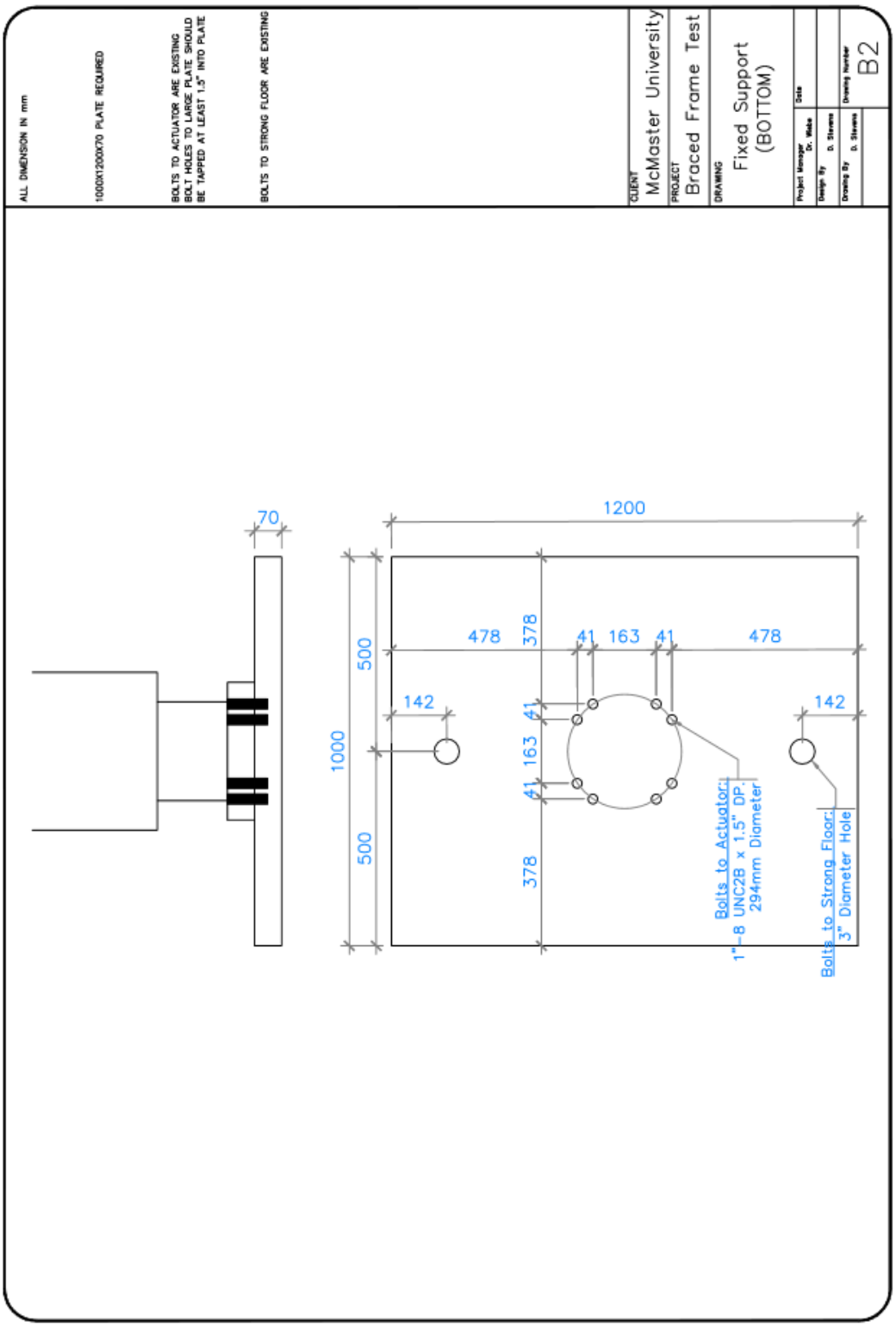
ALL DIMENSION IN mm
1000X1200X70 PLATE REQUIRED
BOLTS TO ACTUATOR ARE EXISTING BOLT HOLES TO LARGE PLATE SHOULD BE TAPPED AT LEAST 1.5" INTO PLATE
BOLTS TO STRONG FLOOR ARE EXISTING
CLIENT McMaster University
PROJECT Braced Frame Test
DRAWING Fixed Support (BOTTOM)
B2
70
1200
500
500
1000
478
378
41
163
41
478
142
142
41
163
41
378
Bolts to Actuator:
1"–8 UNC2B x 1.5" DP.
294mm Diameter
Bolts to Strong Floor:
3" Diameter Hole

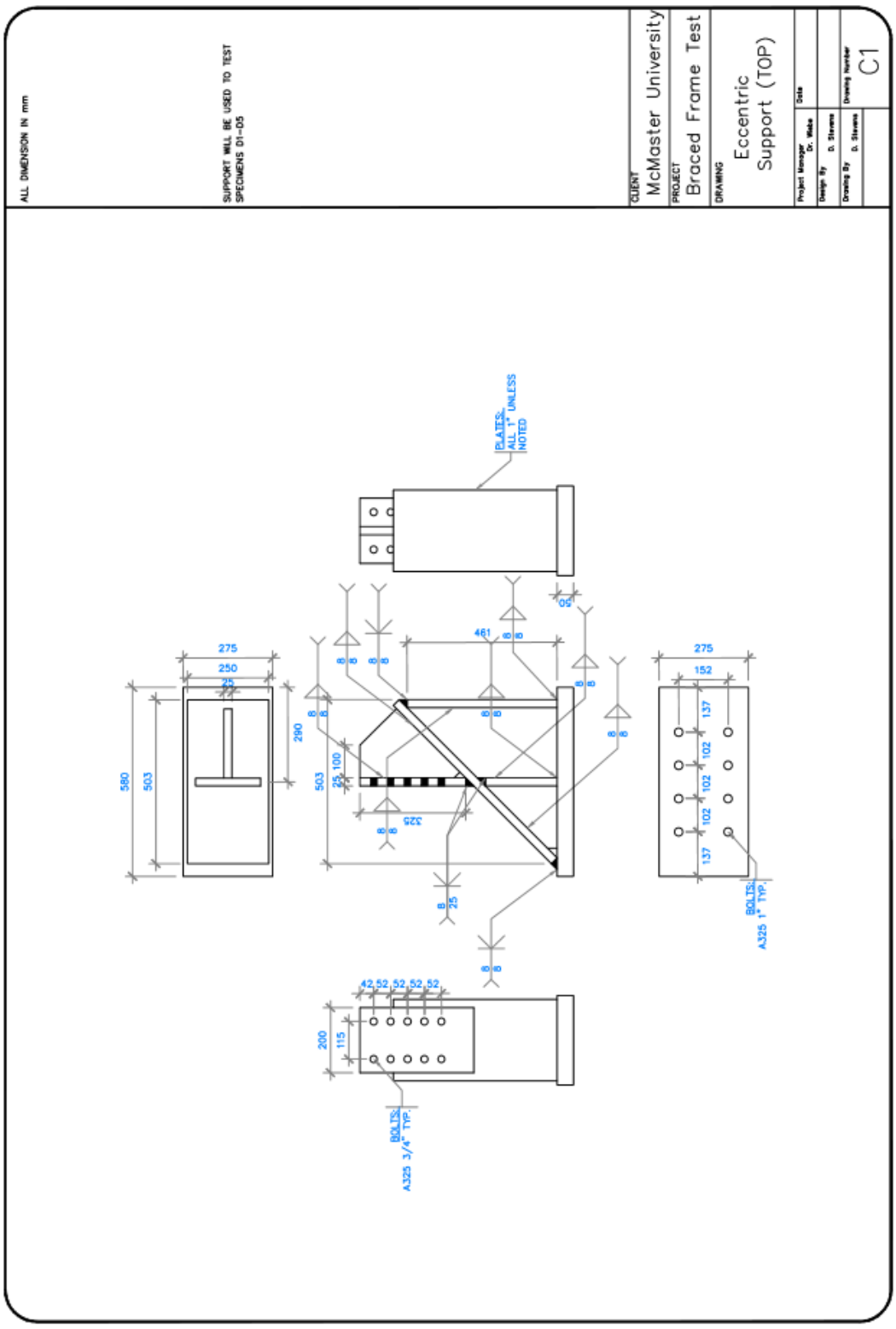
ALL DIMENSION IN mm
SUPPORT WILL BE USED TO TEST SPECIMENS D1-D5
CLIENT
McMaster University
PROJECT
Braced Frame Test
DRAWING
Eccentric Support (TOP)
Project Manager
Dr. Weda
Design By
D. Stevens
Drawing By
D. Stevens
Date
Drawing Number
C1
PLATES ALL 1" UNLESS NOTED
275
250
25
580
503
290
461
50
503
25
100
25
152
137
102
102
102
137
BOLTS A325 1" TYP.
42
52
52
52
52
200
115
BOLTS A325 3/4" TYP.

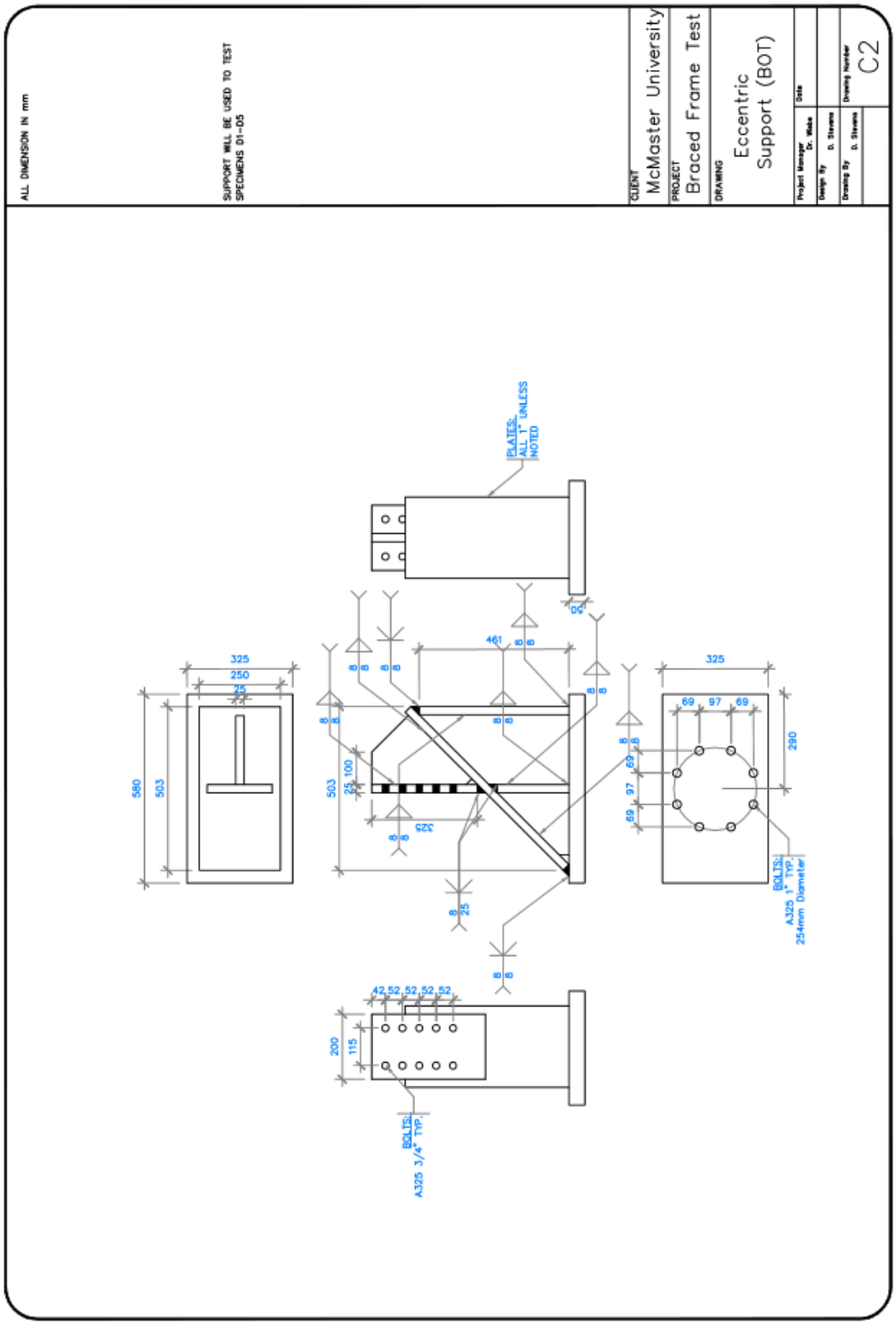
ALL DIMENSION IN mm
SUPPORT WILL BE USED TO TEST SPECIMENS D1-D5
CLIENT
McMaster University
PROJECT
Braced Frame Test
DRAWING
Eccentric Support (BOT)
Project Manager Dr. Kobe
Design By D. Stevens
Drawing By D. Stevens
Date
Drawing Number
C2
PLATES: A572 50 UNLESS NOTED
BOLTS: A325 3/4" TYP.
BOLTS: A325 1" TYP. 254mm Diameter

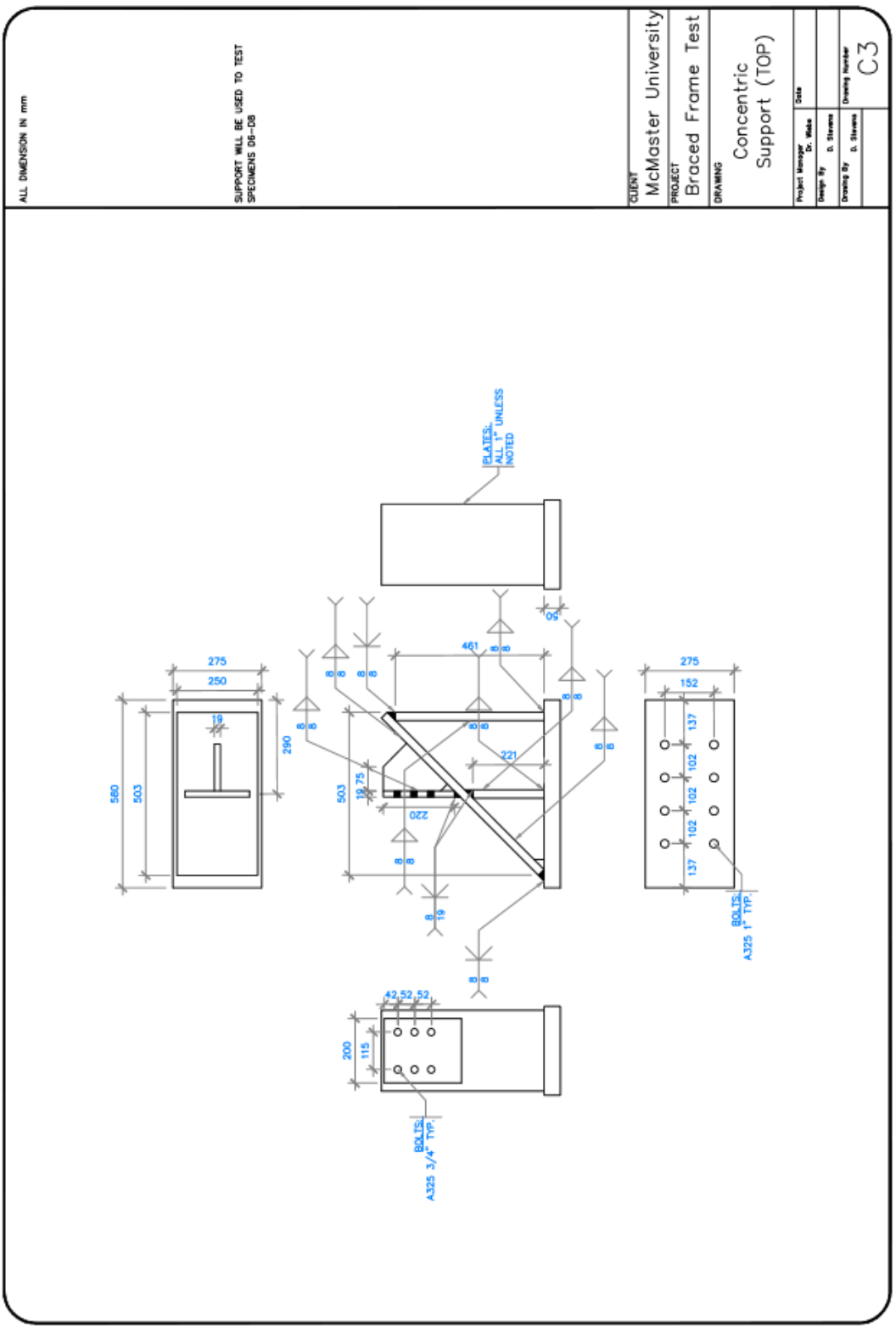
ALL DIMENSION IN mm
SUPPORT WILL BE USED TO TEST SPECIMENS D6-D8
CLIENT
McMaster University
PROJECT
Braced Frame Test
DRAWING
Concentric Support (TOP)
Project Manager Dr. Wake
Design By D. Stevens
Drawing By D. Stevens
Date
Drawing Number
C3
PLATES: ALL 1" UNLESS NOTED
275
250
580
503
290
19
461
221
220
19.75
503
275
152
137
102
102
102
137
BOLTS: A325 1" TYP.
42
52
52
200
115
BOLTS: A325 3/4" TYP.

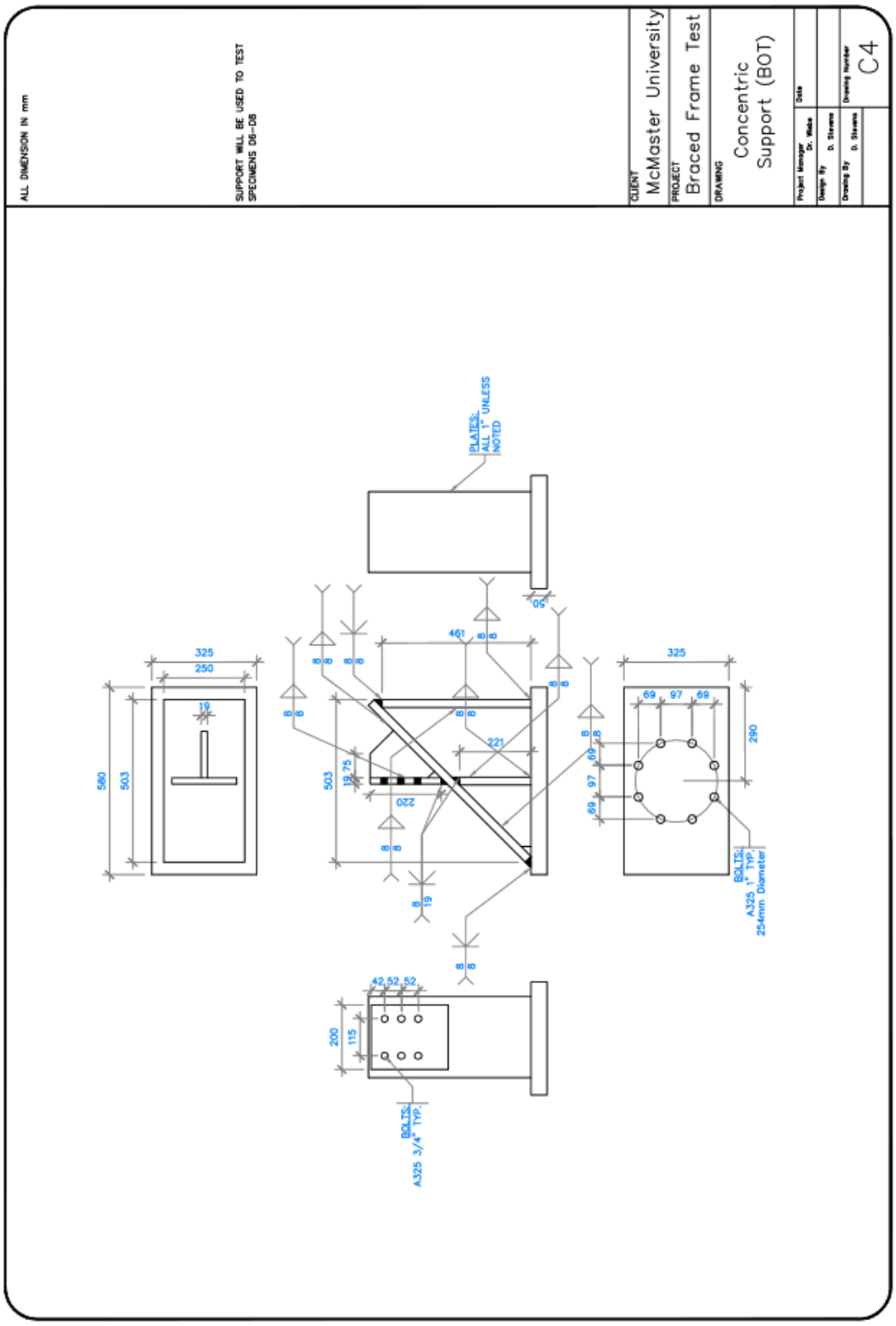
ALL DIMENSION IN mm
SUPPORT WILL BE USED TO TEST SPECIMENS D5-D8
CLIENT
McMaster University
PROJECT
Braced Frame Test
DRAWING
Concentric Support (BOT)
Project Manager Dr. Wake
Design By D. Stevens
Drawing By D. Stevens
Date
Drawing Number
C4
PLATES: ALL 1" UNLESS NOTED
325
250
580
503
19
461
221
220
19.75
50
69
97
290
BOLTS: A325 1" TYP. 254mm Diameter
42
52
200
115
BOLTS: A325 3/4" TYP.

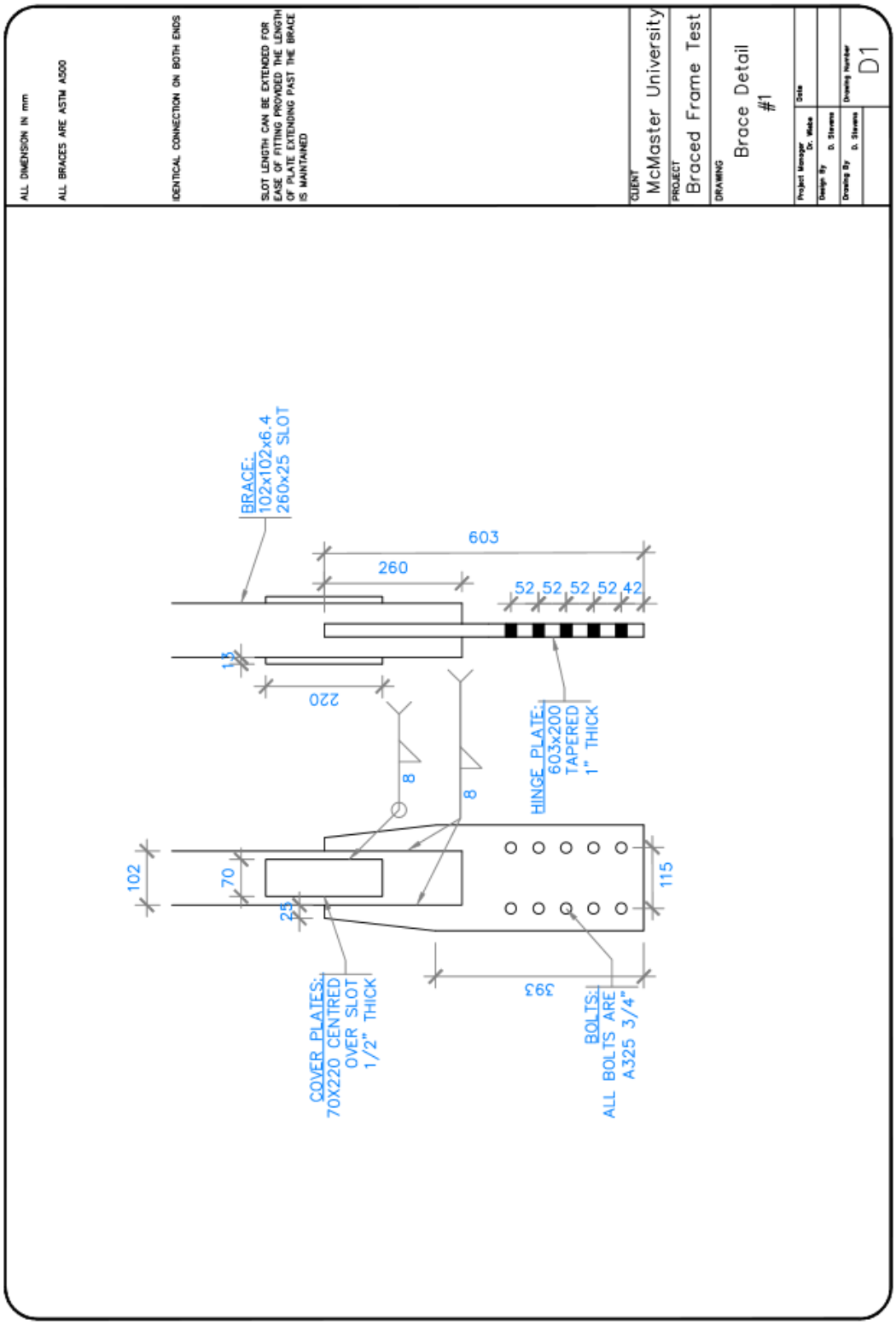
ALL DIMENSION IN mm
ALL BRACES ARE ASTM A500
IDENTICAL CONNECTION ON BOTH ENDS
SLOT LENGTH CAN BE EXTENDED FOR EASE OF FITTING PROVIDED THE LENGTH OF PLATE EXTENDING PAST THE BRACE IS MAINTAINED
CLIENT McMaster University
PROJECT Braced Frame Test
DRAWING Brace Detail #1
Project Manager Dr. Wiebe
Design By D. Stevens
Drawing By D. Stevens
Date
Drawing Number D1
BRACE: 102x102x6.4 260x25 SLOT
603
260
52 52 52 52 42
12
220
8
8
HINGE PLATE: 603x200 TAPERED 1" THICK
102
70
25
115
592
COVER PLATES: 70X220 CENTRED OVER SLOT 1/2" THICK
BOLTS: ALL BOLTS ARE A325 3/4"

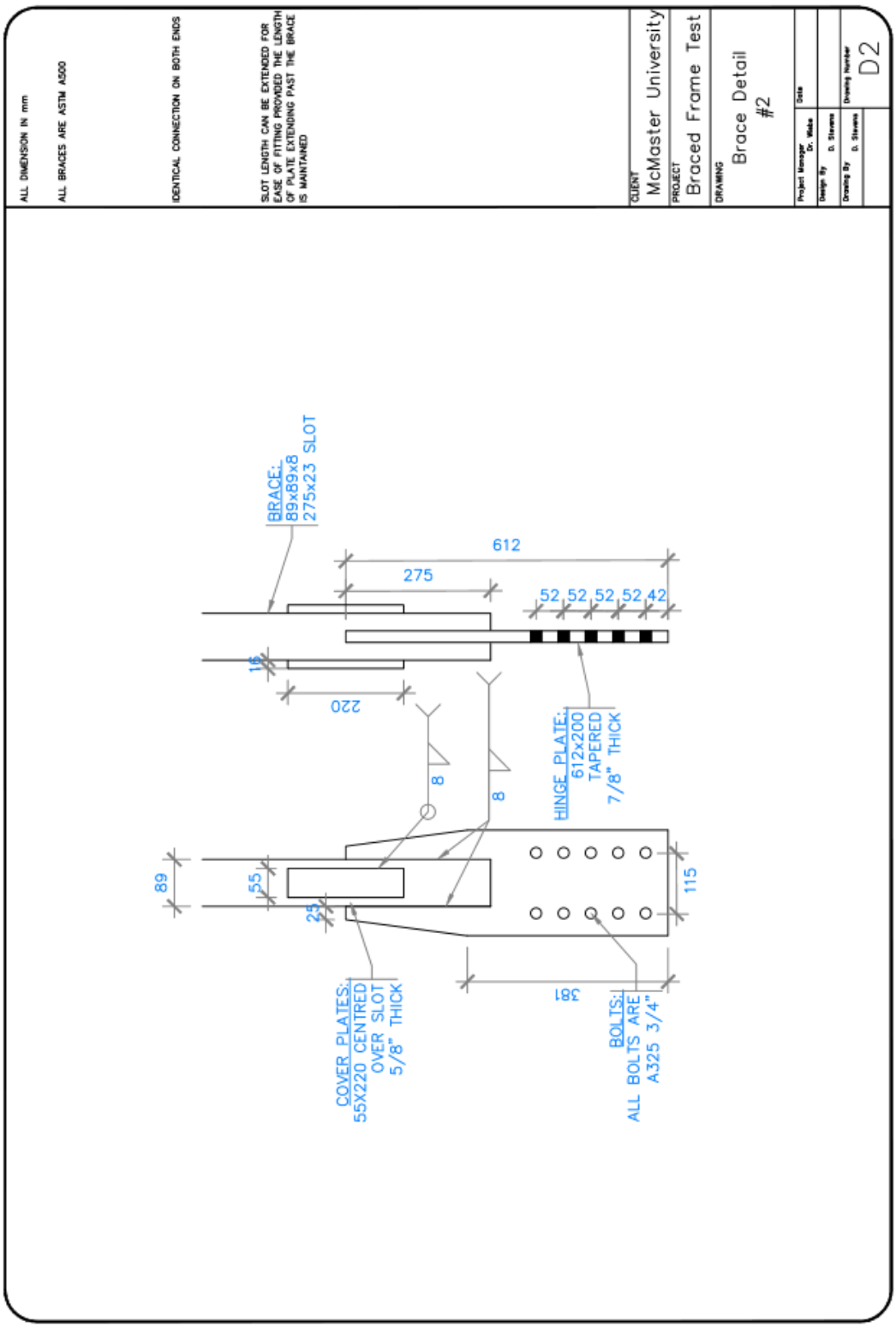
ALL DIMENSION IN mm
ALL BRACES ARE ASTM A500
IDENTICAL CONNECTION ON BOTH ENDS
SLOT LENGTH CAN BE EXTENDED FOR EASE OF FITTING PROVIDED THE LENGTH OF PLATE EXTENDING PAST THE BRACE IS MAINTAINED
CLIENT McMaster University
PROJECT Braced Frame Test
DRAWING Brace Detail #2
Project Manager Dr. Mahe
Design By D. Stevens
Drawing By D. Stevens
Date
Drawing Number D2
BRACE: 89x89x8 275x23 SLOT
612
275
52 52 52 52 42
16
220
8
8
HINGE PLATE: 612x200 TAPERED 7/8" THICK
89
55
25
115
381
COVER PLATES: 55X220 CENTRED OVER SLOT 5/8" THICK
BOLTS: ALL BOLTS ARE A325 3/4"

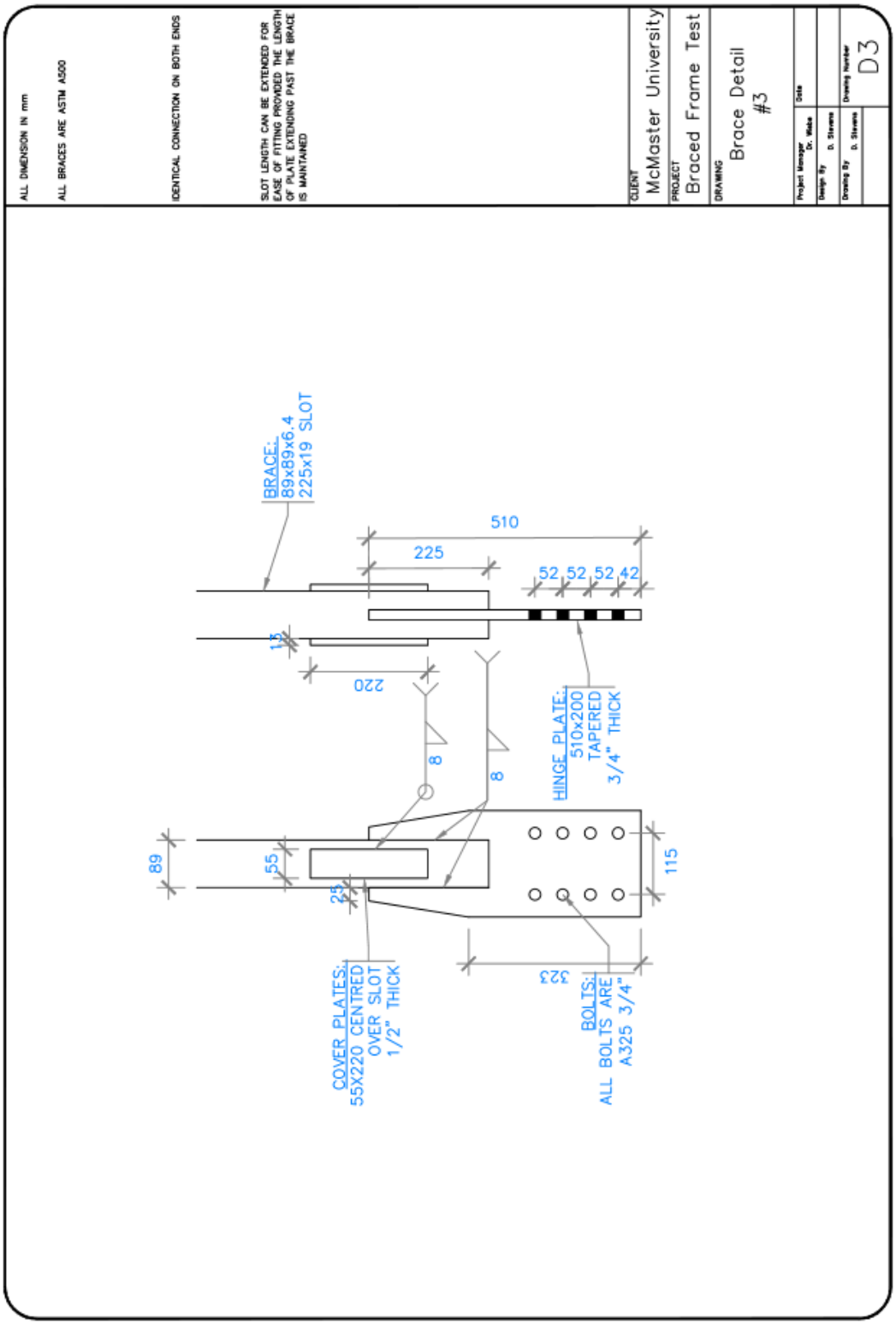
ALL DIMENSION IN mm
ALL BRACES ARE ASTM A500
IDENTICAL CONNECTION ON BOTH ENDS
SLOT LENGTH CAN BE EXTENDED FOR EASE OF FITTING PROVIDED THE LENGTH OF PLATE EXTENDING PAST THE BRACE IS MAINTAINED
CLIENT
McMaster University
PROJECT
Braced Frame Test
DRAWING
Brace Detail #3
Project Manager Dr. Rasa
Design By D. Stevens
Drawing By D. Stevens
Date
Drawing Number
D3
BRACE:
89x89x6.4
225x19 SLOT
510
225
52 52 52 42
15
220
8
8
HINGE PLATE:
510x200
TAPERED
3/4" THICK
89
55
25
115
COVER PLATES:
55X220 CENTRED
OVER SLOT
1/2" THICK
323
BOLTS:
ALL BOLTS ARE
A325 3/4"

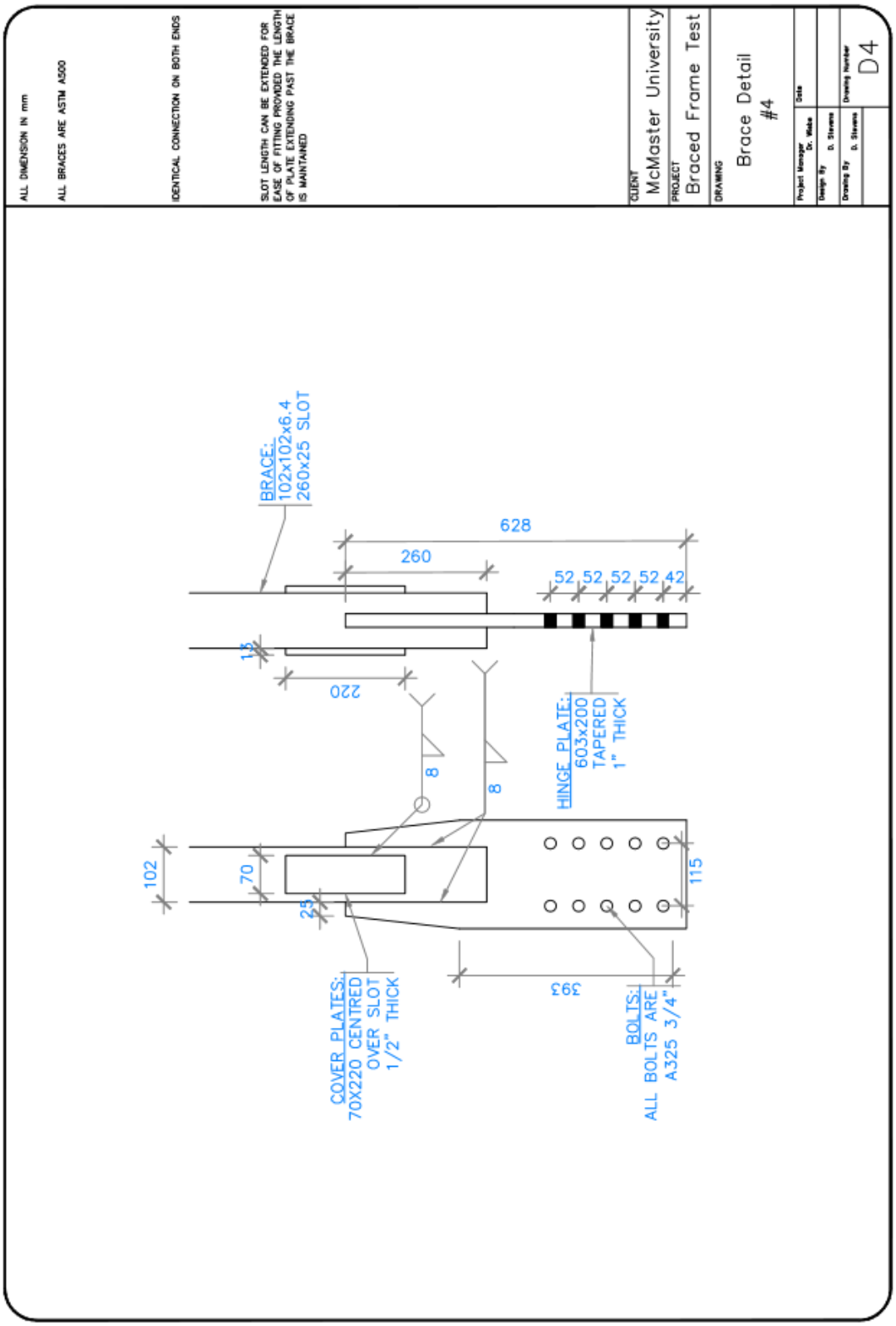
ALL DIMENSION IN mm
ALL BRACES ARE ASTM A500
IDENTICAL CONNECTION ON BOTH ENDS
SLOT LENGTH CAN BE EXTENDED FOR EASE OF FITTING PROVIDED THE LENGTH OF PLATE EXTENDING PAST THE BRACE IS MAINTAINED
CLIENT McMaster University
PROJECT Braced Frame Test
DRAWING Brace Detail #4
Project Manager Dr. Wiebe
Design By D. Stevens
Drawing By D. Stevens
Date
Drawing Number D4
BRACE: 102x102x6.4 260x25 SLOT
628
260
52 52 52 52 42
15
220
8
8
HINGE PLATE: 603x200 TAPERED 1" THICK
102
70
25
115
93
COVER PLATES: 70X220 CENTRED OVER SLOT 1/2" THICK
BOLTS: ALL BOLTS ARE A325 3/4"

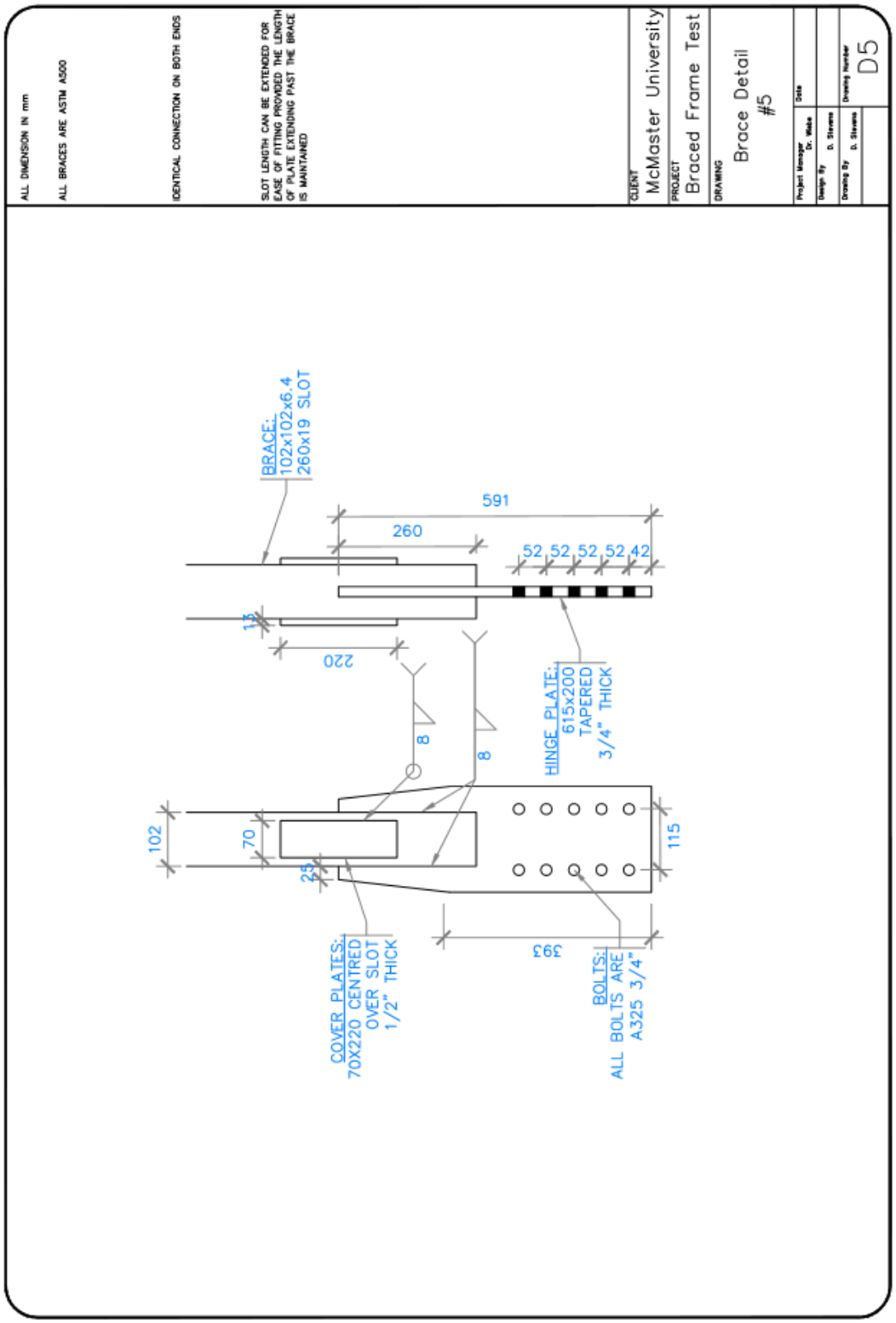
ALL DIMENSION IN mm
ALL BRACES ARE ASTM A500
IDENTICAL CONNECTION ON BOTH ENDS
SLOT LENGTH CAN BE EXTENDED FOR EASE OF FITTING PROVIDED THE LENGTH OF PLATE EXTENDING PAST THE BRACE IS MAINTAINED
CLIENT
McMaster University
PROJECT
Braced Frame Test
DRAWING
Brace Detail #5
Project Manager
Dr. Weiss
Design By
D. Stevens
Drawing By
D. Stevens
Date
Drawing Number
D5
BRACE:
102x102x6.4
260x19 SLOT
591
260
52 52 52 52 42
15
220
8
8
HINGE PLATE:
615x200
TAPERED
3/4" THICK
102
70
25
115
393
COVER PLATES:
70X220 CENTRED
OVER SLOT
1/2" THICK
BOLTS:
ALL BOLTS ARE
A325 3/4"

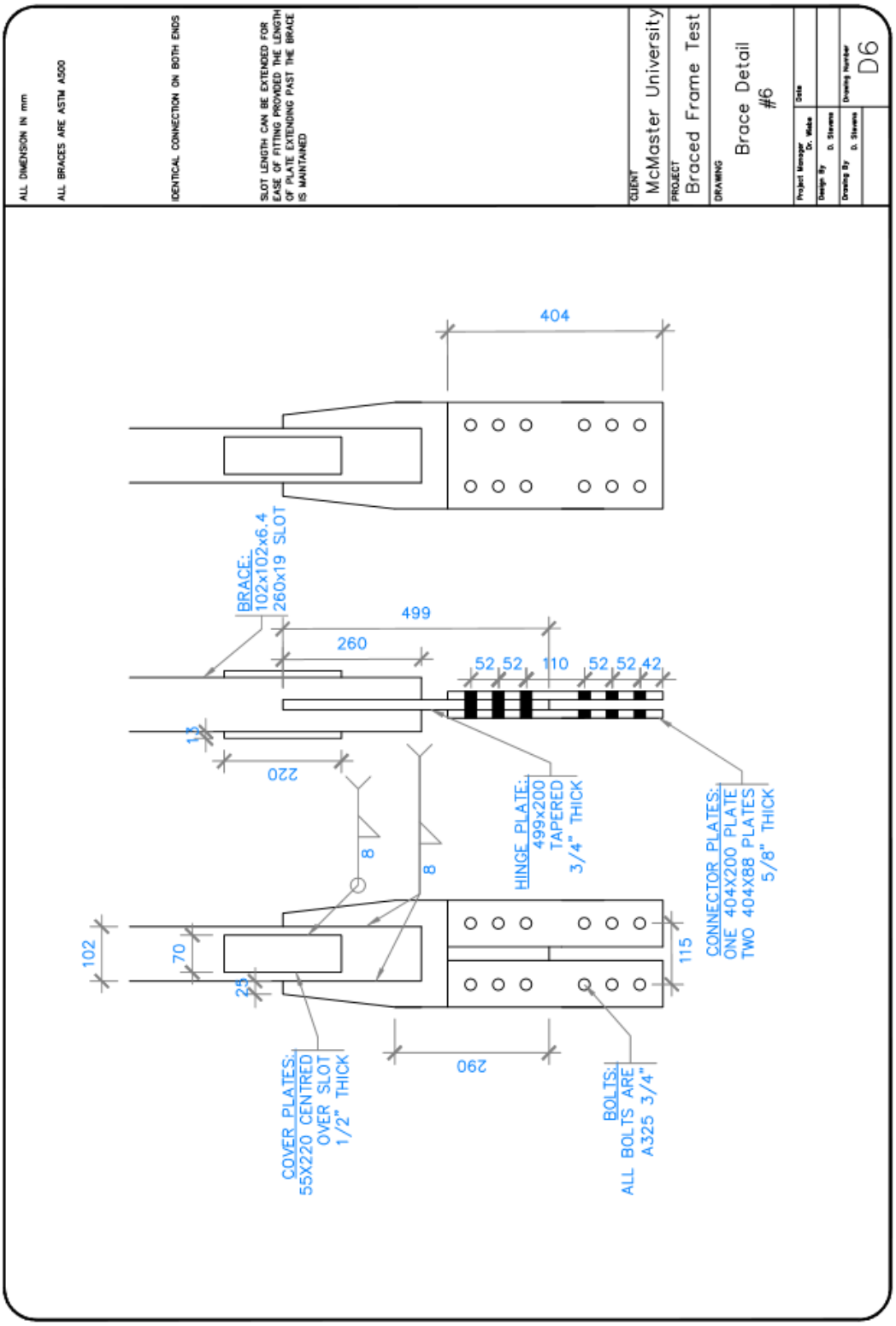
ALL DIMENSION IN mm
ALL BRACES ARE ASTM A500
IDENTICAL CONNECTION ON BOTH ENDS
SLOT LENGTH CAN BE EXTENDED FOR EASE OF FITTING PROVIDED THE LENGTH OF PLATE EXTENDING PAST THE BRACE IS MAINTAINED
CLIENT McMaster University
PROJECT Braced Frame Test
DRAWING Brace Detail #6
Project Manager Dr. Wake
Design By D. Stevens
Drawing By D. Stevens
Date
Drawing Number D6
404
BRACE:
102x102x6.4
260x19 SLOT
499
260
52 52 110 52 52 42
13
220
8
8
HINGE PLATE:
499x200
TAPERED
3/4" THICK
CONNECTOR PLATES:
ONE 404X200 PLATE
TWO 404X88 PLATES
5/8" THICK
102
70
25
115
290
COVER PLATES:
55X220 CENTRED
OVER SLOT
1/2" THICK
BOLTS:
ALL BOLTS ARE
A325 3/4"

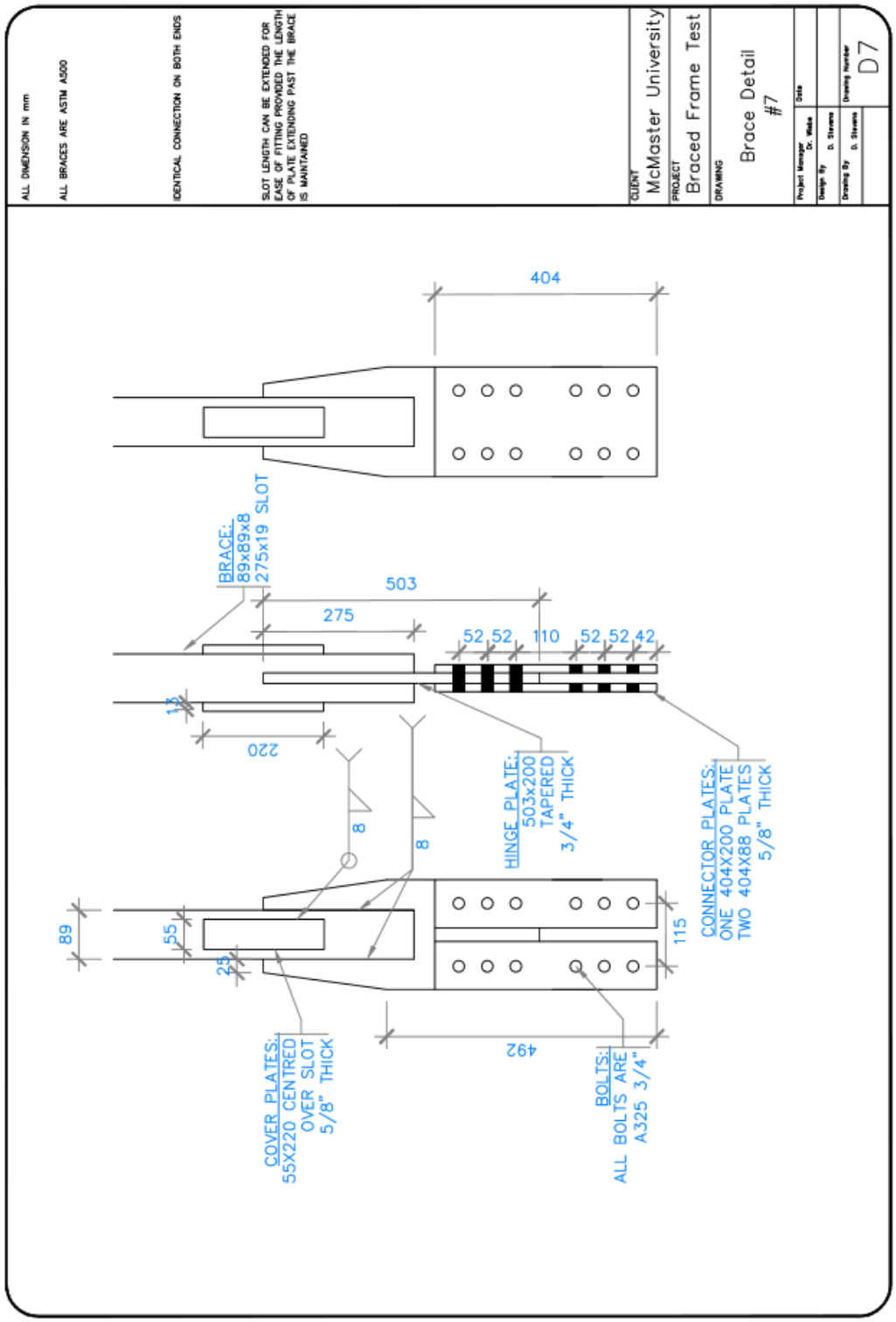
ALL DIMENSION IN mm
ALL BRACES ARE ASTM A500
IDENTICAL CONNECTION ON BOTH ENDS
SLOT LENGTH CAN BE EXTENDED FOR EASE OF FITTING PROVIDED THE LENGTH OF PLATE EXTENDING PAST THE BRACE IS MAINTAINED
CLIENT McMaster University
PROJECT Braced Frame Test
DRAWING Brace Detail #7
Project Manager Dr. Rebs
Design By D. Stevens
Drawing By D. Stevens
Date
Drawing Number D7
404
BRACE: 89x89x8 275x19 SLOT
503
275
52 52 110 52 52 42
13
220
8
8
HINGE PLATE: 503x200 TAPERED 3/4" THICK
CONNECTOR PLATES: ONE 404X200 PLATE TWO 404X88 PLATES 5/8" THICK
89
55
25
115
492
COVER PLATES: 55X220 CENTRED OVER SLOT 5/8" THICK
BOLTS: ALL BOLTS ARE A325 3/4"

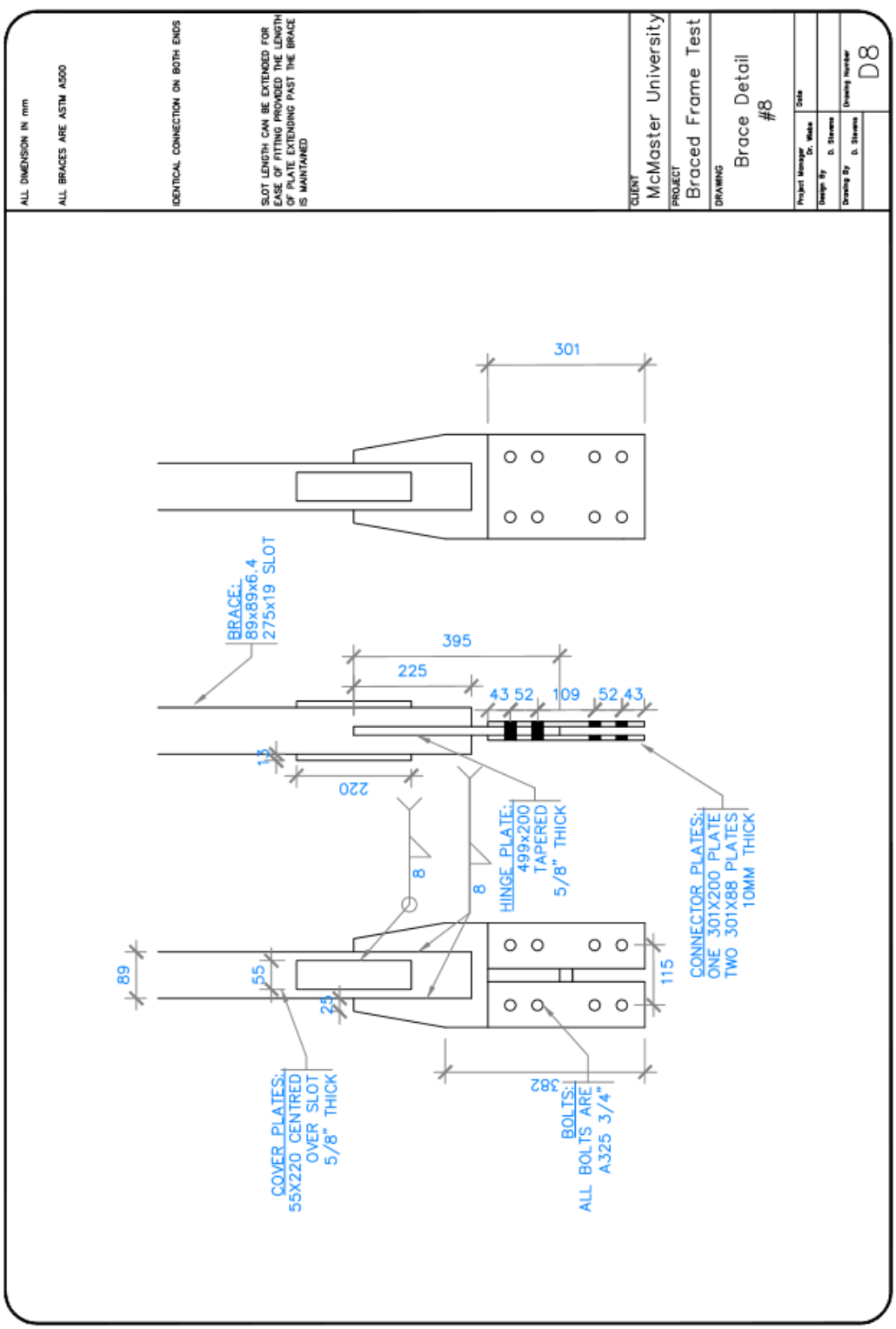
ALL DIMENSION IN mm
ALL BRACES ARE ASTM A500
IDENTICAL CONNECTION ON BOTH ENDS
SLOT LENGTH CAN BE EXTENDED FOR EASE OF FITTING PROVIDED THE LENGTH OF PLATE EXTENDING PAST THE BRACE IS MAINTAINED
CLIENT McMaster University
PROJECT Braced Frame Test
DRAWING Brace Detail #8
Project Manager Dr. Weba
Design By D. Stevens
Drawing By D. Stevens
Date
Drawing Number D8
301
BRACE: 89x89x6.4 275x19 SLOT
395
225
43 52 109 52 43
13
220
8
8
HINGE PLATE: 499x200 TAPERED 5/8" THICK
CONNECTOR PLATES: ONE 301X200 PLATE TWO 301X88 PLATES 10MM THICK
89
55
25
115
382
COVER PLATES: 55X220 CENTRED OVER SLOT 5/8" THICK
BOLTS: ALL BOLTS ARE A325 3/4"

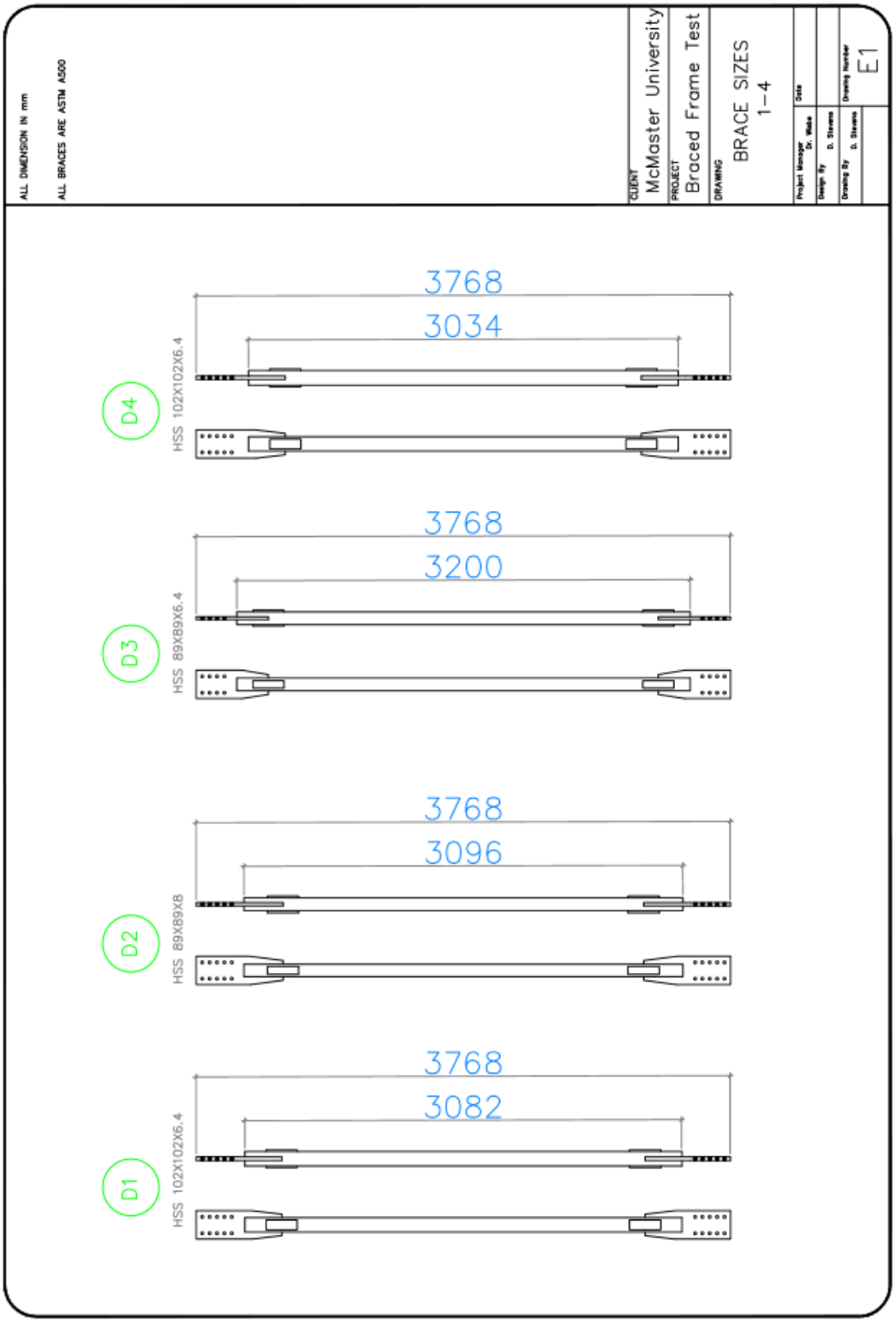
ALL DIMENSION IN mm
ALL BRACES ARE ASTM A500
CLIENT
McMaster University
PROJECT
Braced Frame Test
DRAWING
BRACE SIZES
1-4
Date
Project Manager
Dr. Wade
Design By
D. Stevens
Drawing By
D. Stevens
Drawing Number
E1
D4
HSS 102X102X6.4
3768
3034
D3
HSS 89X89X6.4
3768
3200
D2
HSS 89X89X8
3768
3096
D1
HSS 102X102X6.4
3768
3082

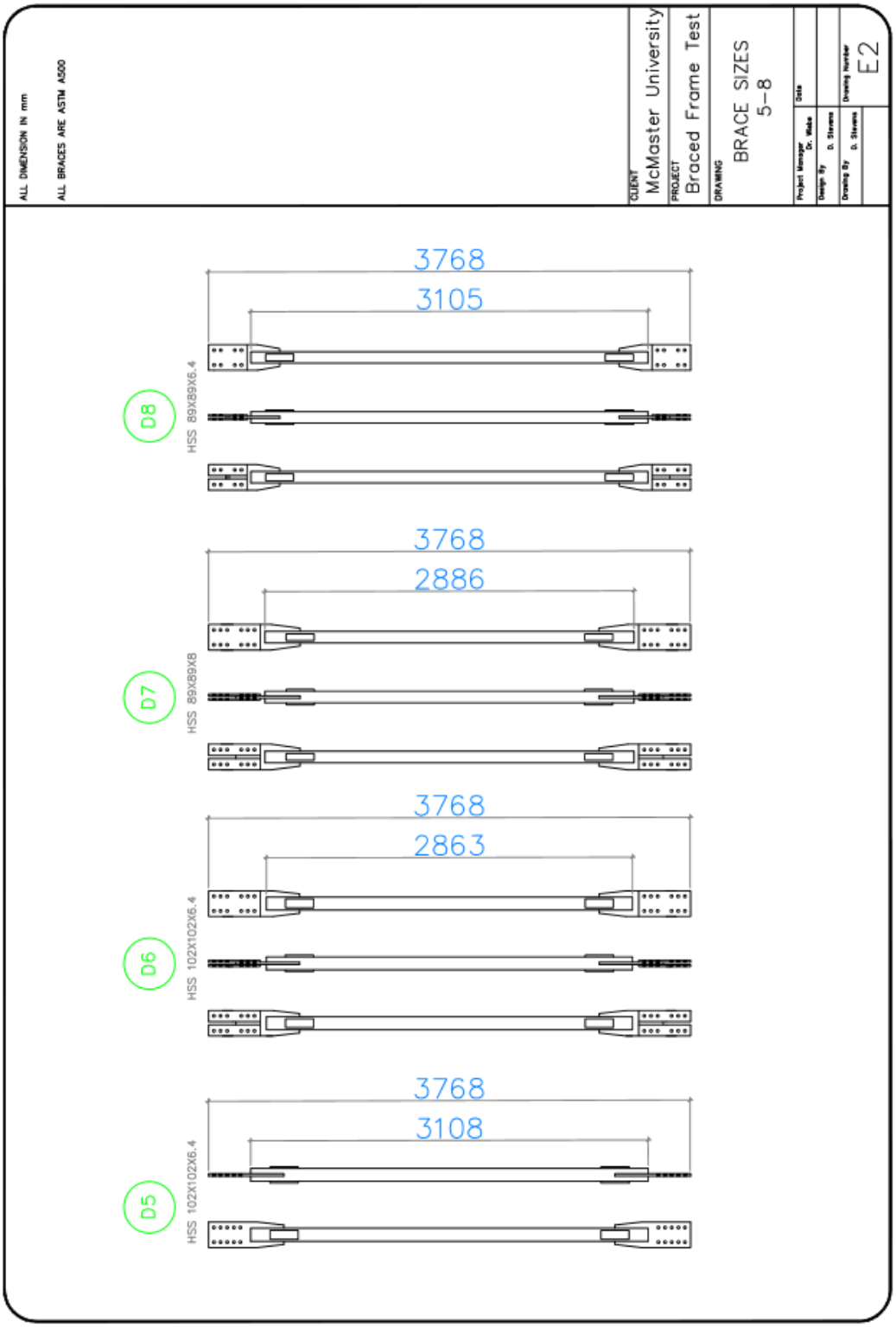
ALL DIMENSION IN mm
ALL BRACES ARE ASTM A500
CLIENT
McMaster University
PROJECT
Braced Frame Test
DRAWING
BRACE SIZES
5-8
Project Manager
Dr. Wake
Design By
D. Stevens
Drawing By
D. Stevens
Date
Drawing Number
E2
3768
3105
D8
HSS 89X89X6.4
3768
2886
D7
HSS 89X89X8
3768
2863
D6
HSS 102X102X6.4
3768
3108
D5
HSS 102X102X6.4